UNIVERSITÀ DEGLI STUDI DI NAPOLI FEDERICO II

PHD IN INDUSTRIAL PRODUCT AND PROCESS ENGINEERING

XXXVI CYCLE

VERSATILE MICROPARTICLE-BASED MICRONEEDLES PLATFORM FOR INTRADERMAL DELIVERY

Supervisor

Prof. Paolo Antonio Netti

Ph.D Candidate

Ing. Alessandro Attanasio

Advisor

Ph.D Ing. Raffaele Vecchione

Coordinator

Prof. Andrea D'Anna

2020/2024

Ai miei genitori

“Tra gli uomini non esiste grande
differenza di intelligenza.
La vera differenza si concretizza fra
l’uomo che pensa poco e
l’uomo che pensa molto.
L’uomo che pensa molto migliora
se stesso, le cose che fa e gli altri uomini”

Salvatore Tonti

Table of Contents

General Abstract

Transdermal delivery complements the list of administration routes alongside oral and parenteral ones, but only a limited class of active principles may be absorbed through the skin passively. Microneedles (MNs) represent an ideal delivery platform capable of facing several challenges in the transdermal administration field. They permit to access to the intradermal and transdermal routes without reaching nerve endings, and enabling molecules with molecular mass > 500 Da to pass through the stratum corneum, the natural barrier of the human organism. MNs constitute an attractive technology within drug delivery field since they can be used to deliver substances, also overcoming some of the main limitations of conventional hypodermic needles which require administration by trained healthcare personnel and risk of diseases transmission. Moreover, MNs offer an ideal solution for the patient compliance by mitigating pain and needle-phobia discomfort. Despite being introduced over twenty years ago, there are still challenges in achieving the desired characteristics. Among different MNs categories Polymer MNs are interesting for easy scale up, low cost and possibility to control drug release depending on their properties. However, they are typically characterized by low drug loading. limiting the number of applications, and incomplete penetration in the skin, making the delivery less effective and not reproducible. In addition, the stability of labile molecules is often affected by MNs fabrication process. The current work aims to design and realize a MN-based technology patch able to provide complete indentation, namely implantation, and a low invasive fabrication procedure allowing the encapsulation of different drugs in an active form and its sustained release. The proposed technological platform is constituted by a bi-compartmental array of microparticle-based MNs where a fast dissolvable tip, along with slow release polymer microparticles (µPs) are assembled together and integrated onto polymethyl methacrylate (PMMA) pillars. The combination of PLGA µPs with microneedle technology, makes µPs-based MNs versatile for a wide range of implementations. Based on a renewed fabrication process, the versatility of µPs-based MNs was explored in different contexts to evaluate the robustness of the platform. Based on the achieved results, microparticle-based MNs are under investigation for mRNA delivery currently.

1 Introduction

1.1 A painless world

Before introducing microneedles (MNs) from a technological point of view, it would be interesting to try explaining their establishment by starting from the analysis of society that humans use to live every day. Technological advances have made life easier and more comfortable century by century and recently year by year (Ebadi & Asadi, n.d.); it is not necessary to list the machines and the instruments that have replaced the man figure, since everyone may make experience of them. The very concept of society is equal to a massive machine made of smaller machines, where humankind is a functionary of a particular apparatus (Anders, 1956). One of the first reflections about the technique, where technology comes from, belongs to "Prometeo Incatenato" of Eschilo (Galimberti, 2013). It was a first attempt to think critically about the chance of dominating nature, as the unchangeable, by using technique. The progression in this direction has totally changed the meaning of fatigue in the XXI century: physical effort belongs to a confined category of jobs nowadays. In line with this, even the concept of pain has undergone a retelling. Ernst Jünger used to say: "Tell me your relation to pain, and I will tell you who you are!" (Jünger, 1997). The relation with pain reveals the world we are living in. The experience of pain is a negative event in modern society: people need to keep away from it. It is something that avoids maintaining a high level of performance, that is out of the worldwide logic driven to the optimization as a goal. Thus, the pain has triggered the fear of pain: which means living a life in search of whatever anesthetizes and leads to pain relief (Han, 2021). In this scenario, would patient's compliance assume a different meaning?

Skipping the answer to this question, which is only an invitation to reflect on the inheritance of this society, it is remarkable how in the 90s scientific literature has been produced to investigate the effectiveness of patient compliance in terms of quantifiable results according to the medical treatment of interest (Morris & Schulz, 1992; Roter et al., 1998). Following this logic, microneedles come under that kind of emerging painless technology whose key point is the capacity to link the world of transdermal and intradermal delivery to patient's needs. As a matter of fact, they are identified as the only means capable of making painless drug delivery possible (Prausnitz, 2004).

Before facing every category of this scientific field, a brief history of microneedle technology and how it gained a foothold is reported, to better make clear the background. Martin S. Gerstel and Virgil A. Place, from Alza corporation, filed a patent in 1976 where hollow and solid MNs were spotted as painless systems for both local and systemic delivery (Donnelly, 2012). Even with that patent, advances in microfabrication systems, by introducing the microelectronic industry, were necessary to obtain efficient drug delivery systems. In 1995, Hashimi published the first-ever paper on the hollow MNs device thought to inject bacterial plasmid for the genetic transformation of nematodes (Hashmi et al., 1995). In 1998, S. Henry published some analyses to investigate the permeability of silicon MNs in the case of *in vitro* and *in vivo* human epidermal skin (Henry et al., 1998). Successively, Mikszta published the first *in vivo* usage of a microneedle array as a platform for the delivery of genetic material in the vaccine field (Mikszta et al., 2002). Then, Mark Prausnitz reported how microneedles can be used to deliver several macromolecules as oligonucleotides, proteins, peptides, and even supramolecular complexes, and not only for small molecular weight molecules (Prausnitz, 2004). These have been the crucial stages in order to get the microneedles established in the state of art. Since then, several papers have been published where researchers showed the usage of microneedles in pharmaceutical applications (Sadeghi et al., 2021). Even if microneedle devices have gained approval by the regulatory authorities for the influenza vaccination, they are not yet large-scale devices as most of them are under investigation in preclinical and clinical studies (Sabri et al., 2019).

Especially in the vaccine field, the concept of Emergency Use Authorization (EUA) as a mechanism to facilitate the availability and use of medical countermeasures, including vaccines, became clear during the Covid-19 pandemic [https://www.fda.gov/vaccines-blood-biologics/vaccines/emergency-use-authorization-vaccines-explained]. Because of that, mRNA vaccine potentialities have been exploited and might represent a solution to several pathologies, including cancer, not only for Coronavirus diseases (Y. Wang et al., 2021). Although hypodermic needles represent an effective via to deliver mRNA vaccines, there is still poor compliance in undergoing this delivery path, mostly for children and adolescents (Orenius et al., 2018), and initiating and adhering to needle-dependent therapies, such as insulin for diabetic patients (Gill & Prausnitz, 2007). Furthermore, patients (an estimation between 11.5 to 66 million of U.S. adults) experiencing vasovagal syncope because of needle phobia, actually considered a mental disorder, skipped Covid-19 vaccination due to that anxiety behavior (Love & Love, 2021).

Proceeding in this direction, needlestick injuries are still a severe hazard among healthcare workers. They are responsible for the potential transmission of more than 20 pathogens (Elseviers et al., 2014). In the last official report of the World Health Organization, there was still incidence of HBV (37%), HCV (39%), and HIV (4.4%) among healthcare workers due to this type of injury (Rapiti et al., 2005). Even if almost two decades have passed since that report, this risk has not been repressed (Hosseinipalangi et al., 2022). The key to reading this introduction was the patient's adherence to this administration domain, but healthcare workers' safety is significant as well. In the investigation concerning the perception and the acceptability of microneedle technology, health care workers assumed a primary role as well as the patients. The clinical benefits of MNs devices are driven by an acceptance of all of the end-users (Marshall et al., 2016).

Based on this introduction, MNs equipment may represent a huge step forward in painless technologies and emerge as leading appliance among the existing tools in transdermal and intradermal delivery in the very near future. In order to assert that, it is necessary to follow the scientific method and point out the surroundings in which they are involved and what they consist of, firstly; then, why they may be considered a real alternative and how they find their *raison d'être* in mRNA delivery. Once all of this is presented, the multicompartmental concept of microneedle and the successful improvements will be shown. Finally, it will be clear how they appear as a versatile platform to be applied in distinct scenarios and explored for mRNA delivery

1.2 Transdermal delivery

Drug delivery embraces everything around the way of carrying and releasing pharmacologically active substances to specific cells, tissues, and organs in order to obtain the specific effect of interest while minimizing side effects (Jeong et al., 2021). This significantly influences both the routes of administration and the physicochemical properties of drugs. Transdermal delivery, historically, has played a primary role among various administration routes. Even in ancient civilizations such as Babylonian and Egyptian, the application of salves, plant, and animal extract patches through the skin was common (Joshi et al., 2023). While the term "transdermal" is commonly associated with the skin, distinctions exist based on the site of action of the active principle. A drug delivery system is defined topical when the site of action is on the superficial layers of the skin, instead when the intended goal is the deeper layers of the skin, such as the dermis, it corresponds to intradermal. Actually, transdermal corresponds to cases where systemic

circulation needs to be reached (Sabri et al., 2019). For simplicity, from now on "transdermal delivery" will be used interchangeably for all of the three circumstances. Transdermal delivery complements the list of administration routes alongside oral and parenteral ones. Despite the importance of oral and injection routes, they come with disadvantages. For oral administration, the gastrointestinal tract can affect drug stability, and a first pass in metabolism is necessary. Enzymatic reactions or the acidic environment in the stomach may lead to the degradation of active ingredients. Furthermore, especially for peptide or protein-based substances, low bioavailability may be induced by the poor solubility of the drugs in the intestinal tract which turns into drug absorption issues (Dahan et al., 2009; Marschuk Tz et al., 2000). The parenteral administration mode is mostly poor compliant and adherent for the patients due to its invasive and painful nature, requiring qualified personnel and significant disposal costs (Ramadon et al., 2022).

Transdermal delivery introduces multiple advantages. It is minimally invasive, enhancing patient compliance and is suitable for unconscious individuals or those suffering from needle phobia. Self-administration is possible, avoiding first-pass metabolism and improving bioavailability. The pharmacokinetic profiles of drugs are more uniform, reducing the risk of toxic side effects while maintaining drug levels above the minimal therapeutic concentration. In addition, when it comes to vaccination strategies, the skin is a promising site for delivering therapeutic proteins and peptides. This is because skin contains dendritic cells in both the epidermal and dermal layers that are crucial for triggering immune responses. Hence, transdermal delivery can be an effective way to administer vaccines (Alkilani et al., 2015a; Ramadon et al., 2022). Before focusing on the subsequent aspects of this topic, it would be preferable to understand the structure of the skin.

1.3 Skin

The skin acts as one of the main players in transdermal delivery, serving as a crucial interface from both pharmaceutical and mechanical perspectives. It is essential to provide a comprehensive overview of its significance. The skin, the body's largest tissue, covers an area of approximately 2 square meters and serves multiple purposes, including body temperature regulation and protection from external threats. Acting as a physical barrier, it shields against mechanical injuries, UV rays, external agents, and microorganisms. The skin is made up of three main layers - the outermost layer called the epidermis, the middle layer known as the dermis, and the innermost layer called the hypodermis (Kanitakis, 2002).

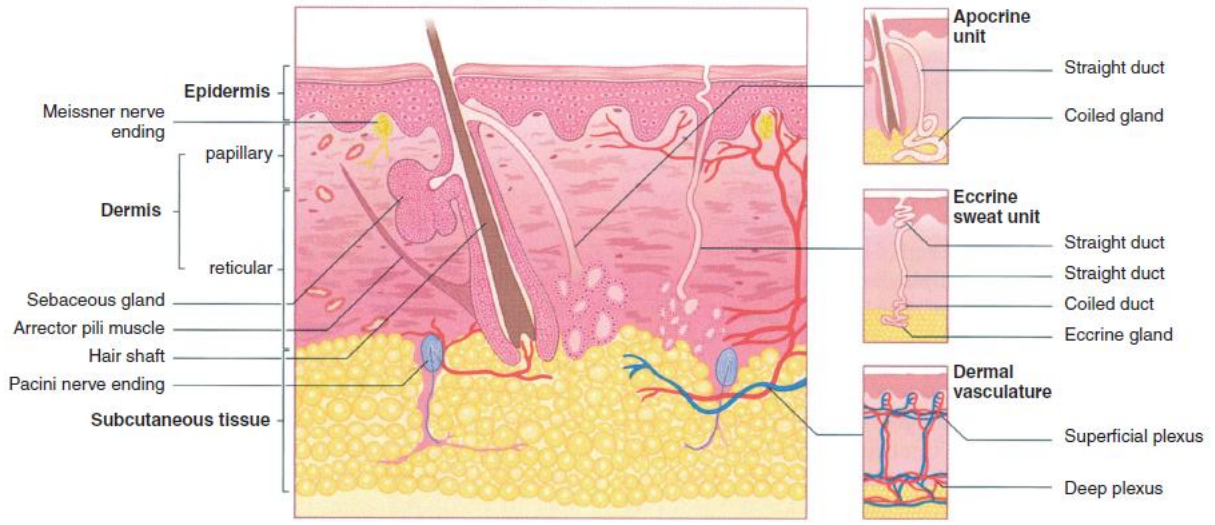

Figure 1 Structure of the skin (Kolarsick et al., 2006)

The epidermis, the outermost layer of the skin, exhibits varying thickness, being around 0.8 mm on the palms of the hands and soles of the feet (Alkilani et al., 2015b). The epidermis is a layer of stratified, squamous epithelium that mainly comprises two types of cells - keratinocytes and dendritic cells. Although there are other cell types like Langerhans and Merkel cells, keratinocytes constitute the majority. The epidermis is usually divided into four layers based on the differentiation of keratinocytes, progressing from the basal cell layer (stratum germinativum) to the squamous cell layer (stratum spinosum), the granular cell layer (stratum granulosum), and finally, the horny or cornified cell layer (stratum corneum) (Kolarsick et al., 2006).

The epidermis is a dynamic tissue that constantly renews itself, which emphasizes the importance of understanding the staminal cell cycle. Over 80% of epidermal cells are keratinocytes derived from the ectoderm. As these cells move from the basal layer to the skin surface, they undergo a differentiation process called keratinization. During this process, keratinocytes first undergo a synthetic phase followed by a degradative phase. In the synthetic phase, the cell builds up a cytoplasmic supply of keratin, which is a fibrous intermediate filament arranged in an alpha-helical coil pattern, and serves as part of the cell's cytoskeleton. Bundles of these keratin filaments merge and attach to the plasma membrane, creating intercellular attachment plates known as desmosomes. The subsequent degradative phase of keratinization involves the loss of organelles,

consolidation of cell contents into filaments and amorphous cell envelopes, ultimately resulting in the formation of a horny or corneocyte.

The maturation process leading to cell death is known as terminal differentiation. The skin's basal layer, or stratum germinativum, consistes of column-shaped keratinocytes attaching to the basement membrane zone perpendicular to the dermis. Connected through desmosomal junctions, basal cells also adhere to superficial squamous cells. Basal cells feature dark-staining oval or elongated nuclei containing melanin pigment transferred from nearby melanocytes. The basal layer is the primary site of mitotically active cells generating outer epidermal layers. Epidermal stem cells in the basal layer are clonogenic with a long lifespan, progressing slowly through the cell cycle under normal conditions. In humans, the migration of a basal cell from the basal layer to the cornified layer takes at least 14 days.

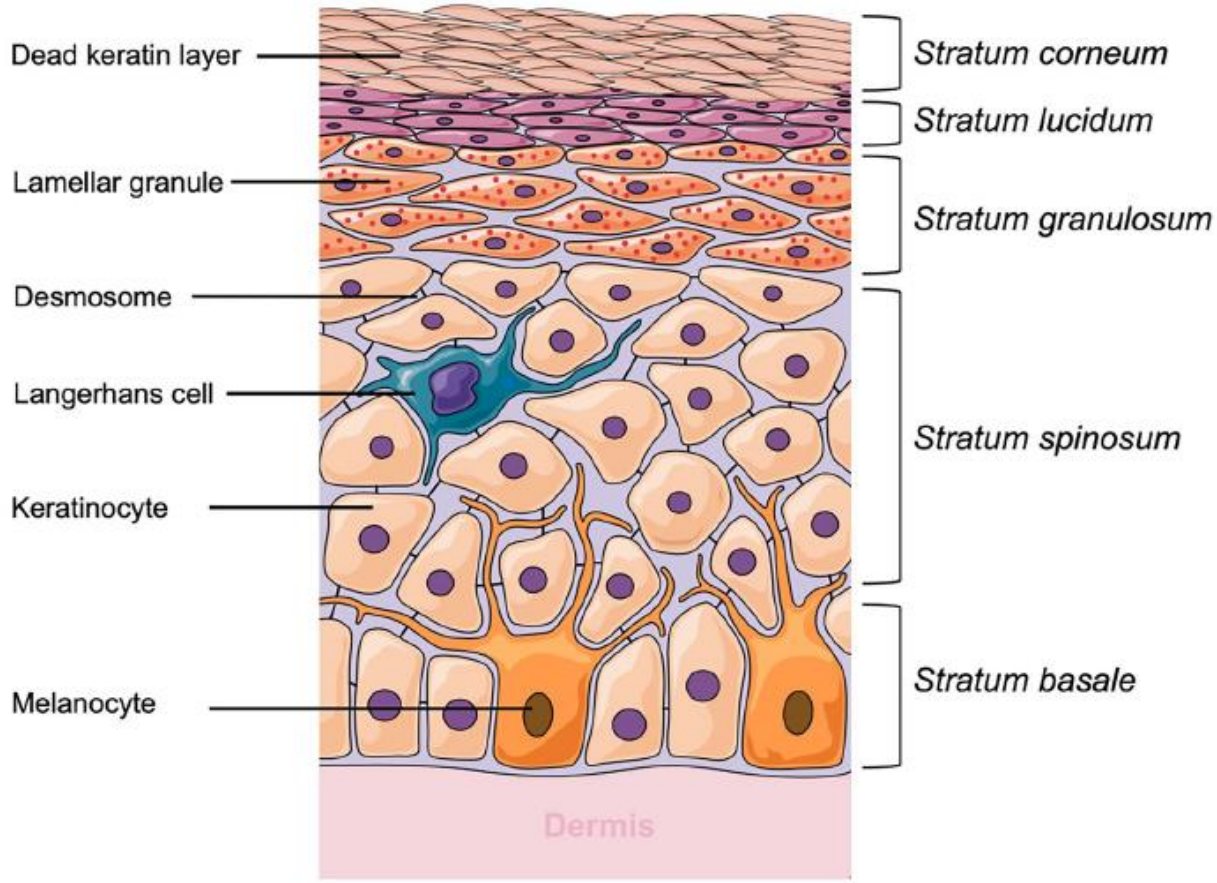

The squamous cell layer or stratum spinosum, situated above the stratum germinativum, consists of 5-10 cell in thickness. This layer consists of different cells that vary in shape, structure, and

subcellular properties depending on their location. Suprabasal spinous cells have a polyhedral shape with a rounded nucleus, while cells in the upper spinous layers are generally larger, become flatter as they move towards the skin's surface, and contain a lamellar granule. The lamellar granules are fascinating organelles found in cells at the interface between the granular and cornified layers. They contain various enzymes, such as lipases, proteases, and glycosidases, resembling lysosomes. The main function of these granules is to deliver precursors of stratum corneum lipids into the intercellular space, but they also play a role in the upper spinous layer. Desmosomes bridge intercellular spaces between spinous cells providing mechanical strength and resistance to physical stresses. Keratin filaments in the cytoplasm are organized concentrically around the nucleus and are bound to desmosomal plaques at one end, while the other end remains free. The numerous desmosomes along cell margins give the stratum spinosum its spine-like appearance. The granular layer or stratum granulosum, the most superficial layer containing living cells, is composed of flattened cells holding abundant keratohyaline granules in their cytoplasm. These cells are responsible for further synthesis and modification of proteins involved in keratinization, whereas the keratohyaline granules found in this layer are important for the formation of the interfibrillary matrix and the inner lining of horny cells. The granular layer thickness varies proportionally to that of the overlying horny cell layer. For example, under thin cornified layer areas, the granular layer may be only 1–3 cell layers in thickness, while under hands palms and the soles of the feet the granular layer may be ten times thicker. Lysosomal enzymes are also present in this layer, with the function to dissolve cellular organelles during the terminal differentiation process. The horny cells of the cornified layer provide mechanical protection and prevent water loss and invasion by foreign substances. These cells are rich in protein, primarily composed of keratins, surrounded by a continuous extracellular lipid matrix. Melanocytes produce melanine pigment transferred to keratinocytes. Merkel cells, found in high tactile sensitivity sites, generate action potentials in the adjoining afferent neurons. Langerhans cells recognize and process soluble antigens found in epidermal tissue. The interface between the epidermis and dermis is formed by a porous basement membrane zone that holds the two layers together, with basal keratinocytes and dermal fibroblasts being crucial. The basal lamina, synthesized by basal cells, mainly comprises type IV collagen, anchoring fibrils and dermal microfibrils. This includes an electron-lucent zone known as the lamina lucida as well as the lamina densa. The plasma membranes of basal cells are attached to the basal lamina by hemidesmosomes resembling rivets,

which distribute tensile or shearing forces throughout the epithelium. The dermal-epidermal junction provides support for the epidermis, establishes cell polarity and growth direction, directs the organization of the cytoskeleton in basal cells, offers developmental signals, and functions as a semipermeable barrier between layers. Some appendages are located here, including eccrine sweat glands involved in the regulation of heat, apocrine sweat glands for scent release, hair follicles whose purpose is to protect from elements and distribute sweat gland products. The dermis is a complex system of fibrous, filamentous, and amorphous connective tissue that accommodates stimulus-induced entry by nerve and vascular networks, epidermally derived appendages, fibroblasts, macrophages, and mast cells. Blood-borne cells including lymphocytes, plasma cells, and leukocytes, enter the dermis in response to various stimuli. The dermis comprises the bulk of the skin, providing pliability, elasticity, and tensile strength. It protects the body against mechanical injury, binds water, aids in thermal regulation, and houses sensory receptors. The dermis interacts with the epidermis to maintain the properties of both tissues. The two regions collaborate during development in the morphogenesis of the dermal-epidermal junction and epidermal appendages and interact in repairing and remodeling the skin during wound healing. The dermis, unlike the epidermis, does not undergo a clear pattern of differentiation. The connective tissue components of the dermis have a predictable structure and organization varying in a depth-dependent manner. Matrix components such as collagen and elastic connective tissue also vary in a depth-dependent manner and undergo remodeling and turnover in response to external stimuli, normal skin processes, and pathological conditions. Except for nerves and melanocytes, which originate from the neural crest, the constituents of the dermis come from mesodermal origin. Collagen, a fibrous protein family and the primary component of the dermis, is responsible for the skin's stress-resistant quality. There exist at least 15 genetically different types of collagen in human skin along with its presence in tendons, ligaments, bones' lining. Elastic fibers play a role in maintaining elasticity but contribute less to resisting deformation and tearing of the skin. The fibrillar collagens found in the skin are the most abundant proteins in the body and type I collagen is the major constituent of the dermis. Collagen type IV is present in the basement membrane zone, and keratinocytes primarily produce the major structural component of anchoring fibrils, collagen type VII. The elastic fiber differs structurally and chemically from collagen and consists of two components: protein filaments and elastin, an amorphous protein. The fibroblast fuses the elastic fiber to the dermis's extracellular matrix, which comprises

glycosaminoglycans. The papillary and adventitial dermis contains fine fibers, wherease the reticular dermis has significant collagen bundles. Hyaluronic acid is a minor component of the normal dermis but accumulates in pathologic states. The dermal vasculature has two intercommunicating plexuses: the subpapillary or superficial plexus and the lower plexus at the dermal-subcutaneous interface. The subpapillary or superficial plexus is composed of postcapillary venules located at the junction of the papillary and reticular dermis. The capillaries, arterioles, and venules of the superficial plexus supply the dermal papillae. The deeper plexus, surrounding adnexal structures, is more complex and supplied by larger blood vessels. Blood flow in human skin fluctuates significantly in response to thermal stress, regulated by the preoptic-anterior hypothalamus. Vasodilation, increased skin blood flow, and sweating are crucial for heat dissipation during heat exposure and exercise, while vasoconstriction reduces heat loss from the body to prevent hypothermia during cold exposure. Furthermore, the dermis contains numerous neurovascular bundles that contain nerve endings, arterioles, and venules (Kolarsick et al., 2006).

1.4 Transdermal routes of drug absorption

Intradermal and transdermal delivery involve the passive release of chemical agents, allowing them to penetrate the healthy and intact skin and reach the dermis or systemic circulation respectively. This diffusive process, known as percutaneous absorption, is governed by Fick's laws (Donnelly, 2012). The nature of the *stratum corneum* (SC), the outer layer of the epidermis, dictates a specific route for a drug to reach the systemic circulation or deeper layers of the skin. As mentioned above, the structure of SC is constituted by dead keratinocytes in a "bumper-to-bumper" conFiguretion, along with lipid components creating a dense architecture known as "brick-and-mortar" arrangement. Consequently, the SC acts as a barrier for most of external substances. Generally, there are two pathways for percutaneous absorption: the transepidermal and the transappendageal routes (Fig. 3).

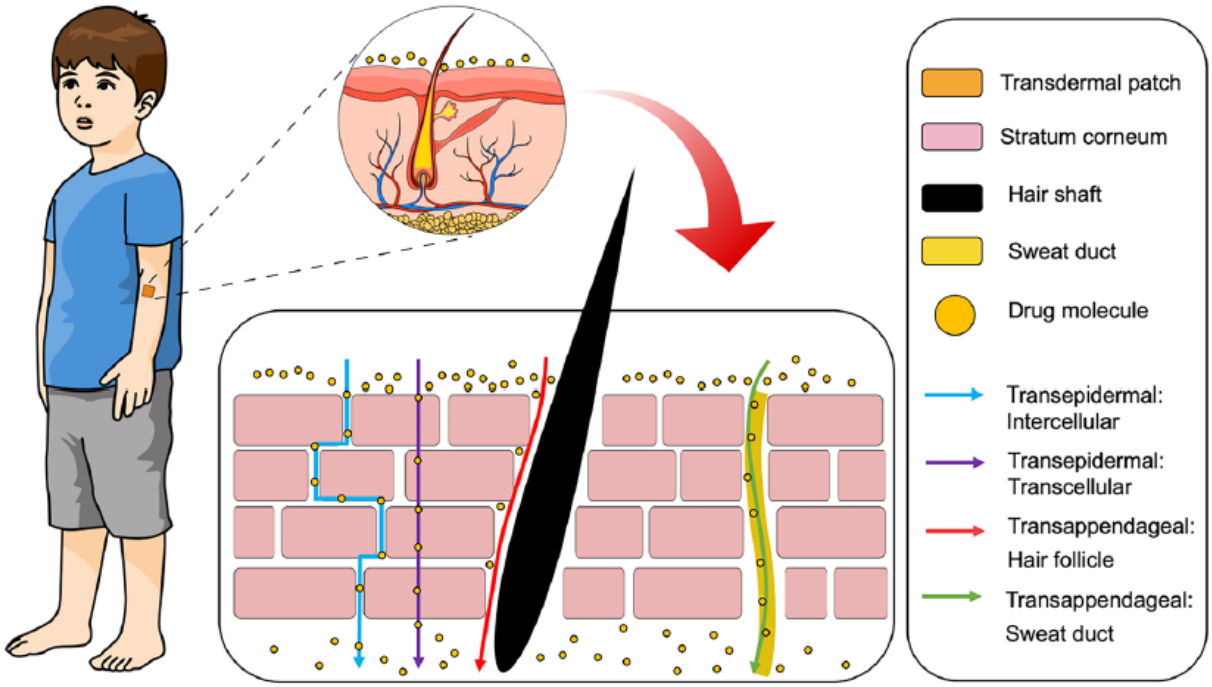

Figure 2 Schematic representation of percutaneous absorption (Ramadon et al., 2022)

The primary route for drug absorption through intact skin is termed transepidermal, which can be further divided into two routes: transcellular and intercellular. The transcellular route is the shortest path but involve diffusion through both lipophilic and hydrophilic structures, posing resistance to the permeation. Hydrophobic drugs typically utilize this route due to the hydrophobic properties of the lipid complex in the cell membranes of the SC. On the contrary, the intercellular route is employed by hydrophilic compounds or small molecules. These substances must diffuse through the lipid matrix of the intercellular space between keratinocytes in the SC to reach vascular capillaries in the dermis. This pathway is predominant in drug absorption and relies on a specific balance of the drug molecule being sufficiently lipid and aqueous soluble. The second pathway for drug absorption through the skin is transappendageal, involving drug delivery via hair follicles or sweat glands. This route is essential for transporting polar or ionizable compounds and is useful for large macromolecules facing challenges passing through epidermal cells due to the molecular size and different partition properties. However, the transappendageal pathway has a smaller absorption area (~ 0.1% of total skin area) compared to the transepidermal route. All three types of administration are influenced by the anatomical properties of the skin (skin type and skin condition), drug characteristics (lipophilicity, particle size, protein binding capacity), and formulation features (vehicle composition, rheological properties)(Ramadon et al., 2022;

Trommer & Neubert, 2006). The SC is macroscopically more resistant to the transit of water and polar solutes than the lipophilic ones. Lipophilic molecules are commonly employed in conventional transdermal delivery, where diffusion is driven by the drug concentration gradient across the SC barrier (Donnelly, 2012). According to Fick's laws, the molecule passage follows a specific curve based on concentration gradients:

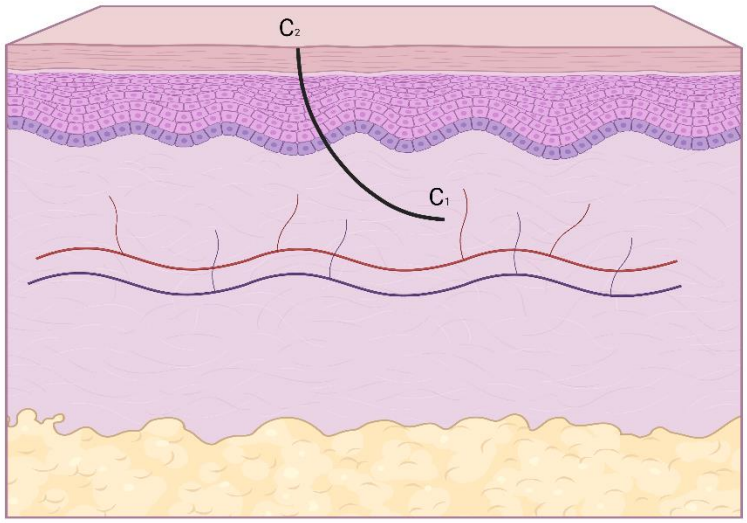

Figure 3 Description of flux across the skin from a transdermal patch. C_2 is the concentration of the active molecule in the patch, C_1 is the concentration of the active molecule within the body

$$J = -D\frac{\partial C(x,t)}{\partial x}$$

where D is the diffusion coefficient and $\frac{\partial C(x,t)}{\partial x}$ is the concentration gradient. Starting from this evidence, typically the goal is to obtain the lag time:

$$t_l = \frac{L^2}{6D}$$

where L is the overall thickness of skin tissues. Thereby, the lag time represents that necessary value to make the concentration gradient become constant. The cumulative permeation curve (Fig. 5) is composed of two distinct portions. The initial part represents non-steady state diffusion, while the linear portion corresponds to steady-state diffusion. It is important to note that Fick's second law can be utilized to describe the non-steady portion of the curve mathematically, while Fick's first law can be used to express the linear portion. Additionally, the time required to reach steady

state is referred to as the lag time and it can be determined by extrapolating the linear part of the permeation vs. time curve to the time axis (Alkilani et al., 2015; Ronnander et al., 2020).

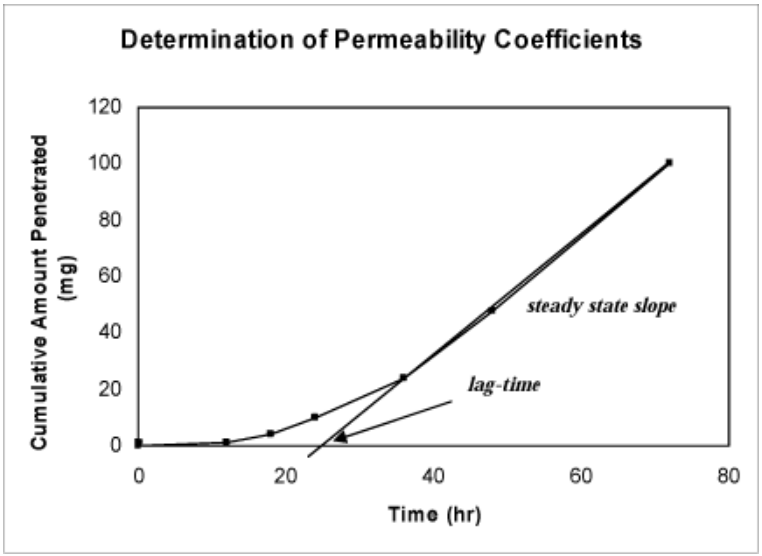

Figure 4 A typical plot of a permeation study

Considering the effective barrier function of the SC, the range of therapeutics available for percutaneous absorption in transdermal and intradermal delivery is limited. For a compound to traverse the intact SC, without an enhancing methodology, certain ideal features are required. Firstly, the drug molecule should have a small molecular weight, Mw < 500 Da, to facilitate easy passage through the barrier. Then, the solubility characteristics should be balanced for both water and oil phases, which means having a log partition coefficient (Log P) in this range: 1.0–3.0. The presence of hydrogen-bonding groups principally influence the ability to diffuse through the SC, with mono or di-substituted drug molecules containing hydrogen-groups having a higher likelihood of crossing, meaning hydrogen-bonding groups ≤2. A low melting point of the compound gives higher solubility, potentially resulting in a greater amount of drug permeating into the skin (Supe & Takudage, 2021).

1.5 Strategies to modify SC properties

Given the limited amount of molecules that can passively cross the healthy SC, different techniques have been explored to alter SC properties and deliver a wider range of drugs in this field (Joshi et al., 2023). There are two classes of procedures to induce skin permeation: passive and active methods. Among passive methods, drug permeability enhancers can increase skin permeation and absorption of drugs. An ideal enhancer should be biocompatible with the

biosystems it is applied to, as well as odorless, colorless and tasteless. It should be chemically and physically stable, sterile, non-toxic, and non-reactive to the drug, without any adverse pharmacological activity. The enhancer should not affect the zero-order skin permeation rate and should result in rapid, sustainable and reproducible absorption, without causing body fluid leakage These permeation enhancer agents are functional excipients included in the formulation cocktail. Chemical enhancers work by modifying lipids, changing their polarity and, thus altering the drug's permeability. The rate at which the drug passes through the skin is the limiting factor for transdermal drug absorption. However, using multiple enhancers at varying concentrations simultaneously is not advisable, and the same amount of a single enhancer cannot be used for different drugs in a single transdermal drug delivery system. Solvents, natural and synthetic polymers, surfactants, and other miscellaneous agents such as fatty acids, constitute the firstgeneration of chemical enhancers (Akhtar et al., 2020). However, these have often resulted in skin irritation, allergy and toxicity. Advanced chemical approaches such as miciroemulsions, nanostructured lipid carriers, invasomes, liposomes, dendrimers, etc, are expected to offer advantages over the previous passive agents but rely on more intricate processes, and most of them are under investigation (Phatale et al., 2022). Active methods are employed to transport drugs across the skin by exploiting external energy as a driving force or by physically disrupting the stratum corneum (Fig. 6).

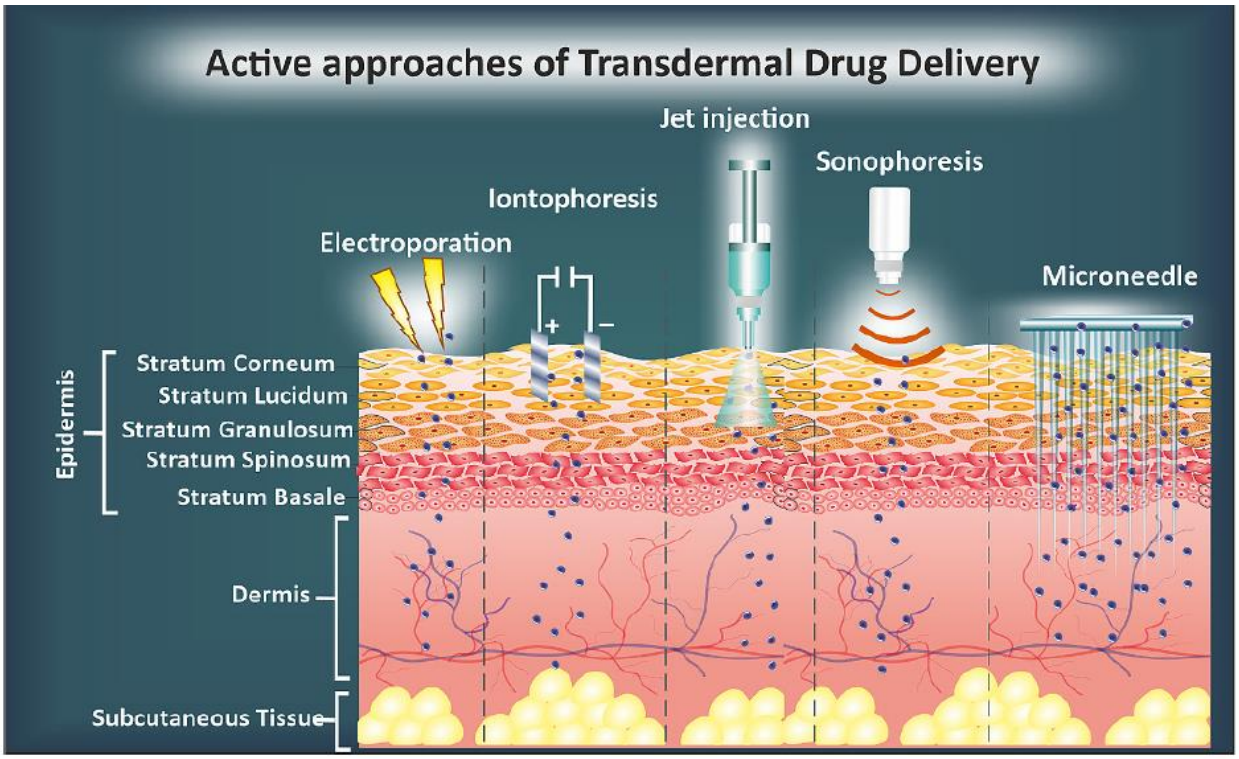

Figure 6 Active methods of transdermal drug delivery (Phatale et al., 2022)

This extensively broadens the range of drugs that can be successfully delivered across the skin. These methods include ultrasound, electrically assisted techniques (such as electroporation and iontophoresis), velocity-based devices (like powder injection and jet injectors), thermal approaches (such as lasers and radio-frequency heating), and mechanical methodologies such as microneedles. Such approaches provide better control over the reproducibility of the delivery profiles of drugs, allowing for a reduction in the lag time compared to passive approaches (Alkilani et al., 2015).

Iontophoresis is a highly effective technique that uses an electric current to transport drugs across the skin. The application of electric current significantly enhances the permeation of both charged and uncharged molecules through appendages. The electrophoretic device consists of an anode, cathode, and power suppliers that attract ions towards and away from the electrode. This promotes the entry of drug molecules into the skin by taking advantage of an ionic flux. The flux generated for drug permeation occurs due to two main kinetic mechanisms: electron repulsion and electroosmosis. The mechanism behind electrorepulsion involves the direct supply of an electric field for only charged drug molecules toward their possible transfollicular delivery. In contrast, electroosmosis is used for both charged and neutral drug molecules. It occurs at a skin

physiological pH of 4.0–4.5. However, an increase in pH will ionize carboxylic acid groups of lipids, which tend to increase the negative charge of the skin, acting as a driving force for permeation. When neutral molecules pass through the skin, an enhanced transport can be observed due to the bulk solvent flow that is carried with some velocity by the solvent stream. This is because electroosmotic flow plays a dominant role in this process. On the other hand, when an electric current is applied, the appendageal pathway predominates because the minimum resistance passage is preferred by the flux of ions. However, it is important to note that the intercellular route, which comprises polar regimes in lipid lamellae, has also been recognized as a significant player in iontophoretic delivery. The application of the electrical current is followed by the opening of polar aqueous pores because of the typical flip-flop movement of polypeptide helices in the stratum corneum. This provides a different route for drug transport. This approach can also be coupled with other passive methods to obtain an additive effect in permeation.

Sonophoresis is a technique that involves the use of ultrasound waves to deliver therapeutic agents through the skin membrane. This technique operates in a wide frequency range, specifically from 20 kHz to 16 MHz. When using sonophoresis, the intensity and time of application are crucial factors to consider. Applying the technique for an extended period can lead to tissue destruction.

Electroporation is an active physical method that uses high-voltage electric pulses for a brief duration (ranging from a microsecond to a millisecond) to transport therapeutic agents into cells and tissues. The efficacy of electroporation-induced transdermal permeation is dependent on the formulation parameters and physicochemical properties of the drug molecule. An increase in the electrical parameters such as pulse voltage, duration, and rate boosts drug transport. Electroporation also enables the permeation of high molecular weight hydrophilic drugs and biomolecules like insulin and DNA. In the process of electroporation, high amplitude pulses are applied for a short duration that disrupts the lipid bilayer structure of the stratum corneum, creating a new temporary path that facilitates transdermal drug absorption.

A needleless jet injector is a drug delivery system that administers proteins and peptides without using a needle. It has many advantages over conventional systems, including better penetration, enhanced absorbability and bioavailability, minor injury, and painless delivery. The injector uses a high-pressure power source (such as a spring or compressed gas) to fire a flow of liquid or solid particles (powders) at high velocity (60–140 m/s) and deliver the drug through the skin membrane through which the drug is delivered. The delivery of drug molecules at different sites

(subcutaneous, intradermal, and intramuscular) depends on the jet velocity and orifice diameter (Phatale et al., 2022).

These techniques explore different strategies to promote percutaneous absorption, but they are not without disadvantages. In the case of electrical methods such as iontophoresis and electroporation, several drawbacks have been reported. With iontophoresis, the electrical current is limited to 1 mA to avoid inducing patient discomfort and avoid the risk of non-specific vasodilation reactions. Local skin irritation (i.e. burns) or current-induced skin damage may occur if an area is solicited for more than 3 min or when the current exceeds 0.5 mA/cm2. Additionally, iontophoresis is more effective in delivering compounds with a molecular weight lower than 10 kDa. Finally, the iontophoresis device is costly and complex from the point of view of instrument setup. This latter limitation also applies to electroporation, since it is based on expensive and sophisticated devices. Other weak points of the electroporation include a small drug delivery load and restricted pore area, time-consuming treatment applications, and the need for qualified personnel. High-voltage applications pose intrinsic risks of cell damage or death, as well as heat-induced drug degradation. Time-consuming treatments and complicated instruments also apply to sonophoresis. Healthy skin is required for this kind of method, and the working principle is not entirely clear, with patient safety not definitely ensured. Regarding needleless jet injection, it is not a friendly-user device. This tool requires optimization for the dose accuracy due to the dependence on skin variability among distinct patients. Moreover, the reusable version is bulky and inconvenient, while the convenient variant is wasteful and raises environmental concerns (Nguyen, 2023).

In the end, thermal ablation is another method to disrupt SC and induce permeation absorption of molecules outside the specified above. This effect relies on lasers and radiofrequency as thermal energy sources, allowing heating of the skin area of interest until reaching about 100 C degrees and triggering the vaporization of keratin. The higher the temperature, the greater the alteration of SC induced, providing an accurate mode to control drug delivery, without causing damage to the deeper layer of the skin. Despite these characteristics, thermal ablation necessitates further investigation because structural changes in the skin are plausible and may cause distress due to the feasibility of the machines used (Jeong et al., 2021).

Although numerous approaches have been acknowledged to enhance crossing the SC barrier, patients are always in search of a balance among safety, compliance and cost. Microneedles may satisfy this requisite.

2 Microneedles (MNs)

Microneedles (MNs) have been depicted as the most desirable and promising technology in transdermal drug delivery over the past twenty years, both in academia and industrial sector. Between 2004 to 2013, the number of publications in this field increased by 77.9%. Currently, MNs constitute 30% of all papers in transdermal delivery technologies (Nguyen, 2023). It is essential to scientifically define what MNs are. They are downscaled version of widely used needles, designed to physically pierce the *stratum corneum* and establish contact between the outer agents and the inner part of the body. This allows drugs to cross the viable epidermis mechanically. Due to their dimensions, MNs are considered minimally invasive devices. Their length does not reach nerve endings or blood vessels, and the micropores in the skin are large enough to allow drug delivery but still small enough to prevent any damage to the tissue (Gill & Prausnitz, 2007; Nagarkar et al., 2020). MNs are in the micron scale, ranging from 50 to 900 µm in height and assembled into arrays covering up to 2000 μm^2 area. Considering that SC thickness is about 10-20 µm and the epidermis is in 100-150 µm window, MNs can fulfill their function (Fig. 7) (Ahmed Saeed AL-Japairai et al., 2020).

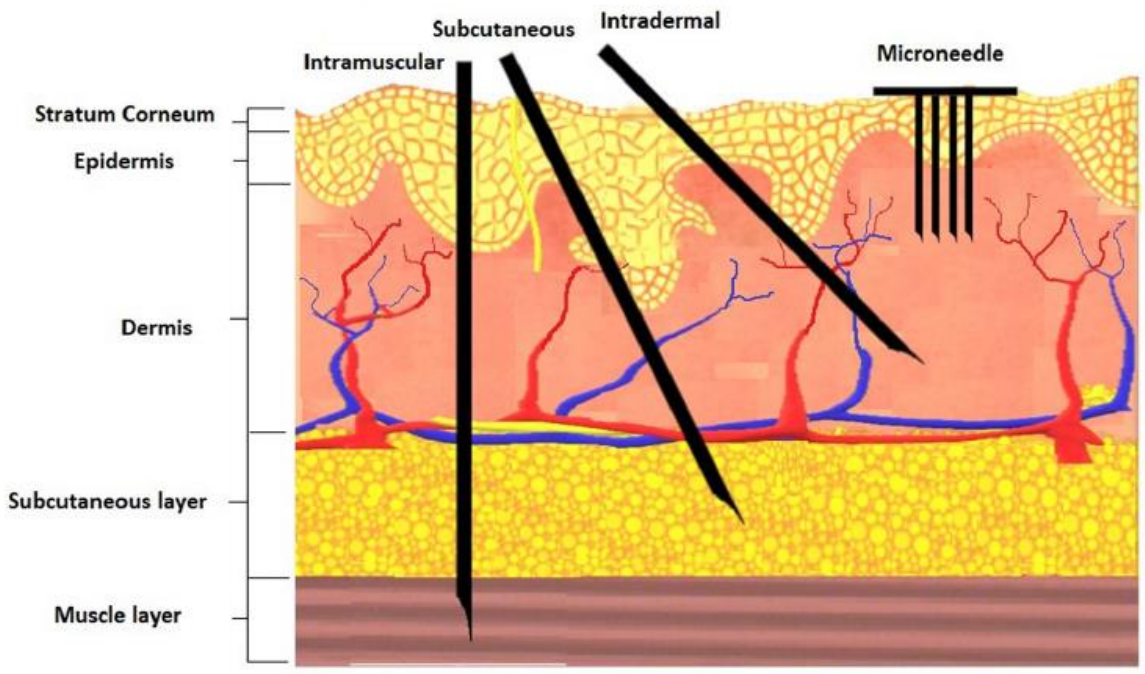

Figure 7 Comparison of microneedles with traditional injectable form of delivery (Nagarkar et al., 2020).

MNs devices have been proposed and investigated for the delivery of various molecules (Ita, 2015; Prausnitz, 2004), offering several advantages. One notable benefit is the potential to reduce anxiety in patients who may experience fear or discomfort during needle-based procedures. The discrete nature of the microneedle patch, due to its small size enhances ease of administration and reduces the need for a trained health care professional. Unconstrained delivery through a microneedle-based approach can decrease administration errors and enable patients to self-administer, improving overall convenience. Conventional hypodermic needles require careful handling and disposal to prevent the transmission of bloodborne pathogens, and despite precautions, needle stick injuries remain common. MNs represent an effective solution for the reduction or elimination (depending on the choice of MNs type) of needle-stick injuries. In addition, these devices do not generate biohazardous waste, minimizing the environmental impact of medical procedures. They also decrease the risk of microbial penetration and contamination, ensuring a higher standard of safety and hygiene compared to traditional hypodermic needles (Donnelly, Singh, et al., 2009; Sabri et al., 2019). The main characteristics of the MNs technology including painlessness, minimally invasive nature, ease of administration, ability to deliver multiple substances, and the elimination of needle-stick injuries, seriously improve patient's compliance. These advantages make MNs a promising candidate for widespread clinical translation compared to previous active methods designed to bypass SC.

2.1 Categories of MNs

MNs are categorized into five distinct types: solid, coated, dissolvable, hollow, and hydrogel-forming. The chosen category strongly influences the intended use and functionality of the MNs.

Once applied to the skin, solid MNs (Fig. 8A) create transient aqueous microchannels in the stratum corneum. A conventional drug formulation (transdermal patch, solution, cream, or gel) is then applied, resulting in an external drug reservoir. However, the two-step application process required is a limiting factor. Common materials used include silicon, metals, and polymers.

A further method involves coating solid micro-needles (Fig. 8B) with a drug formulation before application. Upon insertion of the coated MN arrays into the skin, the drug formulation is released and delivered into the skin. This method offers a simple one-step application process, but is mainly limited by the amount of drug that can be coated onto the finite surface area of the MN structures.

The third type of MNs is dissolving MNs (Fig. 8C). They are made from soluble matrices, typically biocompatible polymers or sugar, containing the active ingredient. Upon insertion into the skin, they dissolve upon contact with interstitial fluid, releasing the drug over time. The release rate of the drug is determined by the dissolution rate of the constituent polymers. Dissolving MNs differ from the other types of MNs for a series of advantages. They are made of relatively inexpensive polymeric materials and may be easily fabricated using micro-molding processes at ambient temperatures, so potentially scalable to industrial mass production. Importantly, the use of water-soluble materials leaves out the risk of biohazardous sharp waste. Conversely, their mechanical properties are not excellent due to the influence of several factors on this kind of materials, and drug stability during the fabrication process could be an issue.

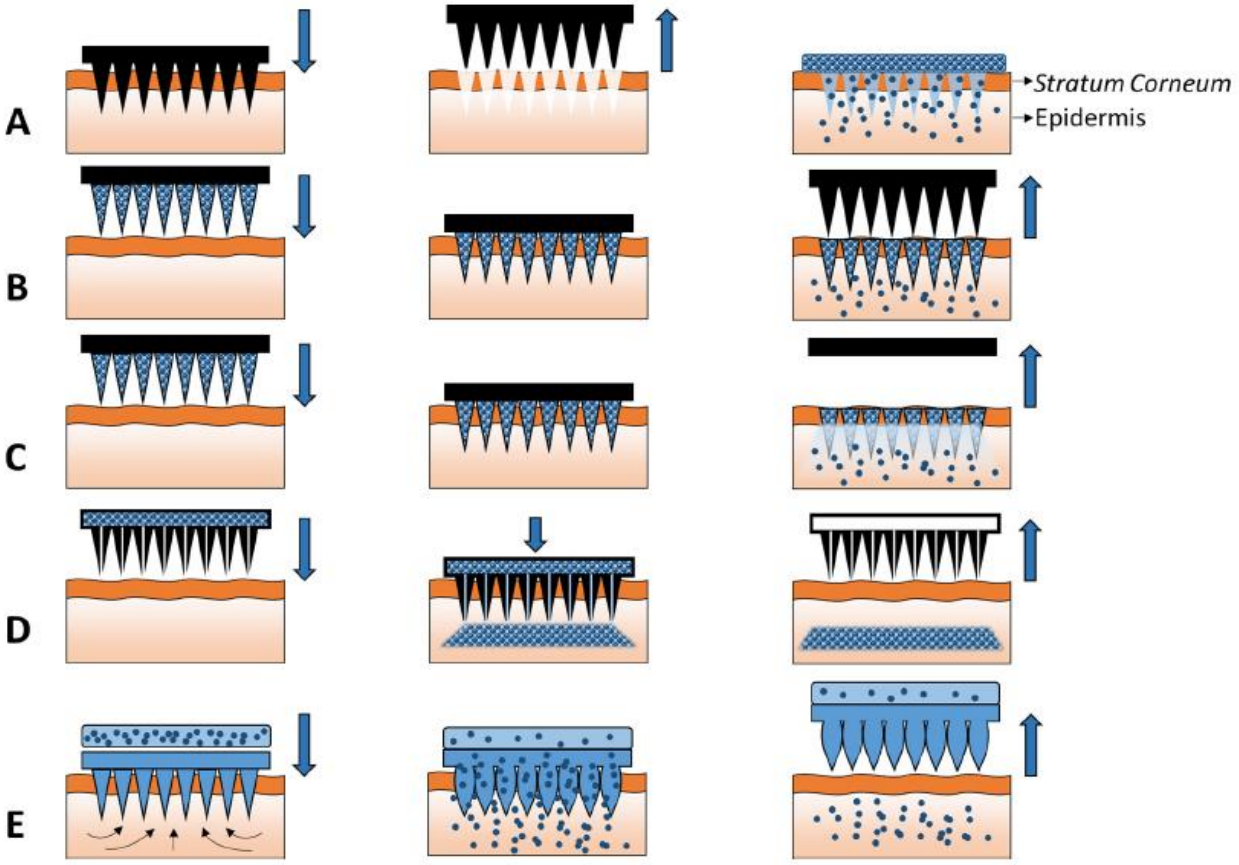

Figure 8 A schematic illustration of five different types of MNs for drug delivery(Larrañeta et al., 2016)

Hollow microneedles (MNs) (Fig. 8D) are a micron-scaled version of hypodermic needles to deliver drugs into the skin. They work by injecting a fluid formulation through the hollow needles, which allows for the continuous delivery of molecules across the skin. Hollow MNs can deliver

larger amounts of drug substances compared to solid, coated, and dissolving MNs. These MNs are made from various materials such as silicon, metal, glass, polymers, and ceramic. However, the skin insertion process could pose challenges, as needle openings may get stuck with tissue, and there could be flow resistance due to dense dermal tissue compressed around the MN tips during insertion.

A more recent type of MNs is derived from hydrogel-forming matrices (Fig. 8E). These systems consist of crosslinked drug-free polymeric MNs placed on a solid baseplate which serves drug reservoir. When the MN array is applied to the skin, the needle tips take up interstitial fluid from the tissue. This process triggers the drug to diffuse from the reservoir through the swollen MNs(Larrañeta et al., 2016).

2.2 Design of MNs

The design of MNs calls is a complex process that takes into account several parameters, with each parameter influencing the physicochemical properties of the MNs. The biomedical application strongly guides the design considerations. These factors include MNs dimensions, category, material choice, fabrication methods, cargo within the microneedle, mode of force application, sterilization, and storage stability (Le et al., 2023). Initially, the behavior and thickness of the skin exhibit intrinsic variability due to factors such as age, sex, anatomical area, race and hormonal balance. When considering the target application, dimensional aspects such as length, tip diameter and width/base diameter, geometrical arrangement (inter-spacing distance) and shape (conical, hexagonal, pyramidal), should be throughly analyzed before proceeding with the array fabrication (K. J. Lee et al., 2020). MNs structural features affect patch performance when the array is to be implanted within the skin. As mentioned earlier, the length ranges from a few microns to about 1 mm, while the base width varies between 50-300 μm. The aspect ratio typically falls within the range of 2:1-10:1. Wider MNs with smaller aspect ratios are stronger and less prone to fracture or deformation, but they can be more painful and harder to penetrate deeply into the skin. MNs tip diameter is crucial for proper skin implantation and usually ranges from 1 to 10 μm in size, ensuring sharpness for effective penetration. These needles are arranged into arrays that can range from tens to tens of thousands of microneedles. The number of microneedles in an array determines the MNs density. Higher density requires thinner and shorter needles, potentially leading to a "bed-of-nails" effect where the force is distributed among too many needles, making skin penetration

challenging. To address this, sharper needles and stronger insertion forces are required. Conversely, lower density makes skin insertion easier and allows for longer needles but reducing the amount of delivered drug. Increasing the array area accommodates more needles but may increase pain during insertion. Moreover, a larger array area makes it more challenging to insert microneedles into nonplanar and deformable skin surfaces. The overall size of the microneedle patch is typically larger than the microneedle array to make the patch easier for patients to handle (Prausnitz, 2017).

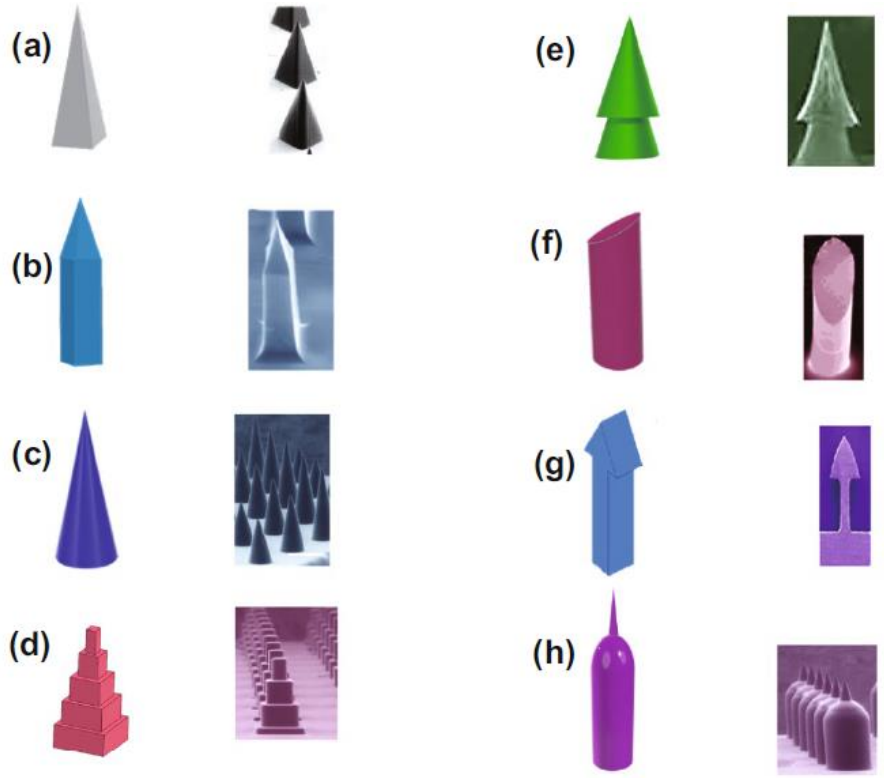

Figure 9 Different geometries of MNs (Makvandi et al., 2021)

2.3 Choice of material

There are six main types of materials used for MNs: silicon, glass, metals, ceramics, sugars, and polymers. Silicon, recognized as the earliest material for microneedle fabrication, offers substantial mechanical strength and allows for the realization of various shapes and dimensions. However, its brittle nature poses challenges, potentially leading to fractures post-penetration and the deposition of silicon residues in the skin, fostering the formation of granulomas. Moreover, its use involve considerable expenses and requires the maintenance of clean room conditions.

Glass, primarily used for the production of hollow microneedles designed for drug delivery and sampling applications, exhibits tissue penetration capabilities similar to silicon microneedles. However, manual processing makes glass microneedle fabrication a time-intensive process.

Metals, including stainless steel, titanium, palladium, palladium-cobalt alloys, and nickel, provide a cost-effective alternative for manufacturing solid, hollow, or coated microneedles. Notably, certain metals, like stainless steel, possess a long-standing clinical history, potentially expediting regulatory approval processes.

Ceramic compounds, combining metallic and non-metallic constituents such as alumina, calcium sulfate dihydrate, and zirconia, serve as viable materials for microneedle construction. Ceramic MNs offer elevated mechanical strength and resistance to high temperature and humidity, providing control over drug release kinetics through modulation of needle porosity.

Sugar emerges as an appealing resource for microneedle fabrication due to its natural origin, safety profile, and rapid dissolving attributes. Commonly used sugars include maltose, trehalose, sucrose, mannitol, xylitol, sorbitol, and galactose. Integrating sugars with various polymers enhances the mechanical strength and stability of MNs.

Polymers, favored for their flexibility, cost-effectiveness, and ease of production, are a preferred choice for generating solid, dissolving/biodegradable, and hydrogel-forming MNs. This category includes synthetic polymers and natural polymers, such as polysaccharides, carbohydrate polymers, polypeptides, and protein polymers. The metabolites of natural polymers exhibit non-toxic characteristics and can be safely eliminated from the human body. The investigation of polymers extends to dissolving/biodegradable polymers, comprising both synthetic (e.g., poly(vinyl alcohol), poly(vinyl pyrrolidone), poly(methyl vinyl ether-co-maleic acid)) and biodegradable polymers (e.g., poly(lactic acid), poly(glycolic acid), poly(lactic-co-glycolic acid)). Additionally, synthetic crosslinking polymers play a crucial role in the fabrication of hydrogel-forming MNs, primarily through covalent conjugation induced by thermal or ultraviolet (UV) reactions. The choice between thermosetting and UV curing methods imparts distinct properties to the resulting hydrogel-forming microneedles, such as varied swelling ratios and mechanical strengths. Young's modulus, characterizing a material, is also relevant for the compressive stiffness of MNs, with ceramic material having the highest Young's modulus values and polymeric ones having the lowest (Larrañeta et al., 2016; Le et al., 2023).

2.4 Dissolvable MNs

Dissolvable microneedles (DMNs) have emerged as a transformative approach in transdermal drug delivery, harnessing the potential of microfabrication technology to revolutionize topical medication application. These microneedles are ingeniously produced by encapsulating drugs within various biodegradable polymers, including dextran, albumin, chondroitin sulphate, polyvinylpyrrolidone, polyvinyl alcohol, and hyaluronic acid. Biodegradable polymers typically undergo either hydrolytic or enzymatic degradation processes, with natural polymers such as collagen and hyaluronic acid transforming into amino acids and saccharides upon degradation. Chitosan primarily undergoes degradation through lysozyme action targeting the hydrolysis of its acetylated residues. Polymers like poly-glycolide and poly-lactide, widely used as co-polymers, undergo hydration, depolymerization and subsequent hydrolysis, ultimately leading to the formation of monomers dissolvable into the intercellular fluid. In particular, the final stage of degradation involves the conversion of L-lactate into carbon dioxide (CO_2) and pyruvate, facilitating major elimination via respiration and minor elimination through excretion in urine and feces. DMNs offers a 'poke and release' mechanism, where MNs dissolve upon penetrating SC, releasing the entrapped medication. This one-step application process eliminates the need for removal post-application, significantly reducing the risk of needle-stick injuries associated with conventional solid microneedles (Dalvi et alsu., 2021; Sartawi et al., 2022).

Research in this domain has been prolific, showcasing various advancements. For instance, Sullivan et al. introduced rapidly dissolving polymer microneedles, demonstrating how to produce robust dissolvable microneedles for the delivery of biomolecules at room temperature (Sullivan et al., 2008). Huang et al. developed novel DMNs using photo-cross-linkable dextran methacrylate (DexMA) for sustained transdermal administration of drugs like Doxorubicin and Trametinib, exhibiting excellent mechanical strength and biological safety (Huang et al., 2020). Zhang et al. researched the safety of polyvinyl alcohol (PVA)-based MNs, confirming their biocompatibility and safety of these materials (X. P. Zhang et al., 2021) through extensive trials on mice. Advancements also include bioresponsive DMNs, such as hyaluronic acid-based MNs developed by Wang et al., integrated with pH-sensitive dextran nanoparticles for targeted treatment like in the case ofmelanoma (C. Wang et al., 2016). Similarly, Yu et al. introduced a groundbreaking glucose-responsive MN patch, loaded with insulin, demonstrating the potential of DMNs in managing diabetes in insulin-deficient animal subjects (Yu et al., 2020). Collectively, these

advancements highlight the vast potential of DMNs in enhancing drug delivery efficacy, ensuring patient safety and comfort. The biodegradability of the polymers used underscores their environmental friendliness, breaking down into harmless by-products post-application. This aspect is crucial, considering the rising concerns about medical waste and environmental impact. The versatility in material choice and innovative design positions DMNs as a promising tool in non-invasive therapeutic delivery, with implications for the treatment of a myriad of health conditions. In the subsequent sections, a list of DMNs a step away from entering the market will be presented.

2.5 Fabrication methods of DMNs

The fabrication of DMNs has evolved to include a diverse array of techniques, each tailored to optimize drug encapsulation and release efficacy. The micromoulding method, especially solvent casting, is a traditional technique involving the realization of negative molds from positive masters of MNs made from materials such as silicon, metal, and polymers. Common methods used for fabricating positive masters include photolithography, etching and two photons polymerization (Larrañeta et al., 2016). These positive masters are then used to replicate microneedle structures in polydimethylsiloxane (PDMS), realizing the negative version of the starting positive master. The solvent casting process (Fig. 10) involves pouring a polymer solution mixed with the active substance into the PDMS mold, followed by solvent evaporation by vacuum/centrifugation, leaving behind a solid microneedle array. While solvent casting is advantageous for its simplicity and low-cost, it can lead to drugs being primarily confined to the baseplate, limiting their release from the needles (Andranilla et al., 2023).

To address these challenges, advanced methods such as the two-step casting method, droplet-born air-blowing (DAB), centrifugal lithography (CL), photopolymerization, and drawing lithography have been developed. The two-step method (Fig. 11) involves realizing a master mold to produce a reusable PDMS or silicone mold, . injecting the drug-polymer mixture into the mold, allowing it to cure, and then adding a blank polymeric solution to have the medication only in the needles. This method offers more precise control over drug distribution within the microneedles, potentially improving drug release efficiency. DAB and CL, both droplet-based techniques, solidify droplets of drug-polymer mixture into microneedle shapes using air blowing or centrifugal force, respectively. These methods allow fine-tuning of drug content in the microneedles while maintaining mechanical integrity and drug stability. Photopolymerization method involves room-

temperature photopolymerization of liquid monomers within microneedle molds, allowing the encapsulation of heat-labile chemicals. However, it requires careful control of UV light exposure to preserve the stability of the encapsulated drugs. Finally, drawing lithography is a mold-free technique that relies on the glass transition temperature of the polymer, enabling precise control of microneedle length by mechanically pulling the polymer(L. Zhang et al., 2021).

These methodologies collectively represent the cutting-edge of DMN fabrication, addressing specific challenges such as structural integrity, drug stability, and release profiles. The choice of method depends on the drug's nature and the desired release characteristics, making DMN fabrication a dynamic and rapidly evolving research area. Innovations in these techniques hold immense potential for enhancing the efficacy and applicability of transdermal drug delivery systems, paving the way for more effective treatments across a variety of medical conditions.

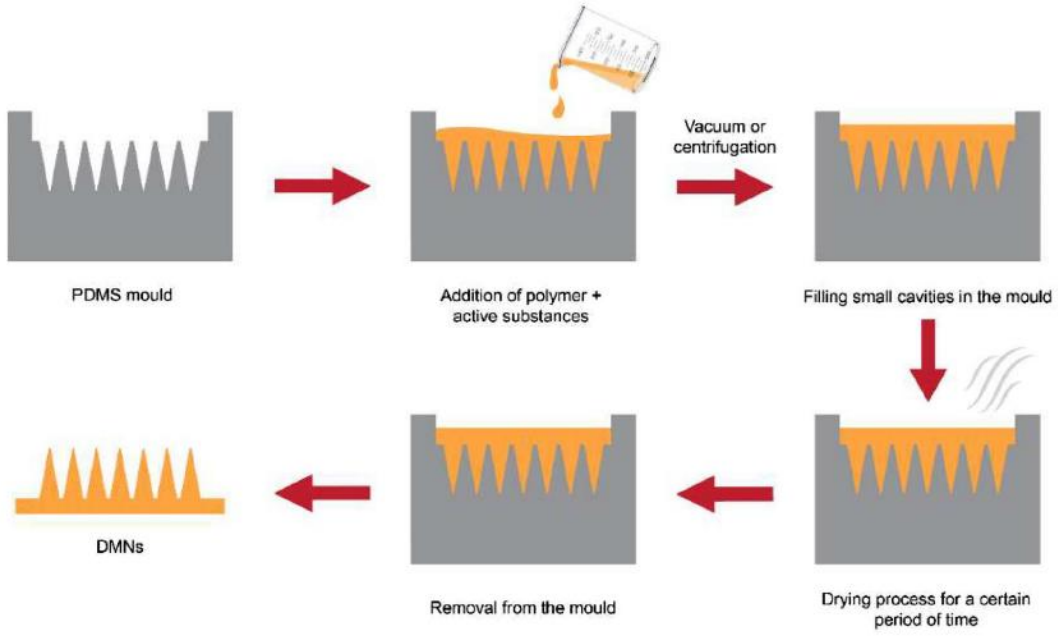

Figure 10 Illustration of one-step solvent casting(Andranilla et al., 2023)

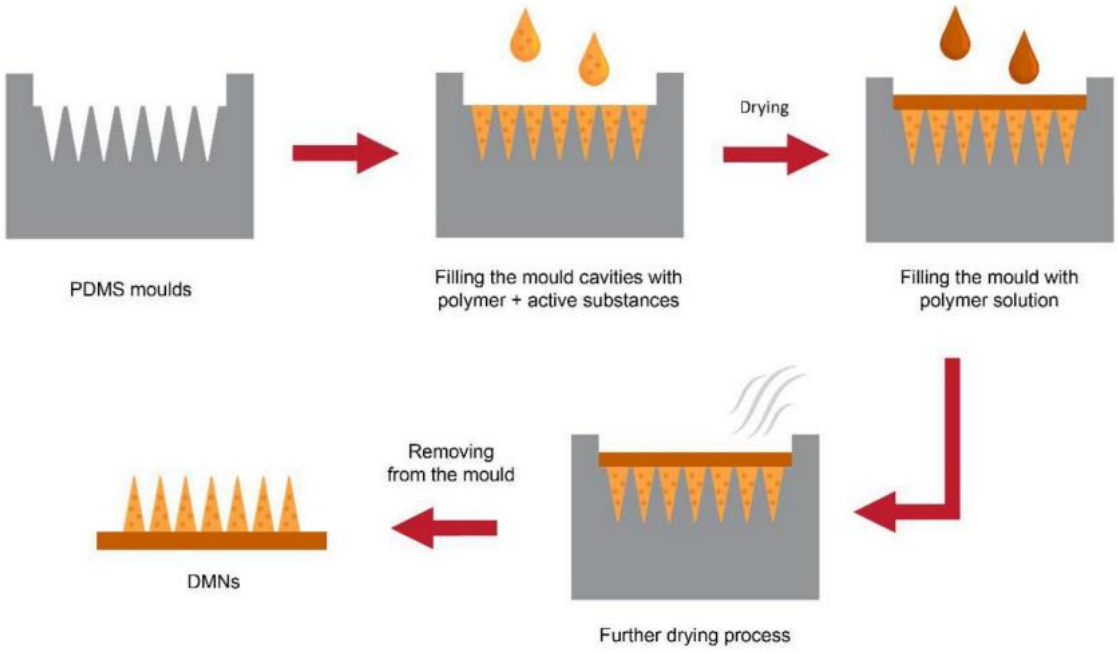

Figure 11 Illustration of two-step solvent casting (Andranilla et al., 2023)

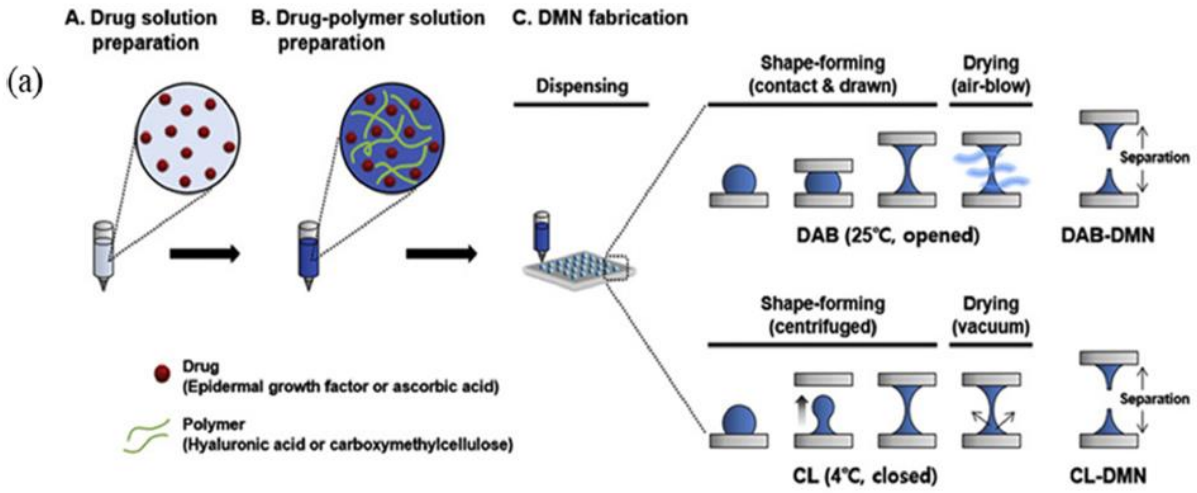

Figure 12 The different operating steps between the droplet-born airblowing (DAB) and the centrifugal lithography (CL) (L. Zhang et al., 2021)

2.6 Limits of DMNs

Drug loading is actually a challenge in MNs field, especially for DMNs (Bauleth-Ramos et al., 2023). The key challenges in this area fall into several categories:

- **Limited Loading Capacity**: The small size and volume of MNs tips result in a very limited loading capacity, typically less than 1 mg and rarely up to 10 mg per patch. This limitation

poses a challenge for drugs requiring higher dosages (Amani et al., 2021; Prausnitz, 2017; Yao et al., 2017).

- **Difficulties in Drug Encapsulation and Localization**: Many drugs can diffuse through the water-soluble MN matrix (Fig. 13), making it challenging to control their encapsulation and localization within the MNs, leading to potential drug loss (Chu et al., 2010; Q. Wang et al., 2015).
- **Restrictions on Co-Encapsulation of Different Drugs**: MNs are usually made from a single material, limiting the opportunity for the co-encapsulation of different drugs based on drug-matrix interactions (Q. L. Wang et al., 2016; P. Yang et al., 2020).
- **Impact of Fabrication Conditions on Drug Stability**: The preparation and manipulation of MNs, including the use of solvents, moisture levels, temperatures, and pressures, can degrade the payload or affect mechanical properties. (Cheng et al., 2022a; Q. L. Wang et al., 2018a)(Chu et al., 2016; Donnelly, Morrow, et al., 2009; Mistilis et al., 2015; Sabri et al., 2020).
- **Skin inherent elasticity**: The microstructural makeup of skin tissue results in a highly nonlinear mechanical response. The inherent elasticity of the skin poses a challenge to the total implantation of the needle (Fig. 14). Achieving reproducible penetration of the skin is crucial, as incomplete implantation can lead to drug loss. This limitation applies to all categories of microneedles being due to the skin behavior (Joodaki & Panzer, 2018; J. Kim et al., 2018; Römgens et al., 2014).

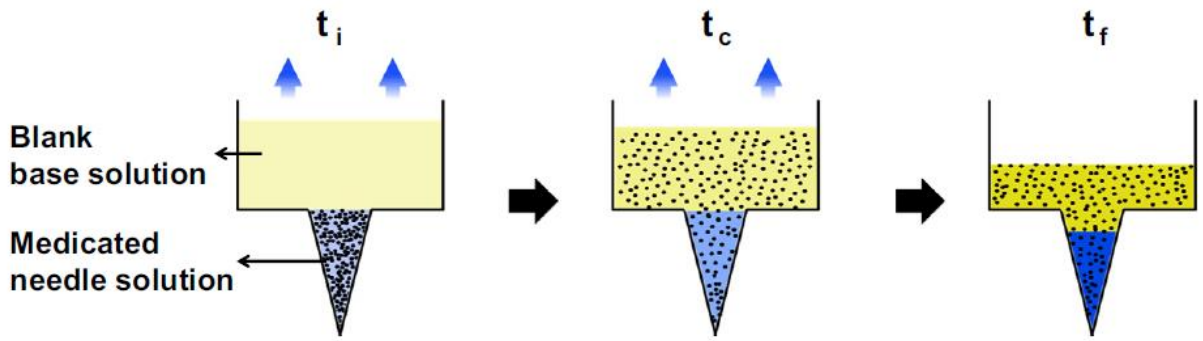

Figure 13 Drug diffusion towards upper baseplate during fabrication of DMNs(Q. Wang et al., 2015)

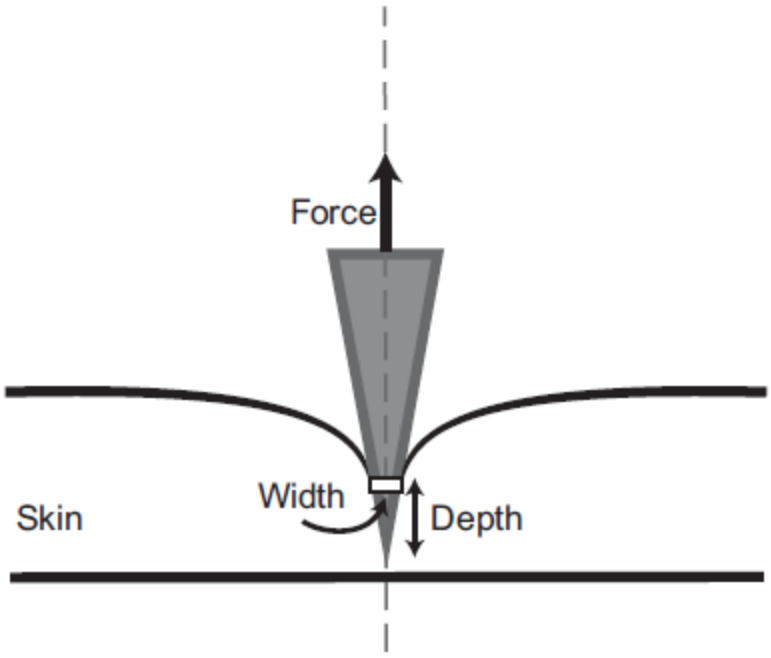

Figure 14 Illustration of incomplete penetration within the skin (Römgens et al., 2014).

It is possible to deduce at this juncture how the combination of the active ingredient to deliver (due to its stability and features), the chosen material, the fabrication method and the conditions which all of them undergo, affects the DMNs properties and the loading capacity.

2.7 DMNs for sustained release

As previously said, DMNs are traditionally manufactured using hydrophilic polymers like hyaluronic acid (HA), polyvinylpyrrolidone (PVP), gelatin, starch, or various sugars. This composition generally results in a rapid release phenomenon, characterized by the rapid dissolution of the polymeric structure of the MNs within seconds to minutes. The "release mechanism" concept refers to the specific processes through which active agents are dispensed from a carrier into the external environment. Comprehending these mechanisms is crucial for the precise control and optimization of biotherapeutic delivery tailored to specific sites and requirements (Jamaledin et al., 2020). In certain applications, such as vaccines or insulin therapy, there is a preference for a sustained release profile to minimize side effects, reduce the frequency of MN administrations, and enhance therapeutic effectiveness. Unlike conventional DMNs that rapidly dissolve and release their cargo upon insertion, sustained release MNs are designed to retain the drug within the

matrix, gradually dispensing the active substances in a controlled manner. This release is governed by the dissolution or degradation characteristics of the polymer matrix (Du & Sun, 2020). The prevalent strategies to modulate the release rate in dissolving MNs encompass four primary methodologies: employing polymers with slower dissolution rate, incorporating micro/nano-particles, utilizing hydrophobic polymers, or cross-linking hydrophilic polymers. These approaches collectively contribute to the controlled and prolonged release of the therapeutic agents from the MNs (Bauleth-Ramos et al., 2023).

In the context of this specific category of DMNS, this PhD thesis work builds upon the multicompartmental concept of dissolvable microneedle (Fig. 15) proposed in previous research (Battisti et al., 2019). This unique design overcomes typical drawbacks in this domain related to improper tunable kinetics (S. C. Park et al., 2019) or time consuming processes (Demuth et al., 2013). Multicompartmental MNs method was developed to realize microparticle-loaded microneedles basically. A stamp-based method was established to come up with polymer dissolvable microneedles presenting a huge empty cavity to be loaded with PLGA microparticles (μPs). First, the stamp cavities were spin-coated with a hydrophilic polymer, PVP, to obtain the fast-dissolvable tips (Vecchione et al., 2016), then the cavities were filled with porous PLGA μPs and assembled using a mild-softening method (De Alteriis et al., 2015), forming the body of the microneedle, which provides the prolonged release of the cargo. Consequently, it is feasible to engineer multi-compartmental microneedles with adjustable drug release characteristics. This design combines the rapid release properties of the needle tip with the extended release of the payload from the μPs, facilitating the potential co-delivery of two distinct molecular ingredients. Notably, this entire fabrication process occurs at room temperature, accommodating the encapsulation of thermolabile (thermo-sensitive) molecules without compromising their structural integrity or functional efficacy.

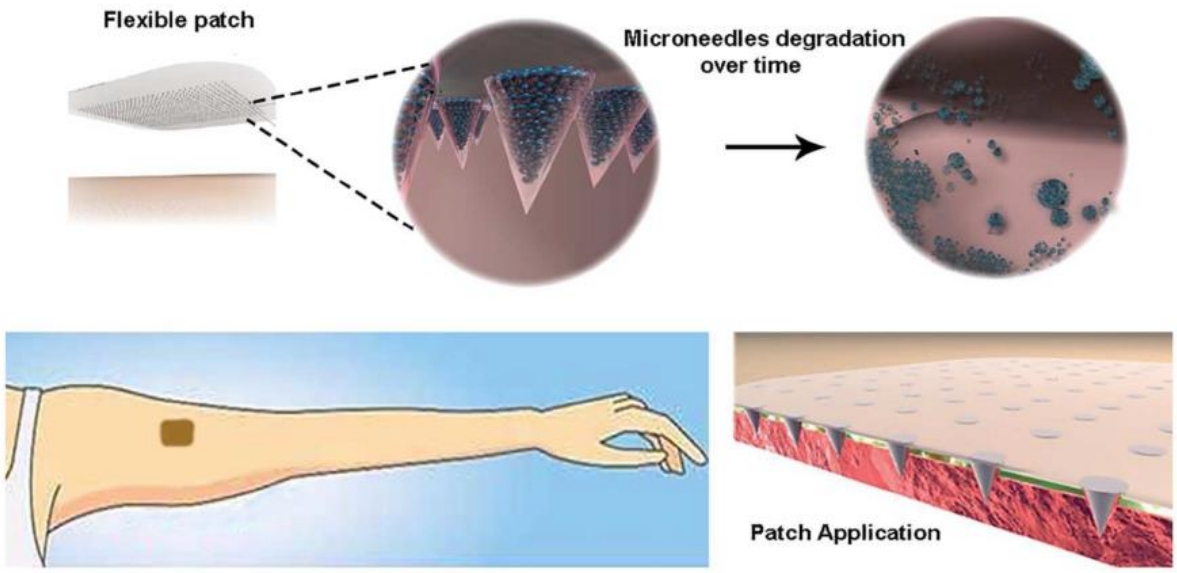

Figure 15 Highly controlled intradermal delivery can be performed with multi-compartmental polymer microneedles that are able to indent the skin and be implanted in it with a fast dissolving tip and a slow degradable body made of porous PLGA μPs (Battisti et al., 2019).

This PhD thesis was carried out to: i) improve the formulation and the fabrication process allowing more reproducible results; ii) investigate the versatility of the multicompartmental platform in different scenarios, even explored in the nascent stage of development for mRNA delivery.

2.8 Applications of DMNs for mRNA delivery

Microneedles have emerged as a focal point of research across a diverse pool of therapeutic domains, extending beyond conventional applications. In recent years, there has been a growing interest in deploying this technology into novel potential areas, particularly in immunotherapy and the management of severe chronic diseases. Microneedle-mediated delivery targets the dermis, a skin layer rich in blood and lymphatic vessels, facilitating access to the skin's extensive immune network (Fig. 16). The use of microneedles to administer agents such as vaccines and anticancer drugs into the dermal lymphatics offers significant clinical advantages. The MN dimensions enable the drug delivery system to easily and painlessly penetrate the immune network. Traditional vaccination methods, involving intramuscular and subcutaneous injections, are performed in areas with a relatively low concentration of antigen-presenting cells, essential for vaccine detection. Consequently, to elicit an adequate immune response in patients, higher vaccine dosages are typically required (Sabri et al., 2020). The skin's lymphatic drainage, providing direct access to lymph nodes, positions cutaneous delivery as a highly preferred vaccine administration route.

Furthermore, the skin is abundant in immune cells, both in terms of quantity and diversity. Notably, the skin's T cell count is double that of those circulating in the bloodstream, emphasizing the critical role of dermal lymphatics in the immune system. The dermal lymphatics are frequently characterized as skin-associated lymphoid tissue, owing to their high concentration of immune cells, including dermal dendritic cells, T cells, and macrophages (Nestle et al., 2009).

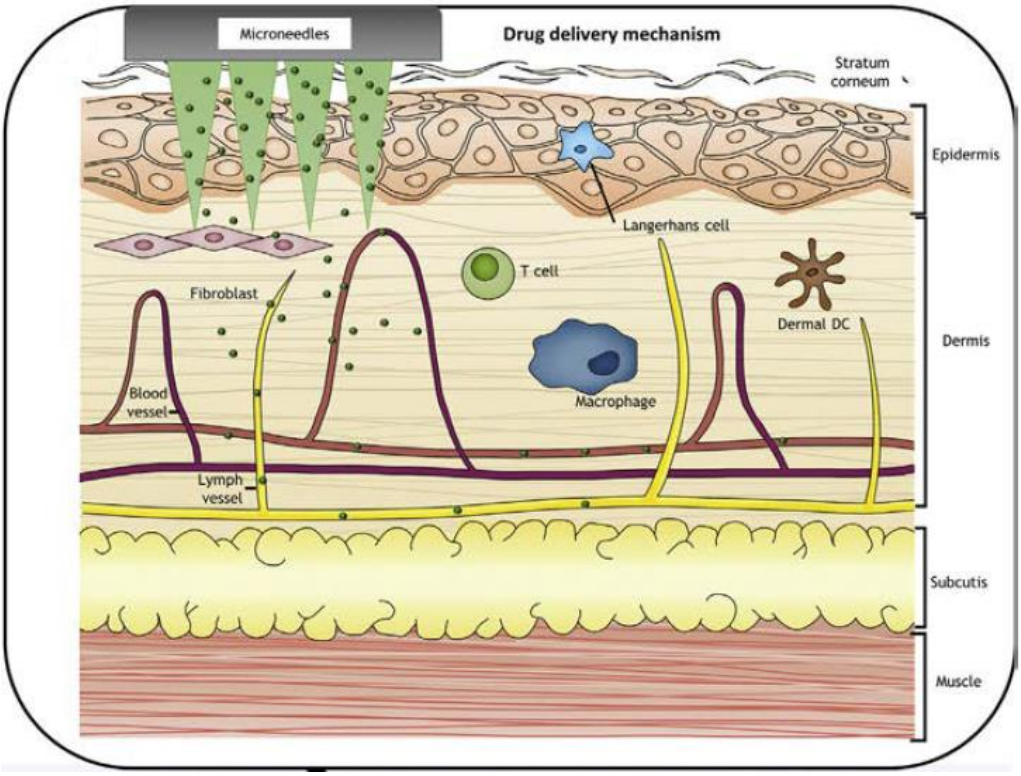

Figure 16 The dermis is rich in blood and lymph vessels and the drug released by MNs in this layer will readily have exposure to various types of immune cells (Sabri et al., 2020).

In the context of stability assessment, the stability of inactivated influenza vaccine encapsulated within dissolving microneedle patches was examined through the microneedle fabrication process and prolonged storage periods. The findings suggest that the enhanced thermostability of the influenza vaccine in dissolving microneedle patches has the potential to improve influenza vaccination practices. This improvement could be realized by reducing dependence on cold chain logistics, eliminating streamlining vaccine distribution (Chu et al., 2016).

In response to the recent COVID-19 pandemic, nucleic acid-based vaccines, such as DNA and mRNA vaccines, have proven safe and effective treatment options with rapid responses to emerging infectious diseases. Nucleic acid-based vaccines offer a rapid and effective approach

against infectious diseases and potentially for cancer treatments, surpassing conventional vaccine methods (Noh et al., 2022). mRNA vaccine technology, blending molecular biology with immunology, stimulates an immune response for antibody production. Similar to gene therapy, this method involves using foreign mRNA to instruct somatic cells to produce specific antigens (Y. Wang et al., 2021). One of the principal benefits of mRNA vaccines, within the broader category of nucleic acid vaccines, is their safety profile, reducing risks of infection and endotoxin exposure associated with pathogen-based therapies. These vaccines operate in the cytoplasm, are suitable for non-dividing cells, and importantly, do not integrate into the host genome, avoiding the risk of insertional mutagenesis. Furthermore, the direct delivery of mRNA eliminates issues related to protein manufacturing, such as denaturation or aggregation. The production of mRNA vaccines is streamlined through in vitro transcription in a cell-free environment, making the process efficient, cost-effective, and scalable. This methodology eliminates the need for microorganisms or cell cultures, facilitating rapid and efficient purification. Despite these benefits, challenges such as mRNA instability, high immunogenicity, and delivery difficulties with success rate of less than 1 in 10 000 molecules in naked state (Qin et al., 2021), initially slowed down research into mRNA therapy. mRNA's susceptibility to nuclease degradation and its ability to trigger an innate immune response limited its expression. The hydrophilic nature and negative charge of mRNA impeded its passage through cell membranes. Successful mRNA-based therapy requires a specialized delivery vehicle, leading to extensive research into tehe impact of the physical features and engineering of nanomaterials for effective carrier development (D. Lee et al., 2023a).

Concurrently, MN-based delivery systems have been studied for nucleic acid delivery. Yang et al. synthesized nanoparticles made of poly(lactic-co-glycolic acid)-poly-L-lysine/γ-polyglutamic acid (PLGA-PLL/γPGA). These nanoparticles were designed for biocompatibility and biodegradability, featuring a positively charged surface suitable for binding EboDNA. This design enables the controlled release of EboDNA, optimizing it for cell transfection over an appropriate timescale. EboDNA-loaded PLGA-PLL/γPGA nanoparticles were incorporated into microneedles patches (Fig. 18B), and then *in vivo* tests revealed robust immune responses post-immunization. The findings of this study point out how nanoparticle-based technology, in conjunction with MNs patches, may address the demand for Ebola vaccination (H. W. Yang et al., 2017). On the other hand, Koh et al. conducted a proof of concept study on the fabrication, characterization, and

therapeutic evaluation of in *vivo* transcribed mRNA loaded in a dissolving microneedle patch. Successful transfection of luciferase mRNA was achieved in the dissolution domain of PVP microneedles in a murine model (Fig. 17,18A). This makes microneedle-based technology viable for mRNA delivery (Koh et al., 2018). As matter of fact, more recently You et al. demonstrated the intradermal delivery of mRNA-loaded extracellular vesicles (EVs) using DMNs for the treatment of photoaged skin. mRNA EVs were firstly conceived, manufactured and then mixed in a hyaluronic acid solution. The fabrication process was based on micromolding. DMNs (Fig. 18C) were implanted in a mouse model, achieving an optimal distribution of COL1A1 mRNA-loaded EVs in in the dermis, resulting in durable collagen-protein engraftment and an improved treatment of wrinkles in photoaged skin (You et al., 2023).

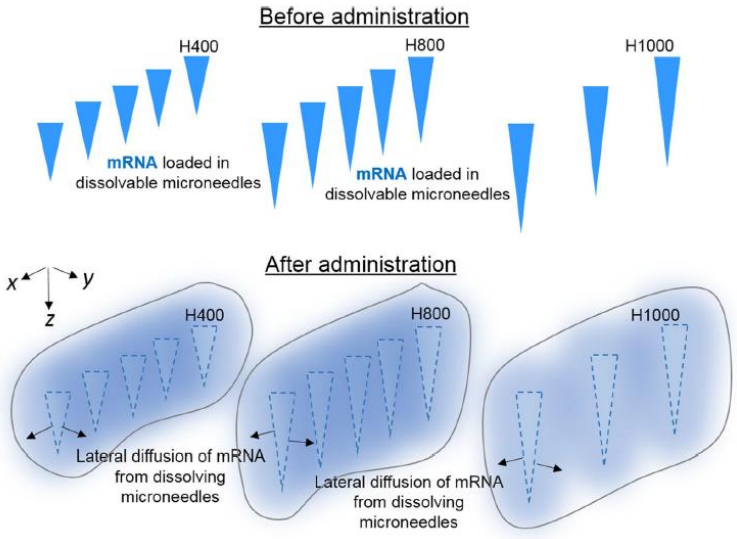

Figure 17 Illustration of lateral mRNA (blue) distribution from dissolving polymeric microneedles (H400, H800 and H1000 state for different geometrical features). The blue regions (within grey outlines) around the faded triangles denote mRNA distribution from dissolving polymeric microneedles (faded triangles) that correlated transfection efficiency data (Koh et al., 2018).

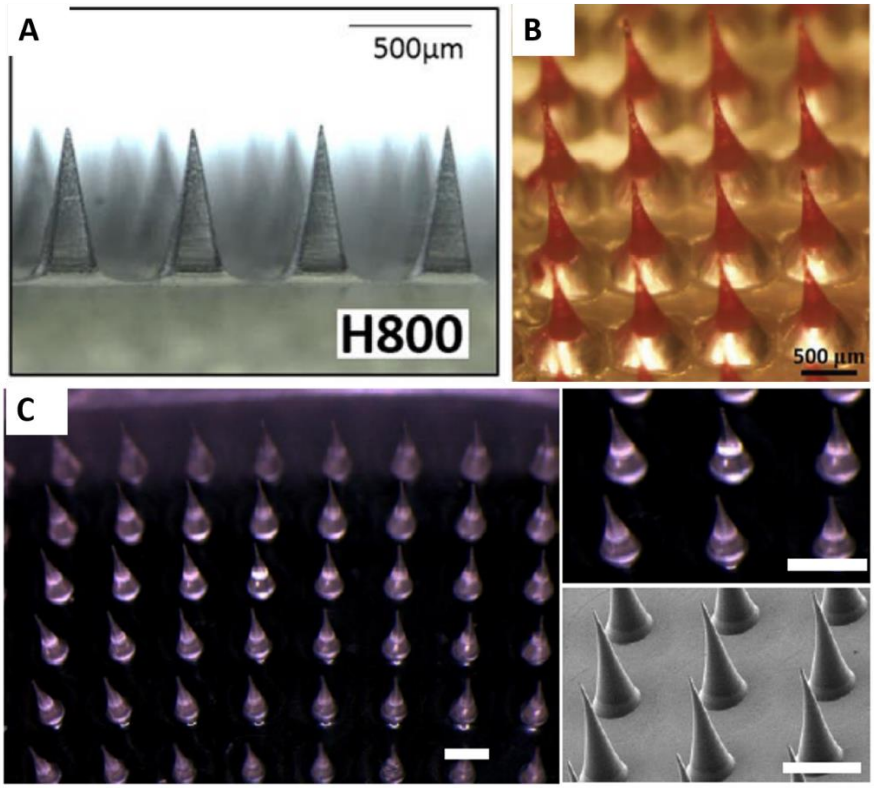

Figure 18 Example of MNs patches. Naked mRNA-loaded PVP MNs patch (A) (Koh et al., 2018). *PLGA-PLL/γPGA nanoparticles-loaded MNs patch for Ebola treatment (B)* (H. W. Yang et al., 2017). *COL1A1 mRNA EVs-loaded MNs patch. Scalebar 500 µm (C)* (You et al., 2023)

2.9 How can MNs rise above challenges facing transdermal drug delivery?

In addition to the typical limitations affecting dissolvable microneedles, as discussed in previous sections, other concerns must be addressed to successfully reach the commercialization of a MN-based product (Donnelly, 2017). Firstly, it is crucial to revisit and comprehensively understand the phenomena of rapid dermal recuperation and the sealing of the microchannels created by microneedles- a process taking a temporal frame of 4 to 24 hours (Gualeni et al., 2018). A profound grasp of the ADME (Absorption, Distribution, Metabolism, and Excretion) profile of any substances encapsulated within these systems is imperative. The focus should be on the duration required for the active compounds to attain peak plasma concentrations. This factor not only indicates the absorptive efficacy achievable via the microneedle matrix but also highlights the localized action potential of the pharmacological agent, a crucial aspect in certain therapeutic contexts (Sartawi et al., 2022).

Furthermore, the trajectory toward clinical implementation of microneedle-based delivery systems encounters multiple limiting factors, including financial implications associated with the active ingredients, excipients, manufacturing process, sterilization procedures, and storage conditions. These elements collectively exert a considerable influence on the temporal and resource investment during the research and development phase. It is noteworthy that the fabrication of microneedles often presents greater complexity compared to conventional dosage forms, such as topical, oral, or injectable preparations. This complexity is inherently tied to the distinctive characteristics of these products, yet it is the sophistication of the structural parameters essential for efficacious drug delivery that introduces a considerable risk for manufacturers aspiring to escalate production to commercially viable batch sizes compliant with current good manufacturing practices. Large-scale manufacturing is mandatory to yield microneedles that can compete with existing hypodermic methods.

Moreover, the regulatory landscape for microneedles remains in a state of flux, with several commercial impediments yet to be clarified. In the context of the United States, governed by the Food and Drug Administration's Code of Federal Regulations (Title 21/ Chapter 1/Sub-chapter A/Part 3/Sub-part A/3.2), dissolvable microneedles are likely to be categorized as a drug/device combination product. Conversely, within the European Union framework, specifically under Directive 2001/83/EC or Regulation No 726/2004, they would presumably be classified as medicinal products. Consequently, development efforts must be aligned with the stringent regulatory framework governing drug development. The evolution of microneedle platforms, as with any drug delivery system, encounters a significant financial bottleneck during the non-clinical stage. The capacity of any microneedle prototype to successfully navigate the evolving regulatory landscape constitutes a formidable barrier to commercialization. Manufacturers invested in the microneedle technology and its scale-up await the establishment of guidelines pertinent to pharmacopeial standards and recognized quality control measures. Additionally, specific regulatory directives pertaining to patient use, encompassing aspects such as sterility, packaging, ease of use, assurance of correct application, disposal, and safety considerations, are essential (Avcil & Çelik, 2021; Dalvi et al., 2021; Sartawi et al., 2022; Yadav et al., 2021).

Based on this awareness, currently, no intradermal microneedle array-based drug delivery product has been marketed (Sartawi et al., 2022). However, the market for microneedles is forecast to continue to grow at a compound annual growth rate of 7.1% through to 2027 (Economidou &

Douroumis, 2021). In fact, several microneedle array-based drug delivery products are currently in advanced stages of development (Fig.) (Sartawi et al., 2022).

Device name	Developer name/ Clinical Phase	length	Type of treatment	Image/Diagram
Dissolvable Microneedle Chip[a]	BioSerenTach Phase I	500 μm	Small molecule drugs, vaccine antigens, insulin, erythropoietin, interferon, growth hormone	
MicroCor®[b]	Corium international Phase 2a	200 μm	Osteoporosis	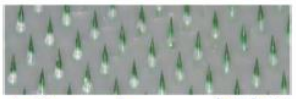
Peel & stick[c]	Georgia Institute of Technology & Micron Biomedical Phase 1/2	Not mentioned	Small molecule drugs, vaccine	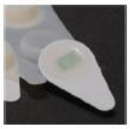
Un-Named[d]	FUJIFILM Pharmaceuticals, Unclear	100–2000 μm	Influenza virus	
Un-Named microneedle patches[e]	Innoture Medical Technology, Preclinical		3D precision printing.	
Micro Array Patch (MAP)[f]	LTS Lohamann, Unclear	200–1000 μm	Small molecule drugs, biologics, and vaccines	
SkinJect™ patch[g,h]	SkinJect, Inc. & University of Pittsburgh, Phase1/2	<1000 μm	Non-melanoma skin cancer, basal cell, and squamous cell carcinoma	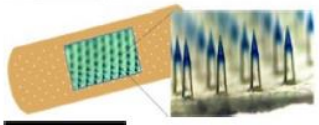
Microneedle Array "Patch Vaccine"[i]	MEDRx INDA application		Large molecule drugs and vaccines	
DrugMAT and VaxMAT[j]	TheraJect, Unclear	500 μm	Small molecule drugs and vaccines	
MIMIX[k]	Vaxess Technologies, Phase 1		Small molecule drugs and vaccines	

Figure 5 List of DMNs products in an advanced stage of development (Sartawi et al., 2022)

3 Aim of the study

Transdermal drug delivery has been a reliable administration route for humankind. Even in ancient civilizations such as Egyptian and Babylonian, it was common to apply salves, plants, and animal extract patches through the skin. It plays an important role in skipping the drawbacks paired with oral and parenteral administration routes. Relying on the ample surface offered by the skin tissue, it has always been perceived with theoretic easiness and self-administration in the assumption of a drug. This is correct when a lotion or a cream is applied to the skin to promote the passage of an ingredient. Cutaneous permeation absorption only occurs for a precise category of substances due to the properties of the skin.

The skin is the largest tissue of the human body, covering an area of about 2 square meters, and serves distinct purposes. An initial subdivision looks at the skin as the overlaying of the epidermis, the dermis, and the hypodermis, from the outer to the inner of the body. The stratum corneum (SC) represents the outer layer of the epidermis and its architecture makes the skin behave as a barrier from the external agents. Due to SC features, only a limited amount of drugs can cross the intact skin leveraging the permeation absorption and they are typically included in creams.

Several strategies have been explored to alter SC characteristics and enable the enhancement of transdermal drug delivery. They belong to two different classifications: passive and active methods. The passive methods encompass chemical enhancers to alter the drug's permeability, but they have raised concerns regarding safety and health. Other sophisticated mechanisms have been exploited, such as miciroemulsions, nanostructured lipid carriers, invasomes, liposomes, ecc, but most of them are under investigation. Active methods are utilized to transport drugs across the skin by exploiting external energy as a driving force or by physically disrupting the stratum corneum. The active methods include ultrasound, electrically assisted techniques (such as electroporation and iontophoresis), velocity-based devices (like powder injection and jet injectors), thermal approaches (such as lasers and radio-frequency heating), and mechanical methodologies such as microneedles. Innovation in drug delivery systems is a key strategy employed to improve the bioavailability of active pharmaceutical ingredients and microneedle-based technology, among the active techniques, is the unique candidate for potentially ensuring a balance in terms of patient compliance, safety, cost-benefits, and effectiveness of the treatment, that is the accommodation of all the patient’s needs.

Microneedles are the micron-scaled version of the hypodermic needles, conceptually. They allow to pierce the SC and create micro-channels for the drugs transition. Owing to their characteristics, nerve endings are not reached, and so representing a painless technology prepared for self-administration as well. Moreover, qualified personnel, wastage, needle-stick injuries and needle phobia do not constitute a concern. This kind of device is subdivided into 5 distinct categories: solid, coated, dissolvable, hollow and hydrogel-forming.

Dissolvable microneedles (DMNs) are made of payload-included biodegradable polymers. They release the cargo over time, depending on the release kinetic of the chosen polymer, once in contact with the skin interstitial fluid. Depending on the application, such as in the cases of vaccines or insulin therapy, there is a preference for a sustained release profile. DMNs for sustained release are supposed to not provide the active ingredient following a logic of a burst profile, but in a controlled manner to arrive at the desired steady state. Among the main limits of DMNs, restricted loading capacity, difficulty in encapsulation and co-encapsulation pose more than one challenge to overcome. This PhD thesis work accepts the inheritance of the multicompartmental concept of microparticle-based microneedle and was carried out to move forward toward the clinical translation of this particular design.

Microparticle-based Microneedle assume an innovative role to conjugate in a precise manner the ability to tune release kinetics to the application of interest by taking advantage of microneedle platform. They are microneedles capable of hosting porous microparticles ready to be delivered intradermally. In order to proceed toward the establishment of this platform, the fabrication process needed to be set up from top to bottom. Additionally, considering that the skin inherent elasticity is an opposing factor for a proper implantation of microneedles in general, improvements were achieved to better reproducibly a complete implantation of microneedles within the skin. This tool was examined and characterized by using a broad sphere of techniques and a mechanical setup was put in place to analyze the implantation abilities. Then, microparticle-based microneedle patch was explored in different scenarios to investigate the versatility and adaptability of this tool.

In response to the recent COVID-19 pandemic, nucleic acid-based vaccines such as DNA and mRNA vaccines have demonstrated their efficacy as safe and effective treatment options with a rapid response to emerging infectious diseases. The skin's lymphatic drainage, providing direct access to lymph nodes, positions cutaneous delivery as a highly preferred vaccine administration

route. The utilization of microneedles to administer agents like vaccines and anticancer drugs into the dermal lymphatics offers significant clinical advantages, considering that the microneedles target is precisely the dermis. The microparticle-based microneedle vehicle is under investigation for mRNA delivery, and promising results at this early stage encourage to persist in this direction.

4 Experimental section: Materials and methods

Materials

Polyvinylpyrrolidone (PVP 856568 Mw 55 kDa), hydroxyethyl cellulose (HEC 09368), Dimethyl Carbonate (DMC, D152927), as solvent of the PLGA, Sulpho Rhodamine (SulphoRh6G, S470899) were purchased by Sigma Aldrich. Hyaluronic acid (HA 200 kDa) was kindly provided by Fidia Farmaceutici. Poly (dimethyl-siloxane) (PDMS), used as flexible support, was provided by Sylgard® (184 Silicone Elastomer Kit, Dow Corning). Poly (lactic-co-glycolic acid) 50:50 (PLGA RESOMER® RG 504H), 38000 -54000 Dalton, was purchased by Boeringer Ingelheim and used as received. Polymethyl Methacrylate (PMMA) was purchased by Prodotti Gianni s.r.l.

PDMS

Polydimethylsiloxane (PDMS), a significant member of the silicone family, represents a versatile class of polymeric compounds renowned for their extensive commercial and industrial applications. PDMS-based polymers demonstrate remarkable diversity in their utility, spanning sectors such as optoelectronics, medical and cosmetic industries, surfactants, industrial cleaning agents, soft lithography, and encapsulation of biomaterials. This family of polymers exhibits a range of common properties, while PDMS specifically possesses certain distinctive characteristics. The mechanical attributes of these polymers are influenced by their molecular architecture, which may include linear, cross-chains, or cross-linked structures. PDMS is notable for its highly cross-linked nature, forming a single super-molecule in a given container.

PDMS is unique for its silicon-oxygen backbone, diverging from the more typical carbon backbone found in other polymers. This structure results in a lower glass transition temperature of -125°C, rendering PDMS less temperature-sensitive compared to other rubber-like polymers. Its remarkable flexibility and biological stability make it an ideal material for sensitive medical equipment, including catheters, drainage tubing, and pacemaker insulation, as well as various prostheses like finger joints and heart valves.

Commercially, PDMS is known under several names, including Siloxanes, Silicone fluids, Dimethicone, and E900. It is produced through a reaction between elemental silicon and methyl chloride (CH_3Cl), leading to the formation of dimethyl dichlorosilane ($Si(CH_3)2Cl_2$). This compound, upon distillation and hydrolysis, forms linear siloxanes that are subsequently

polymerized. The process involves the removal of lower molecular weight siloxanes through thermal treatment or solvent extraction.

Physically, PDMS appears as a clear, odorless liquid with minimal vapor pressure, and its properties vary slightly based on the degree of polymerization, which influences its viscosity. Chemically, it is represented by the formula $(C_2H_6OSi)n$, where 'n' denotes the number of repeating units. Structurally, PDMS comprises an inorganic backbone with organic pendant groups, classifying it as a “semi-inorganic” or “organic-inorganic” polymer. In composites with silica, PDMS exhibits substantial impact strength due to the elastomeric nature of the siloxane component, attributed to its low glass transition temperature.

The surface characteristics of PDMS and its composites have been a subject of interest due to their wide-ranging applications. These properties arise from factors such as the low intermolecular forces and compact size of the methyl group pendants, the high flexibility and bond energy of the siloxane backbone, and the partial ionic nature of the siloxane bond. In its solid state, PDMS is hydrophobic, preventing swelling in water or alcohol-based solvents, making it a preferred choice for mold materials in microneedle fabrication. However, it can swell in the presence of certain organic solvents. Surface treatment with air or argon plasma introduces silanol groups, rendering the surface hydrophilic, further expanding its application scope (Miranda et al., 2022; Raj M & Chakraborty, 2020; Victor et al., 2019).

PVP

N-Vinylpyrrolidone polymerization through a free radical process yields Poly(vinylpyrrolidone) or PVP, establishing both low and medium molecular weight pharmaceutical grade povidone powders. The US Food and Drug Administration has approved its pharmaceutical use, deeming it safe. Initially utilized as an alternative to blood plasma during World War II, its oral intake has since been ceased due to the potential for drug accumulation within the organism. PVP is produced in two variants based on polymerization degree: water-soluble (povidone) and water-insoluble (crospovidone). The soluble variant, povidone, emerges from polymerizing N-vinylpyrrolidone in water or 2-propanol, patented in 1939, with a molecular mass between 8000 and 10000 daltons, serving as a common pharmaceutical excipient and known for its use in Povidone-iodine, a topical disinfectant. Crospovidone, the insoluble form, exhibits a molecular mass over 700000 daltons, created by physically cross-linking PVP in alkaline conditions, and is prominently utilized as a

disintegrant in tablet formulations and for enhancing the solubility of insoluble components through adsorption and complexation.

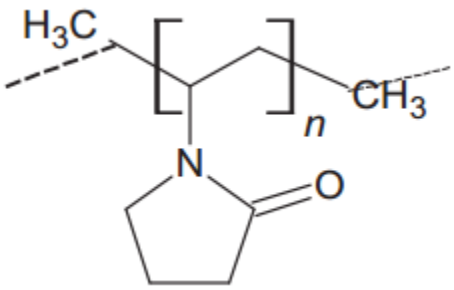

Figure 4.1 Structure of poly(vinylpyrrolidone)

PVP, a homopolymer of vinylpyrrolidone, is marketed as a free-flowing white powder or solid, available in various aqueous solution concentrations, with its molecular weight and the density of its aqueous solutions varying based on synthesis methods and polymer concentration, respectively. Despite being stable under normal conditions and resistant to heat, it is advised to avoid exposure to extreme temperatures due to its hygroscopic nature, which necessitates moisture prevention measures. Its ability to form films and act as a coating agent or additive is attributed to its high polarity, amphiphilic nature, and compatibility with various solvents and resins. PVP stability is maintained even under mildew treatment and repeated heating, though high temperatures may reduce its solubility and alter its color.

As a physiologically inert substance, PVP forms a hard, transparent, glossy, oxygen-permeable film, compatible with numerous cross-linking agents, resins, salts, and chemicals, maintaining transparency and gloss across various solvent systems. Its hygroscopic properties and the moisture equilibrium make it unsuitable for thermoplastic processing and sensitive to environmental conditions, with moisture acting as a plasticizer. To mitigate the tackiness of PVP films in humid environments, acetylated monoglycerides or other commercial modifiers may be added. Shellac, cellulose acetate propionate, and carboxymethyl cellulose can decrease the tackiness, whereas diethyl alcohol, sorbitol, and glycerin increase the tackiness. Its extensive application spans pharmaceuticals, cosmetics, biomedical uses, and the food industry, offering benefits such as reduced toxicity in germicidal products and decreased oral toxicity of certain chemicals. In the end, PVP is generally safe for dermal use (Awasthi et al., 2018; Kurakula & Rao, 2020).

Function	Pharmaceutical form
Binder	Tablets, capsules, granules
Improved bioavailability	Tablets, pellets, suppositories, transdermal systems
Film-forming agent	Tablets, ophthalmic solutions
Solubilizing agent	Oral, parenteral, and topical solutions
Taste masking	Oral solutions, chewing tablets
Lyophilizing agent	Injectables, oral lyophilisates
Stabilizer	Suspensions, dry syrups
Stabilizer	Enzymes in diagnostics, different forms
Hydrophilizer	Sustained release forms of suspensions
Adhesive	Transdermal systems, adhesive gels
Toxicity reducer	Injectables, oral preparations

Figure 4.2 Applications of PVP in various pharmaceutical formulations

Hyaluronic acid

Hyaluronic acid (HA), a pivotal synovial fluid component, functions as a lubricator and shock mitigator. This anionic biopolymer, consisting of D-glucuronic acid and N-acetyl-D-glucosamine disaccharide units in alternating sequence linked by β(1→4) interglycosidic bonds, stands out as the sole non-sulfated glycosaminoglycan (GAG) prevalent in both the synovial fluid and the extracellular matrix (ECM). Predominantly located within the skin, lungs, and intestines, accounting for over half of the body's HA, it also permeates synovial fluid, umbilical cords, and blood. Exhibiting a vast molecular weight spectrum from 1,000 to 10,000,000 Daltons, HA undergoes metabolic degradation through a sequential process involving tissues, lymphatics, lymph nodes, bloodstream, liver, and kidneys. The molecular weight of HA dictates its biological function; high molecular weight HA preserves cell integrity and ECM hydration, whereas its oligosaccharide fragments initiate receptor-mediated intracellular signaling. Leveraging its multifaceted biological roles and superior physicochemical traits, HA and its derivatives find extensive applications in arthritis management, ophthalmic surgery, drug delivery systems, and tissue engineering, attributed to its biodegradability, biocompatibility, non-toxicity, and non-immunogenicity (Kobayashi et al., 1994; Oh et al., 2010).

HEC

Hydroxyethylcellulose (HEC), derived from cellulose, incorporates hydroxyethyl groups (CH_2CH_2OH) into its structure, enhancing water solubility through ether linkages between ethyl cellulose molecules. The solubility varies with the degree of etherification, leading to classifications as either alkali or water soluble. The manufacturing process entails treating starch with sodium hydroxide to yield alkali cellulose, which undergoes etherification with ethylene oxide, converting cellulose hydrogen to a hydroxyethyl group. HEC, a biocompatible, biodegradable, non-toxic, hydrophilic, and non-ionic polysaccharide, is economical and appears as a tasteless, colorless to slightly yellow, odorless powder. It is chosen for its organic solvent solubility, facilitating chemical modifications and exhibiting properties beneficial for thickening, stabilizing, emulsifying, suspending, and dispersing. HEC's wide viscosity range and thermal stability make it versatile for applications in pharmaceuticals, paints, emulsion polymerization, agriculture, cosmetics, wastewater treatment, and more, owing to its effective hydroxyl groups (Noreen et al., 2020)**.**

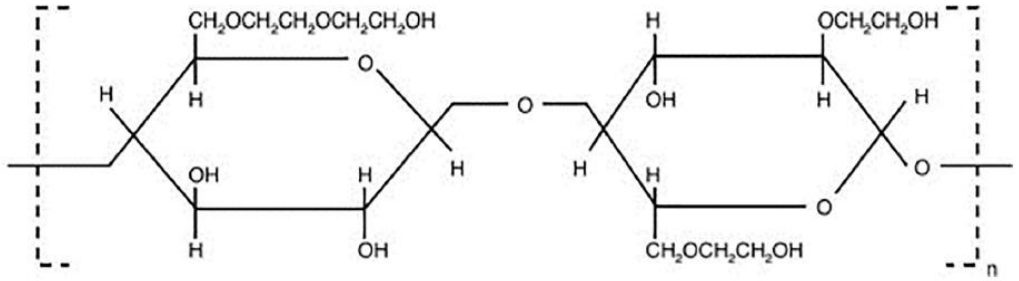

Figure 4.1 Structure of HEC

PLGA

Poly(lactic-co-glycolic acid) (PLGA), a copolymer composed of lactic and glycolic acids, has received approval from the Food and Drug Administration (FDA) for its use in therapeutic applications, owing to its biodegradable and biocompatible nature. Polyglycolide (PGA), characterized as a biodegradable, hydrophilic, and thermoplastic aliphatic polyester, stands as a primary synthetic polymer explored for biomedical purposes. Its notable crystallinity (45–55%) confers a high tensile strength and limited solubility in organic solvents. The polymer exhibits a glass transition temperature between 35 to 40°C and a melting point exceeding 200°C, displaying superior mechanical properties due to its crystallinity and undergoing bulk degradation through

ester backbone scission. Upon hydrolysis, PGA degrades, converting into glycine, which is either excreted or metabolically processed into carbon dioxide and water. However, its rapid degradation and acidic by-products, alongside low solubility, restrict its medical applications, prompting the development of copolymers containing glycolide to address these drawbacks.

Poly(lactic acid) or polylactide (PLA) is recognized for its biodegradability and hydrophobic nature. The chiral nature of lactic acid leads to various polylactide forms, with poly-L-lactide (PLLA) being the most prevalent, resulting from LL-lactide polymerization. PLLA's crystallinity (approximately 37%) is influenced by molecular weight and processing conditions, featuring a glass transition temperature of 60–65°C and a melting point around 175°C. As a slow-degrading polymer with substantial tensile strength and a high modulus (approximately 4.8 GPa), PLLA degrades into lactic acid, a benign metabolic by-product, through hydrolytic degradation involving ester backbone scission. Its hydrophobicity contributes to a slower degradation rate compared to polyglycolide, with high molecular weight PLLA potentially taking 2 to 5.6 years for complete resorption in vivo. The degradation pace is affected by polymer crystallinity and matrix porosity. Despite its strength reduction over six months post-hydrolysis, mass loss occurs over an extended period. This has led to the investigation of co-polymers combining L-lactides and glycolides or DL-lactides to improve polymer properties. PLGA synthesis employs random ring-opening copolymerization of glycolic (PGA) and lactic (PLA) acid cyclic dimers, utilizing catalysts such as tin(II) 2-ethylhexanoate, tin(II) alkoxides, or aluminum isopropoxide. This process links monomeric units through ester bonds, yielding a linear aliphatic polyester. PLGA degrades by hydrolysis of its ester linkages in the presence of water. It has been shown that the time required for degradation of PLGA is related to the monomers' ratio used in production: the higher the content of glycolide units, the lower the time required for degradation. An exception to this rule is the copolymer with 50:50 monomers' ratio which exhibits the faster degradation (about two months).

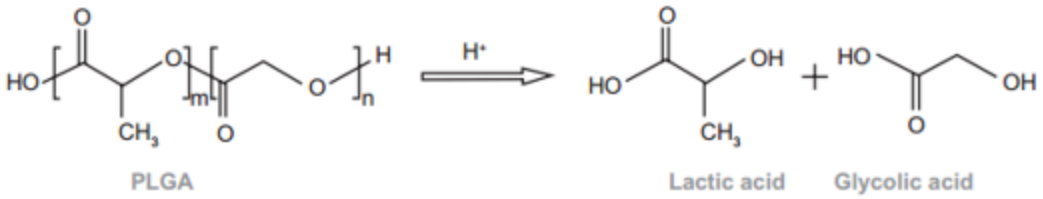

Figure 2.4 Degradation of polylactide-co-glycolide to lactic and glycolic acid

PLGA has been successful as a biodegradable polymer because it undergoes hydrolysis in the body to produce the original monomers, lactic acid and glycolic acid. These two monomers under normal physiological conditions, are by-products of various metabolic pathways in the body. Since the body effectively deals with the two monomers, there is minimal systemic toxicity associated with using PLGA for drug delivery or biomaterial applications. Also, the possibility to tailor the polymer degradation time by altering the ratio of the monomers used during synthesis has made PLGA a common choice in the production of a variety of biomedical devices, such as, grafts, sutures, implants, prosthetic devices, surgical sealant films, micro and nanoparticles (Parikh et al., 2011; Prokop & Davidson, 2008; Vert et al., n.d.).

Glycerol

Glycerol is a colorless and odorless liquid, slightly denser than water, with a sweet taste. It is viscous at room temperature and non-toxic in low concentrations. Its empirical formula is $C_3H_5(OH)_3$.

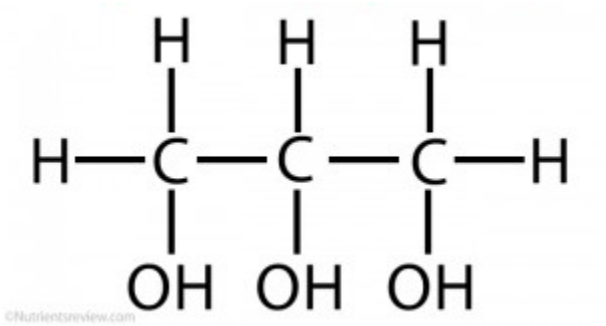

Figure 4.5 Structure of Glycerol

Pure glycerol has a melting point of 17.8°C. Its boiling point is 290°C but it also decomposes at that temperature. The presence of three hydroxyl groups makes the compound hygroscopic, with a tendency to absorb moisture from the air. This also makes it useful as a humectant in cosmetics

and food, retaining water and preventing the substance from drying out. Glycerol is easily soluble in water, due to the ability of the polyols groups to form hydrogen bonds with water molecules. Glycerol is used in a number of industrial applications, in the pharmaceutical industry, in cosmetics and personal care products, in the production of resins, detergents, plastics and tobacco and as a humectant in food (*Glycerol*, n.d.). Due to its qualities, it has been used as plasticizer.

Tween

Polysorbates are a group of nonionic surfactants that consist primarily of fatty acid esters of polyethoxy sorbitan. These polysorbates are marketed under a variety of trade names such as Tween, Sorlate, Monitan, Olothorb, and they find widespread use as emulsifiers, defoamers, dispersants, and stabilizers in food, cosmetics, and biodegradation media (Ayorinde et al., 2000).

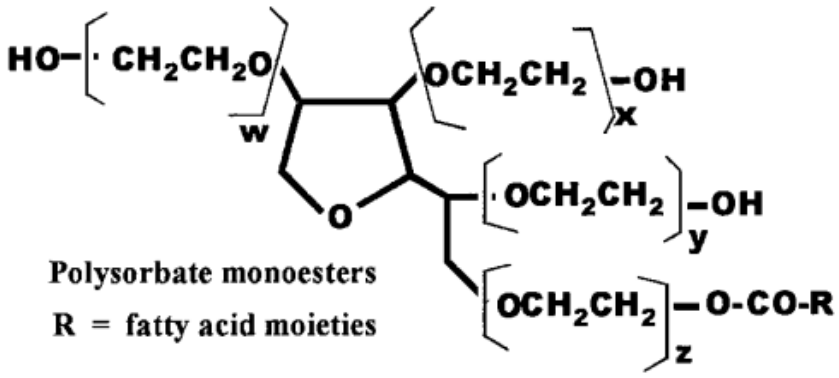

Figure 4.6 Structure of Tween

There are a number of Tweens having different fractions of oxyethylene chains and are named as Tween 21, 61, 65, 81, and 85. The properties of surfactant can be ascribed to the presence of a hydrophilic head group and a hydrophobic chain (or tail) in the molecule. The polar or ionic head group usually interacts strongly with an aqueous environment, in which case it is solvated *via* dipole–dipole or ion–dipole interactions. In fact, it is the nature of the polar head group which is used to divide surfactants into different categories: anionic, cationic, non-ionic and zwitterionic. In aqueous solution dilute concentrations of surfactant act much as normal electrolytes, but at higher concentrations very different behaviour results. This behaviour is explained in terms of the formation of organized aggregates of large numbers of molecules called micelles, in which the lipophilic parts of the surfactants associate in the interior of the aggregate leaving hydrophilic parts

to face the aqueous medium. The formation of micelles in aqueous solution is generally viewed as a compromise between the tendency for alkyl chains to avoid energetically unfavourable contacts with water, and the desire for the polar parts to maintain contact with the aqueous environment. Thus, when surfactant molecules adsorb at an interface they provide an expanding force and cause the interfacial tension to decrease, facilitating a surface wettability or miscibility between two liquids. Surfactants can be found in the production and processing of pharmaceuticals, food, agrochemicals, laundry products etc (Schramm et al., 2003).

Fabrication of the Positive Master

Two photons lithography was used to induce polymerization of resins. Two photons polymerization was performed on a Nanoscribe Photonic Professional GT system (Nanoscribe GmbH). The Nanoscribe system uses a 780 nm Ti-Sapphire laser emitting ≈100 fs pulses at 80 MHz with a maximum power of 150 mW and is equipped with a 25x, NA 0.8 oil immersion objective for printing medium-sized features. The ITO-coated substrate is placed in a holder that fits into a piezoelectric x/y/z stage. A galvo scanner determines the laser trajectories. In the immersion conFiguretion the lens is immersed in the resin with a refractive index matching that of the glass coated with the photoresist; here, because of the refractive index difference between the glass and the photoresist, a laser scattering takes place at the glass-photoresist interface then worsening the fabrication performances of the system. A stl file of a single cone is loaded in Describe software and is converted in GWL document. The array of cones comes from the combination of lines of code by using Describe software. The negative tone IP-S photoresists assures a high resolution and is optimized for the process of multiphoton polymerization. The IP photoresists are exclusively available to users of the Nanoscribe systems.

Negative Mold Fabrication

As mentioned above, polydimethylsiloxane (PDMS) is an optimal polymeric material to be used in biomedical applications, so PDMS molds have been made. Starting off from PDMS preparation, it involves pouring PDMS liquid precursor into a falcon (50 mL) and then the curing agent in a 10:1 ratio. After centrifuging the falcon for 5 min at 1000 rpm, the PDMS is poured in a glass petri where the microneedles master has been previously placed on the bottom, until the petri is almost full of it. Then, PDMS curing is necessary to obtain the final mold, so this step has been made faster introducing the petri in oven at 65°C (higher temperatures would ruin the master material)

for 90 min. After PDMS being cured, mold is removed carefully. By using the same master, several molds are able to be prepared.

Molds Characterization

Optical images of PDMS molds were acquired. The internal morphological structure of the mold was investigated. The PDMS mold was frozen in liquid nitrogen (-196 °C) and sectioned using the Leica CryoUltra Microtome EM-FC7-UC7. 5 μm thickness slices were deposited on a 12 mm round glass cover slip and then mounted on a standard SEM pin stub for SEM imaging.

Fabrication process of microparticle-based microneedles (μPs MNs)

A polymeric solution was blended according to the following volumes per mL: 249 μL of PVP 25% w/V, 592 μL of HA 3% w/V, 140 μL of H_20, 19 μL of Tween 80 10% V/V. It is left stirring overnight. 150 μL of polymeric blend are casted onto PDMS negative stamps (Fig. 4.7 Step 1). The samples are dehydrated by vacuum steps at the beginning and then the final aqueous phase is let evaporating by leaving the samples in a climatic chamber for 90 min at T=23°C and R.H.=47% (Step 2-3). Then μPs are loaded in the concave-shaped microneedles by the aid of a spatula and a stereomicroscope (Step 4). Further, hollow pillars are pressed on the polymeric films (Step 5). This step provides for cracking the polymeric interconnections of the array to make the μPs MNs harvestable in a stand-alone manner. Then the samples undergo the plasticization process through a mixture of vapors of Etoh/DMC (8:1) (Fig. 4.7 Step 6) (Fig. 4.8). The samples are let once again 30 min in climatic chamber T=23°C-R.H=49.5%. For the harvesting step, a beaker is filled with water and warmed with a hot plate at T=70°C. The hot water vapor is used to turn into a glue-like solution the harvesting film. Then bulk pillars are put in contact with the glue-like solution. This makes pillar edges adhesive and then are aligned with the corresponding μPs MNs. The samples are put in climatic chamber for 2 hours at T=23°C and R.H.= 48% (Step 7-11). Then they are ready to be lifted off (Step 12).

Harvesting solution is prepared as mix of PVP 25% w/V and glycerol 0,5% V/V. Then it is casted on a PMMA sheet (0,5 mm) and let it dry with a hot plate.

A detailed explanation of the process, and how it was obtained, is provided in chapter 5.

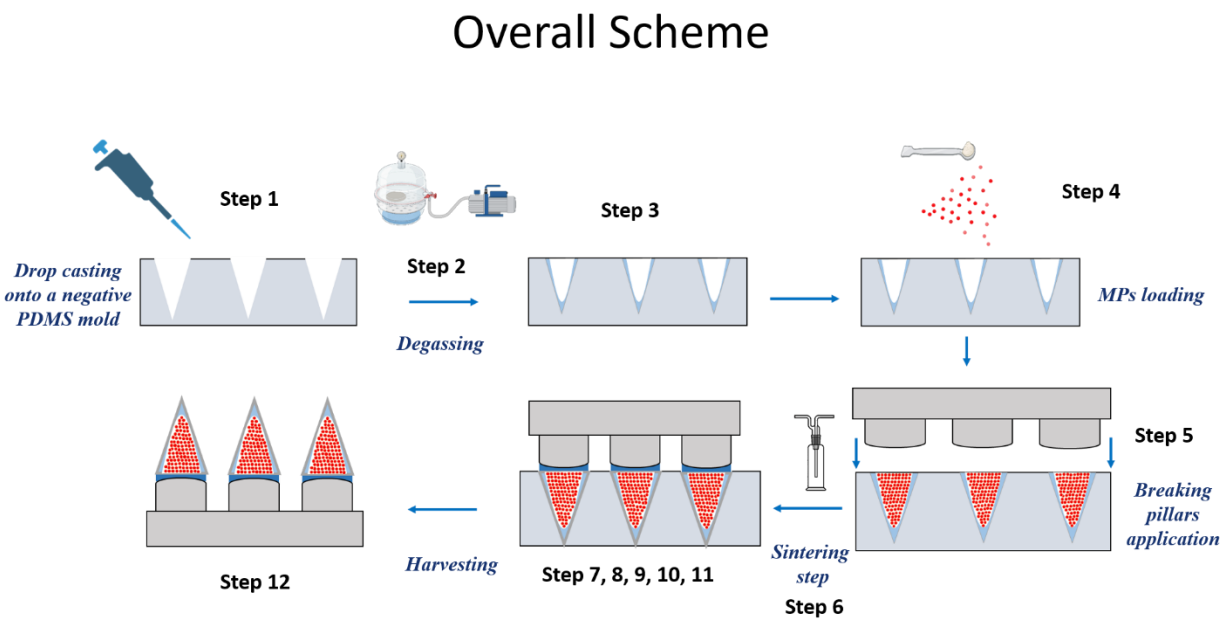

Figure 4.7 Overall fabrication process of dissolvable microparticle-based microneedles

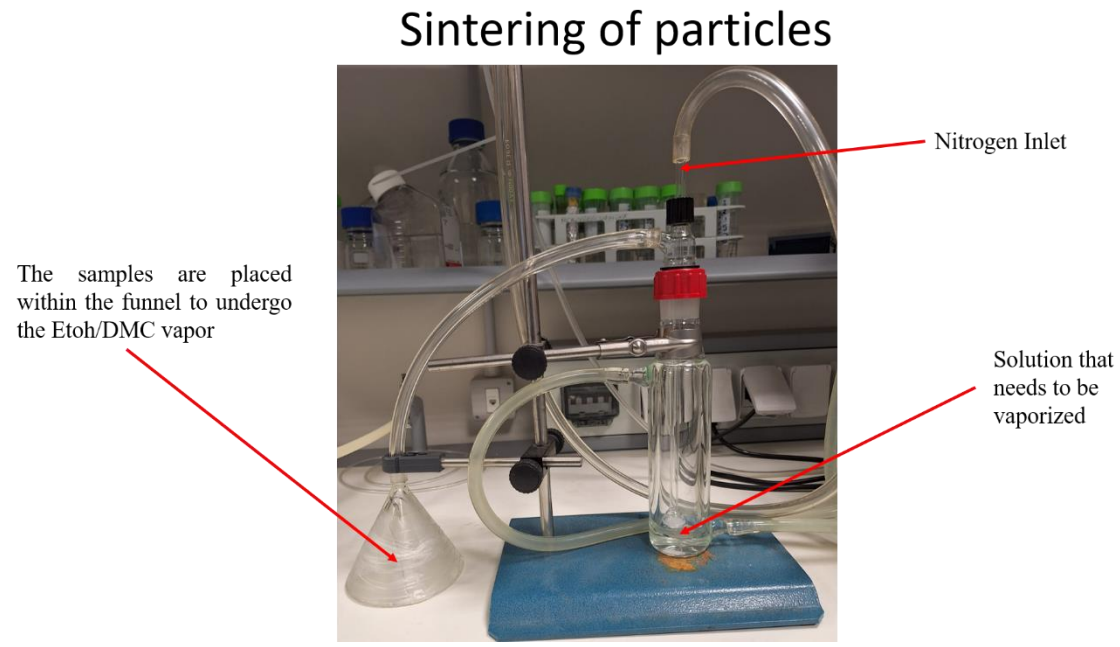

Figure 4.8 Drechsel bottle used to vaporize Etoh/DMC mixture by flowing Nitrogen. A water bath is used to maintain the temperature constant (25,2°C)

Optical microscopy

After fabrication, the microneedles were visualized under a stereomicroscope (Olympus, SZX16 double objective) to investigate the sharpness of the tips and the patter distribution of the microneedles.

Scanning electron microscopy

Microneedles positive masters morphology was investigated through a scanning electron microscope (SEM). SEM samples were prepared attaching the microneedles patch on a cover slip mounted on a standard SEM pin stub. The samples were gold-sputtered with a HR208Cressington sputter coater (15 nm thickness) and analyzed by FESEM ULTRA-PLUS (Zeiss) at 10-20 kV with the SE_2 detector.

Mechanical performance of µPs MN arrays

Polymeric µPs MNs were subjected to compressive test by using a mechanical station (Instron® Model 5943L4717; Instron, Norwood, MA, US). Axial Fracture force using a rate of 1.1 mm/min (ASTM D695-10) was investigated to obtain µPs MNs fracture force. Both 1 kN and 10 N load cells were implemented. Instron station was also used to mimic the effect of an applicator when testing in skin models. A rate of 0,5 mm/s and a pressure of 3 min was set in the latter case. Data were analyzed with BlueHill 3 Testing Software for Mechanical Testing Systems (Instron, Norwood, MA).

Fabrication of pillars

CNC Micro-milling machine (Minitech Machinery Corporation, Norcross, Georgia, US) was used to fabricate hollow and bulk pillars. A sheet of 2 mm thick PMMA was used in combination with the following end mills TR-2-0080-S, TR-2-0100-S, TR-2-0400-S (Performance Micro Tool, Janesvile, Wisconsin, US). DesKam software was used to launch the jobs.

Production and characterization of PLGA microparticles

PLGA porous microparticles (µPs) have been designed, produced and characterized. Every modification to accomplish the target goal of the application of interest is described in chapter 6. Here is reported a general procedure for the ups production, more details are described in the further sections (chapter 6). PLGA µPs were prepared by the double emulsion water/oil/water solvent evaporation method (De Alteriis et al., 2015). First, 100 mg of PLGA were dissolved in 1 mL of dichloromethane (DCM) or dimethilcarbonate (DMC) for oil phase. The aqueous phase was composed of 100 µl of ammonium bicarbonate (ABC) previously dissolved in water. For pH sensible active agent (i.e. mRNA) ammonium bicarbonate is avoided. In this case the oil phase consists in 83 mg of PLGA and 17 mg of Pluronic F-68. Both phases were homogenized (Ultra-

turrax, IKA T- 25 ULTRA-TURRAX Digital High-Speed Homogenizer Systems) for 30 s at 20000 rpm. The first emulsion was immediately poured into 10 mL of 2% (w/v) polyvinyl alcohol PVA solution and further homogenized for 1 min at 25000 rpm. The second emulsion was immediately poured into 40 ml of water under mechanical stirring for 3h at 450 rpm for the complete solvent diffusion and evaporation. The whole process for the preparation of the μPs was carried out under refrigeration on ice. Then, the μPs suspension was centrifuged 4 times for 10 min at 4°C and 10000 rpm (AvantiTM J-25, Beckman, USA) for washing. Finally, μPs were lyophilized (Heto PowerDry PL6000 Freeze Dryer, Thermo Electron Corp., USA; -50°C, 0.73 hPa) over-night. After washing steps, the μPs were characterized by confocal miscroscopy (Leica SP5 microscope), in order to evaluate the signal of the molecule inside porous structures.

Histology

The specimens were fixed using a 10% neutral buffered formalin solution overnight. Subsequent to fixation, gradual dehydration was accomplished through successive immersions in ascending concentrations of alcohol (75%, 85%, 95%, and two cycles of absolute alcohol), each immersion lasting 30 min at room temperature. Post-dehydration, the specimens underwent xylene treatment for 30 min and were then embedded in paraffin. Longitudinal sections measuring 7 μm in thickness were obtained from both the wounded-M2 and wounded+M2 specimens using a microtome (Thermo Scientific HM 355S). The paraffin embedding process creates an anhydrous environment, whereas histological dyes used for tissue staining are water-based. To facilitate the compatibility of aqueous dyes with the tissue sections, the deparaffinization step in xylene was conducted to remove the paraffin. Subsequently, rehydration was executed using a series of ethanol solutions in descending concentrations (100%, 95%, 85%, 75%) concluding with immersion in water. Histological staining involved the application of Hematoxylin and Eosin (H&E) (Bio Optica), Alcian Blue (Sigma Aldrich), and Picrosirius Red (PSR) (Sigma Aldrich Chemical Company). Upon completion of the staining process, sections were mounted onto coverslips using Histomount Mounting Solution (Invitrogen).

5 Results and Discussion

Based on the aforementioned information, the aim of this work was to establish and further investigate the feasibility of the multicompartmental concept of absorbable microneedles (MNs). This concept involves coupling distinct dissolvable/biodegradable polymers in order to provide tunable release kinetics for sustained delivery. Unlike single solid body MNs, our MNs are based on the assembly of two regions (Fig. 5.1). PVP-HA MNs form a concave-shaped cone leaving an internal cavity to accomodate PLGA microparticles (µPs). This approach is supposed to overcome the limited loading ability, and the encapsulation or co-encapsulation challenges of drugs (altered physicochemical characteristics, degradation of the payload, drug diffusion), typically associated to dissolvable MNs category. The cavity-shaped MNs, referred to as the tip compartment, serve as the starting matrix where a drug may be dissolved, while the porous PLGA µPs act as carriers loaded with one or multiple drugs. This approach prevents the dispersion of the drug in the water-soluble matrix and allow to preserving the activity of the molecule. Previous studies have demonstrated how protein-loaded polymeric µPs can protect protein activity (Lagreca et al., 2020). Controlling the release properties involves choices related to polymer, size and microstructure which enable the tuning of drug outflow. Additionally, to ensure mechanical integrity between the tip and the set of particles, a gentle sintering method, developed so far by the group has been employed This method is carried out at room temperature by using solvent vapors that do not affect the bioactivity of drug loaded in the µPs. This process is performed after the insertion of the µPs within the MNs cavities.

This PhD thesis aims to overcome the limitations of the previous fabrication process, ensuring more reproducible results and testing the platform in distinct scenarios. For instance, the polymeric blend of the dissolvable part of the MNs was replaced with another formulation and a drop casting method was settled. A further step which has been optimized is given by the integration of PMMA pillars with the µPs-based MNs taking advantage of a polymeric solution as an adhesive layer. These pillars ensure the harvesting of the needles form the PDMS stamp and promote the implantation of the cones within the skin. Optical and mechanical characterizations were used to analyze the features of µPs-based MNs and the fracture force, respectively. The mechanical setup was customized to test the implantation capabilities in a reproducible manner. Once a robust protocol of µPs-based MNs was established, some adjustments were made to verify its suitability

in specific contexts. With a reliable protocol in place, the platform was ready to be explored for mRNA delivery within the PNRR (National Recovery and Resilience Plan) project "National Center for Gene Therapy and Drugs based on RNA Technology" for a potential application in the vaccine field.

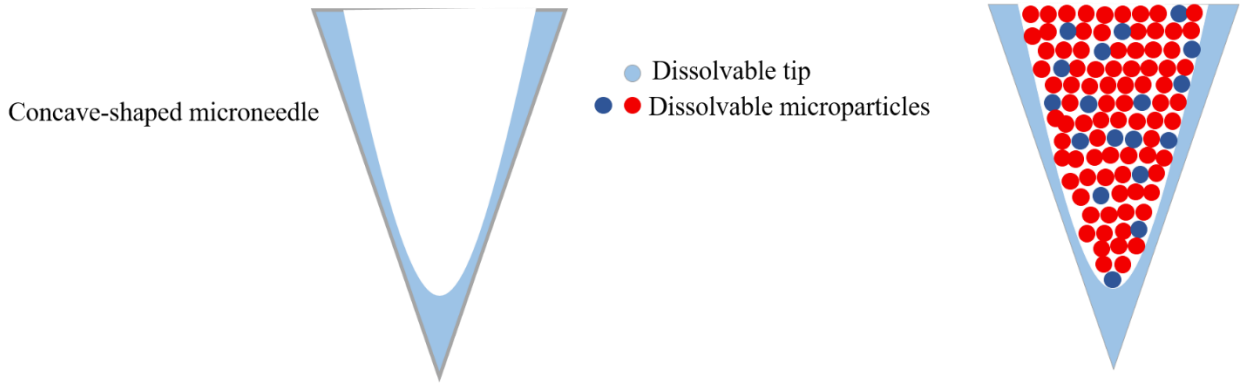

Figure 5.1 Concave-shaped microneedles emerging in combination of several factors. They host a concavity capable of being loaded with PLGA μPs

5.1 Fabrication of the positive master

A positive master is crucial to proceed with the stamp-method process and ultimately attain absorbable MNs. The Nanoscribe system was used to realize a master of microcones using additive manufacturing technology. This technology allows the production of 3D structures with high spatial resolution by exploiting the two photons polymerization effect. This phenomenon depends in a non-linear way on the incident intensity, which turns into the fabrication of constructs with controlled feature size on the order of tens of nanometers, especially when using the most accurate objective (63x). Moreover, Nanoscribe software gives the opportunity to work with complexes 3D CAD accurately reproduced during the reparation of the job file. Due to these benefits, it is preferable over other microfabrication technologies such as deep reactive-ion etching, laser ablation, microstereolithography, drawing lithography, droplet-born air blowing, and chemical isotropic etching (Joshi et al., 2023) (Doraiswamy et al., 2006; Faraji Rad et al., 2021). Especially when realizing MNs arrays, where the piercing ability is highly affected by tip diameter, it is essential to precisely reproduce their geometry. To better tap into Nanoscribe advantages, a positive master of microneedles was obtained by using the setup for medium features, as described in their documentation [https://support.nanoscribe.com/hc/en-gb/articles/360002419574]. It refers to geometries with dimensions on the order of millimeters, ensuring reasonable processing times. Achieving features on the order of 1 μm or a bit lower is challenging, but conceivable. Considering

this, a 25x objective in combination with IP-S polymer was chosen for manufacturing an array of cones as positive master of microneedles, whose geometrical dimensions are:

- Height 600 µm
- Base diameter 300 µm
- Center-to-center distance 600 µm
- 256 cones (16x16) covering an area of 1 cm^2

These dimensions meet the state of art requirements to avoid "bed of nail" effect and enhance penetration efficiency (Battisti et al., 2019; Olatunji et al., 2013; Shu et al., 2021). The 25x objective performs jobs taking advantage of a larger scan field in comparison with the 63x, resulting in decreasing the stage movement and accelerating the printing time. With the purpose of further decreasing the printing time, the combination of shell and scaffold strategy and post-print UV curing was preferred rather than processing the total solid cone model. The shell is only a fraction of the structure and is printed as polymerized resin, preventing the collapse of the structure. The residual resin is cured by a subsequent UV process. In this case, UV-post curing process takes 3 h and in principle can be applied in parallel to more than one master.

A recipe was developed to accomplish the array of cones using a mesoscale setup. Firstly, dose testing was explored to achieve optimal resolution properties. Dose, roughly proportional to laser power and residence time, influences parameters such as degree of polymerization, size and aspect ratio of voxel. According to this evidence, laser power and scan speed were investigated to achieve the resolution capability of the 25x objective. A matrix of trials was arranged, varying laser power along the rows and scan speed along the columns, to find out the optimal combination. In the end, laser power and scan speed were set equal to 100% of Power-scaling (this latter set equal to 1) and 50000 µm/s respectively, resulting in a tip diameter nearly close to 1 (1.147) µm, matching the objective limit. An additional challenge arose due to the discrepancy between the height of cones and the working distance of the objective, fixed at 380 µm from the substrate, while the cone height and center-to-center distance are 600 µm. However, photopolymerizing the cone in a single step was not feasible. Instead, the upper part of the cone was stitched with the lower part (Fig. 5.2). It is necessary to give as input the cone divided in two CADs. The stitching layer, where adhesion occurs, is a crucial part of the process. If the upper part does not fit together with the lower, a sort of "stairstep" comes out after the junction, because the upper part results in sinking within the

lower. This leads to a mechanical stress concentration with subsequent potential breakage of the replicated microneedles during implantation tests. By comparing software simulation results with the manufactured jobs, a proper Z_{offset} equal to -13 µm was found out when approaching the lower part, ensuring a perfect junction between the two portions of the cone and leading to a single solid figure.

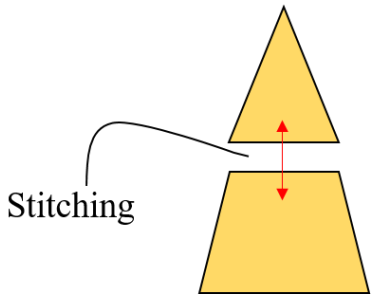

Figure 5.2 Stitching approach. A stairstep emerges if the upper and the lower parts are not combined properly

To ensure the proper adhesion of the microneedles with the glass substrate, a polymeric interface in a hexagonal pattern conFiguretion was realized. In the same job of the array of microcones, an additional layer was added to be printed. To induce photopolymerization of the interlayer to better integrate the cones at the substrate, it was necessary to make the surface of interest printable. Considering that the surface of interest (1 cm^2) exceeds the printing field, it is unavoidable to split it into blocks, each one fitting the scan field of the used objective. The hexagonal pattern was chosen for its geometrical properties, allowing the maximization of the surface with the same perimeter, resulting in the minimization of the side faces, and the implementation of a continuous floor without empty spaces. This led to covering the same area while reducing processing time. Examples of natural hexagonal patterns include beehives for cell organization, and the latest James Webb telescope as technological applications. The implementation of the polymeric interface is crucial to prevent microneedles detaching during resin development or the subsequent step of replica molding. Integrating it in the same job of microcones, eliminates the need for additional surface adhesion enhancements, such as silanization, and other deposition techniques, such as spin coating, which require supplementary fabrication steps. Moreover, it also avoid the step of replacing the original master with a NOA glue master, typically done to extend the lifetime of the original master. This process is susceptible to detaching events .

In the end, the final processing time to print a 16x16 array of highly accurate cones (Fig. 5.4) (tip diameter ~ 1 µm) (Fig. 5.4 B) integrated with a polymeric interface (Fig. 5.3) takes 15 h in comparison with the previously reported 76 h when using a 63x objective. This speeds up the process five times and eliminates the need for the fabrication process of a NOA replica master.

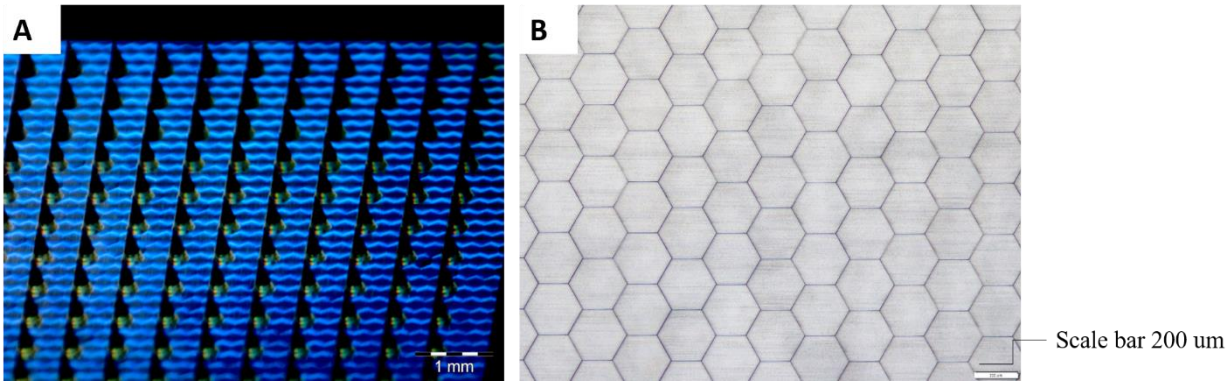

Figure 5.3 Polymeric interface obtained as blocks of hexagons to enhance the adhesion of cones to the glass substrate

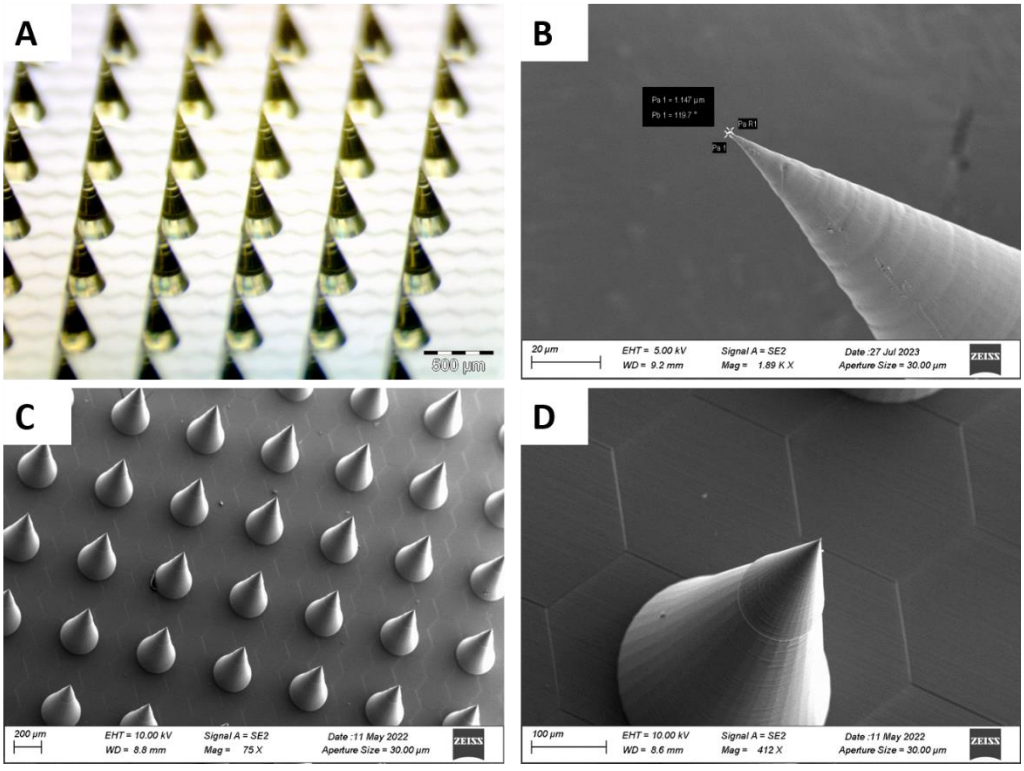

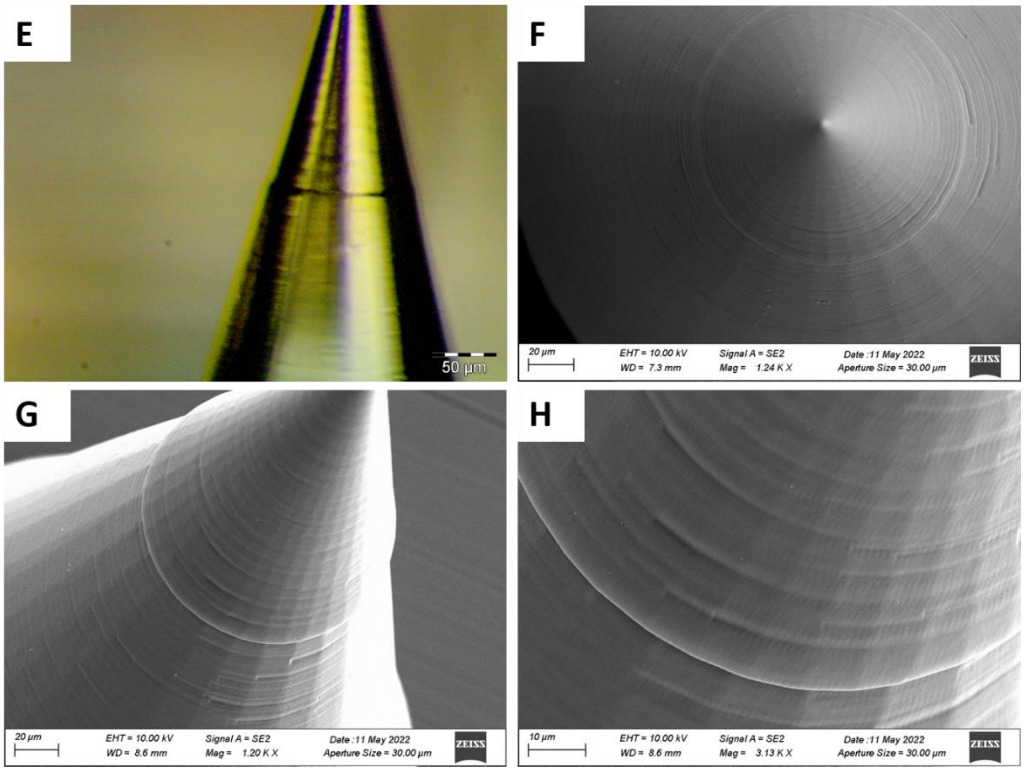

Figure 5.4 Positve master fabricated by two photons polymerization technique. Tip diameter 1.147 µm B

5.2 Fabrication of Microparticle-based Microneedles

Once the positive master was produced, the negative stamp was obtained from it using PDMS, a widely used material in the scientific community for replicating shapes. The cones were accurately reproduced through this process (Fig. 5.5). A drop-casting method was employed to fabricate dissolvable microparticle-based microneedles (µPs MNs). This technique utilizes vacuum conditions to promote the filling of hydrophobic stamp cavities with hydrophilic a hydrophilic solution. When the polymeric solution casted on the stamps undergoes several stages of vacuum conditions, it starts filling the negative replicas of needles while the air flows up. The vacuum conditions are not sustained over time but rather alternate with a return to regular atmospheric pressure conditions. Conversely, continuous vacuum conditions throughout the process would conduct to brittle behavior and subsequent failure. After this stage, a further step of dehydration leaves behind the polymeric needles. As previously reported, upon this process a concave shape within the truncated cone of the microneedle is obtained. The particles are loaded within polymeric microneedles manually by spatula, then the microneedles can be lifted off. The harvesting is shown furtherly.

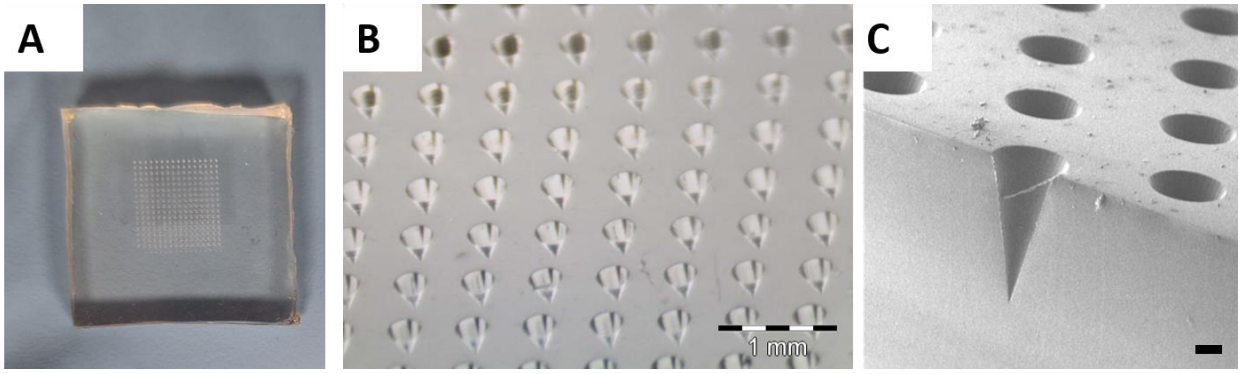

Figure 5.5 PDMS negative stamps. C scale bar 150 micron

In order to determine the appropriate amount of material for the final polymeric blend, several efforts were made to understand the physics of capillary and evaporation phenomena. Firstly, PVP and HA were separately dissolved in water at concentrations of 25% w/V and 3% w/V, respectively. The reasons for choosing these polymers are widely discussed in experimental section. Assuming that the effective volume of 256 cones with the listed dimensions is considerably less than 4µL, which is the empirical volume required for the process, an initial batch of a 5% m/V polymeric solution composed of a blend of PVP and HA was tested. A 200 µL solution was casted onto PDMS stamps and the stamps underwent vacuum conditions and further dehydration. The evaporation forces caused polymer shrinkage and formation of cavities. It resulted that the process was achievable only within 7%-8% m/V range of the polymeric solution. A polymeric solution below 7% m/V contained an insufficient amount of polymer mass to carry out the process, while more than 8% m/V did not result in concave-shaped needles. Consequently, the final conditions to carry out the drop casting method were established as 150 µL of a polymeric solution at 8% m/V, covering the area of interest (1 cm^2) and producing concave-shaped needles (Fig. 5.6). Although the casting method was clarified at this stage, further optimizations were applied to the polymeric solution.

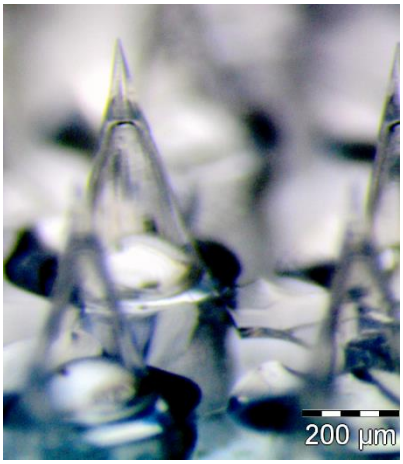

Figure 5.6 Shrinkage phenomenon leading to the emerging of a concavity within the body of the microneedle

The dissolution rate of biodegradable polymers significantly affects the application time of MNs on the skin surface and the drug release performance. The hygroscopicity of water-soluble polymers directly influences their dissolution properties, while mechanical strength is fundamental for skin penetration and can be adversely affected by the moisture absorption (Cheng et al., 2022b; Q. L. Wang et al., 2018b). Since different materials exhibit varying degrees of hygroscopicity, several tests were conducted to better apprehend the behavior of the PVP-HA blend. Considering the brittle nature of PVP, HA was added as plasticizer to realize more flexible MNs patches without compromising hardness properties. The specific properties of the customized HA product from Fidia Farmaceutici were not known, except for its molecular weight (200 kDa). Moreover, detailed explanations of HA behavior are often challenging to find in the literature and are typically investigated experimentally (Leone et al., 2020). Firstly, to understand the moisture absorption ratio of stored PVP and HA powders, both were separately dissolved in water and then lyophilized. The outcome was an increase of powder weight of 3,8% for PVP and 7,64% for HA, so almost 2:1 relation. The viscosity of HA (3% w/V) was measured and shear thinning or thickening phenomena were not observed (Fig. 5.7). The constant behavior of the viscosity [Pa· s] results in low grade of polymeric chain entanglement, and so closer to a polymer characterized by a linear behavior.

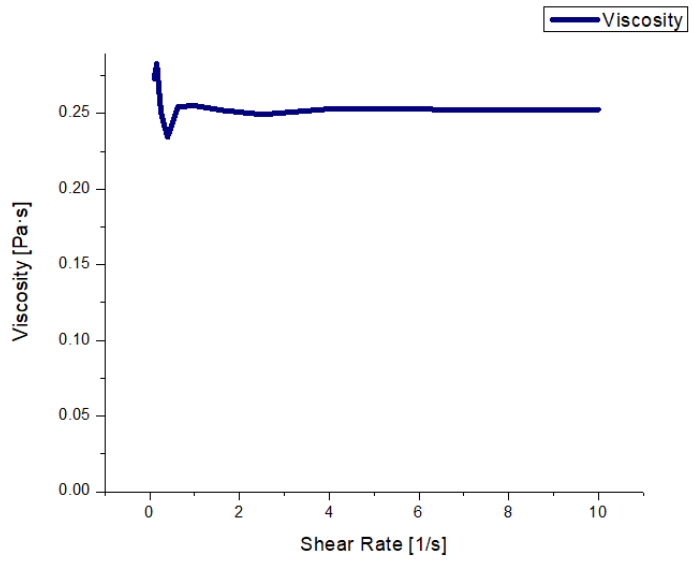

Figure 5.7 Viscosity of HA (3% w/V) (200 kDa, Fidia Farmaceutici)

In light of these data and considering that moisture absorption depends on the type of material, blend of materials, etc, different ratios of PVP and HA were dissolved and mixed together to achieve the final conFiguretion. Different solutions were prepared in order to have:

- PVP+HA=80 mg/mL
- $\frac{\text{PVP}}{\text{HA}}$= 2, 2,5, 3, 4 w/w

Each formulation was stabilized by adding the same amount of Tween 80 as surfactant. The limit of 80 mg/mL is set to make microneedles emerge with cavities, while the ratios of 2, 2.5, 3, 4 represent the polymeric masses tested separately. In order to understand moisture absorption, an analysis of weights was executed. PDMS stamps weights were registered before casting the solution and immediately after dehydration. Five samples for each kind of mass ratio were fabricated, resulting in 20 weights of samples. An ANOVA test was performed on the weights of samples to understand if the amount of HA influenced the weight of the sample and thus the moisture absorption. The tests were conducted at R.T. considering fluctuations in temperature and relative humidity of 21-22 °C and 42%-50% throughout the day. F_0 was compared to an appropriate upper-tail percentage point of Fisher distribution:

$$F_0=22,39 > 5,29= F_{0.01,3,16}$$

Considering P-value of 0,01 and 16 degrees of freedom. The normality assumption was checked and since it was not clear at all if it could be confused with a bimodal distribution, resulting in a normality violation, a Kruskal-Wallis test and Dunn's multiple comparison were performed via GraphPad Prisma software, confirming differences between groups, especially between 2 and 4 ratios of mass amount. This leads to the assumption that the difference is statistically significant when the difference of amount regards the extremes of the range. Based on this evidence, further investigations were conducted on blend solutions characterized by PVP/HA=3, 3.5, 4. Considering qualitative assessment of the samples, such as the bending of the tips of microneedles, a typical behavior of excessive flexibility in a microneedle patch, and weight variation due to moisture absorption (Fig. 5.8), the best ratio for the polymeric blend emerged as PVP/HA=3,5, which means a mass amount of PVP 3,5 times HA amount per mL. A blend outlined in this way, was adaptable to the process both for sustaining the drop casting method and for being less affected by the environmental conditions in terms of moisture absorption. This ensures good mechanical properties, as shown in the subsequent paragraphs.

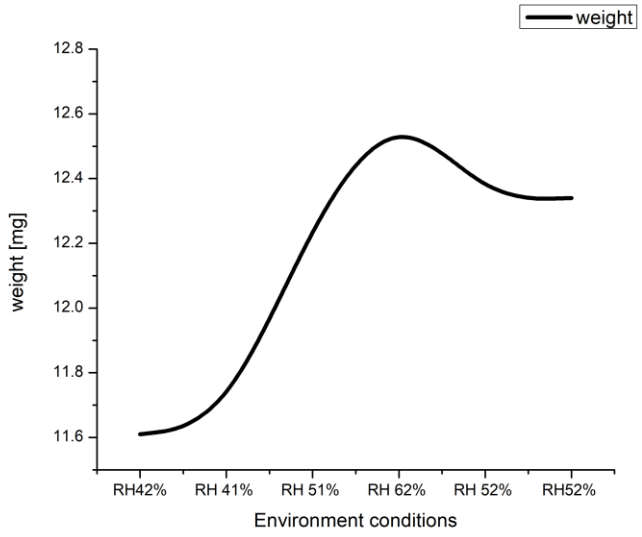

Figure 5.8 Weight variation of sample (blend 3.0) according to variation of moisture. 1) T=21°C-RH 42%, 2)T=21,2°C-RH41%, 3)T=21,3°C-RH51% 4)T=22,3°C-RH62%, 5)T=23,1°C-RH52%; 6)T=20,7°C-RH52%

At this point, after the samples are harvested out of the PDMS stamp, the behavior of the microneedles patches was observed when the environmental conditions changed. It finally resulted in a sample affected by the relative humidity (R.H) with a definite slower rate. This data was important to better understand the reproducibility of the process in terms of durability as well. In

the end, after the exposed optimizations, the durability of the drop casting methods ranges from 45 to 60 min and following dehydration 90-120 min by inserting the samples in a climatic chamber set with T=23 °C and R.H. =47%. This is a time-saving process in comparison with typical casting methods where only the drying steps require 24 h (Ando et al., 2023; Q. Wang et al., 2015).

The loading of the particles occurs after the dehydration of the samples, when they are extracted from the climatic chamber. PLGA particles are inserted manually with the aid of a spatula and a stereomicroscope. They represent a popular carrier and are prepared by a double-emulsion method and provided by the group (Lagreca et al., 2020).

Immediately, the samples are exposed to a solvent mixture of Ethanol and DMC at room temperature using a Drechsel bottle. This technique was developed in the group previously (De Alteriis et al., 2015), and is important to promote the sintering of PLGA particles. This provides mechanical integrity to the body of the microneedle without affecting the bioactivity of the encapsulated drug. Mechanical characterization is exhibited at later stage.

A polymeric layer was used to harvest the microneedles out of the stamp in the earlier period. The preparation of harvesting layers is conducted concurrently with the other steps of the process. The layer is plasticized taking advantage of water vapor, as previously reported, and after one hour in the climatic chamber, it is possible to harvest the µPs MNs out of the PDMS stamp. Glycerol was added as an enhancer of the plasticization effect of the layer, permitting both better integration with the µPs MNs and a more rapid process. This step was replaced by using PMMA pillars, but they are discussed in the following paragraph.

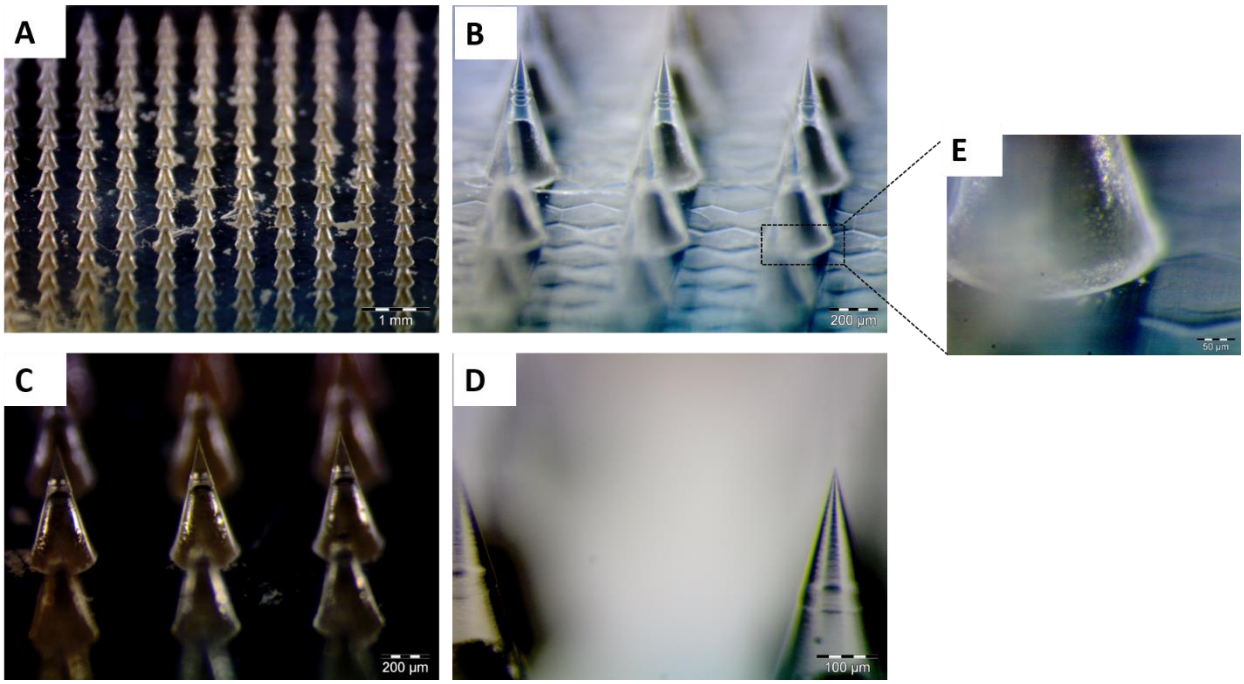

Figure 5.9 Microparticle-based Microneedles not integrated yet with pillars. An harvesting layer was used to collect them out of the PDMS stamp

5.3 Fabrication of PMMA Pillars

An usual limitation of MNs technology is constituted by an incomplete insertion within the skin, even if they fulfil the mechanical requirements to pierce the stratum corneum. This leads to a loss of the drug and reduction of the effectiveness of the treatment. The anisotropic behavior of the skin is responsible for this effect, where collagen and elastin mainly contribute to this phenomenon. The non-linear response is due to the unfolding of collagen fibers with the increasing load until reaching the maximum point where the fibers stretch and align along the load direction and the skin stiffness augments. A single microneedle stretches the skin surface, resulting in high stress in the skin in a ring around the edges of the microneedle (Fig. 6). The size of this ring is equivalent to the circumference of the microneedle tip, which is proportional to r. The force will be also influenced by compression of the volume of skin underneath the microneedle, which is proportional to r^2. Results indicate that the force to stretch the surface dominates over compressing the skin at small tip diameters, while the inverse happens for increasing radii (Römgens et al., 2014).

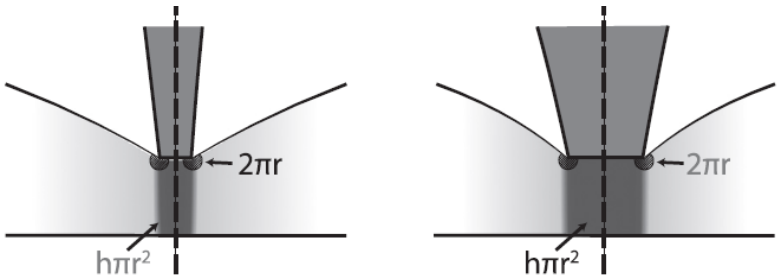

Figure 6 Non-linear behavior of the skin (Römgens et al., 2014)

This leads to the conclusion that the deeper the microneedle is pushed, the higher the force to implant it fully. In light of these elements, PMMA cylinders (Fig. 6.2 C-D) were fabricated using a micro-milling machine to obtain pillar-integrated MNs. They were designed to harvest the µPs MNs out of the stamp and constitute centered pressure points to enhance implantation abilities within the skin. They are meant to avoid the spreading of the pushing force over large areas of the array but to center it on the µPs MNs base. Considering that during implantation, it may occur that the MNs move along the lowering of the skin, pushing the skin without continuing the insertion within, PMMA pillars may sort out this issue by increasing µPs MNs height without being inserted inside the skin.

In order to extract µPs MNs using pillars, some steps need to be discussed. µPs MNs need to be removed out of the stamp as single microneedles, without interconnections given by the polymeric matrix during the fabrication process (Fig. 6.1). For this reason, hollow half PMMA pillars (Fig. 6.2 A-B) were fabricated and called “breaking pillars” to make the µPs MNs harvestable in a stand-alone manner. Hollow half pillars are characterized by a circular crown at the edge, used to crack the bases of microneedles for disconnecting them from the interconnecting polymeric layer. After the loading of the µPs, hollow half pillars are aligned with the cavities of the stamp and then submitted to a delicate pressure.

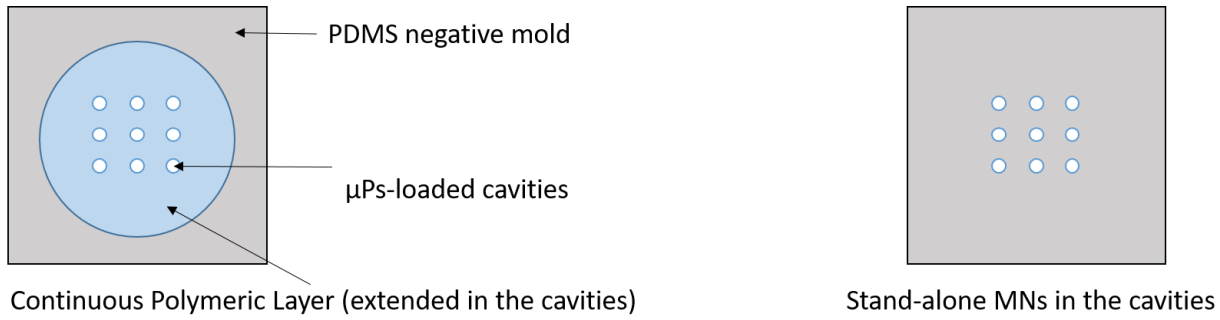

Figure 6.1 Scheme of the removal of polymeric interconnections among microneedles during the fabrication process

The final stage of gathering the µPs MNs using pillars may occur in accordance with the preparation of a glue-like solution with the aim of making the edges of the pillars adhesive. PVP-Gly solution is casted on a sheet of thin PMMA and dried using a hot plate. This step is conducted concurrently with the degassing step. When the harvesting step arrives, the dried solution on the PMMA sheet is turned into a glue-like solution by using warm water vapor. Depending on the environmental conditions, it turns into this state in 4-6 min. After that, pillars are let laying on it (Fig. 6.2 E-F) and immediately aligned with stand-alone µPs MNs still within the PDMS stamp. The samples are kept in climatic chamber for 120 min and finally lifted off.

According to the fabrication of PMMA pillars, two main optimizations assumed a primary role. The first one was to speed up the process, achieved by matching contour caving functions with proper diameter tips to replace the pocket caving function. The fabrication process of pillars takes less than 3 hours in the end. The second mandatory optimization was the achievement of the alignment between the pillars and the cavities within the stamp. The PDMS stamps are obtained from a positive master and because of the shrinkage effect, the center-to-center distances are slightly affected. Consequently, center-to-center distances of PDMS cavities (3 samples) were registered and the average value was pulled out. It resulted in an error of 1,8% with respect to the center-to-center distances of the positive master. This shift was taken into account when designing pillars, and alignment was achievable (Fig. 6.2 G-H). The alignment takes place because of transparency of PMMA and by using stereomicroscope. In the end, each pillar was aligned with the corresponding microneedle (Fig. 6.3).

Other pillar-based methods exist but typically rely on sophisticated methods to fabricate pillars (Chen et al., 2017) or are time consuming processes (S. Kim et al., 2020), which could be an opposing factor to clinical translation. Moreover, the number of needles per array is lower than the

one proposed here (256), leading to lower drug amount. The method presented here is a time-saving process, considering dissolvable microneedles patches and PMMA pillars may be fabricated in one day concurrently. Considering that, automation studies are under investigation right now.

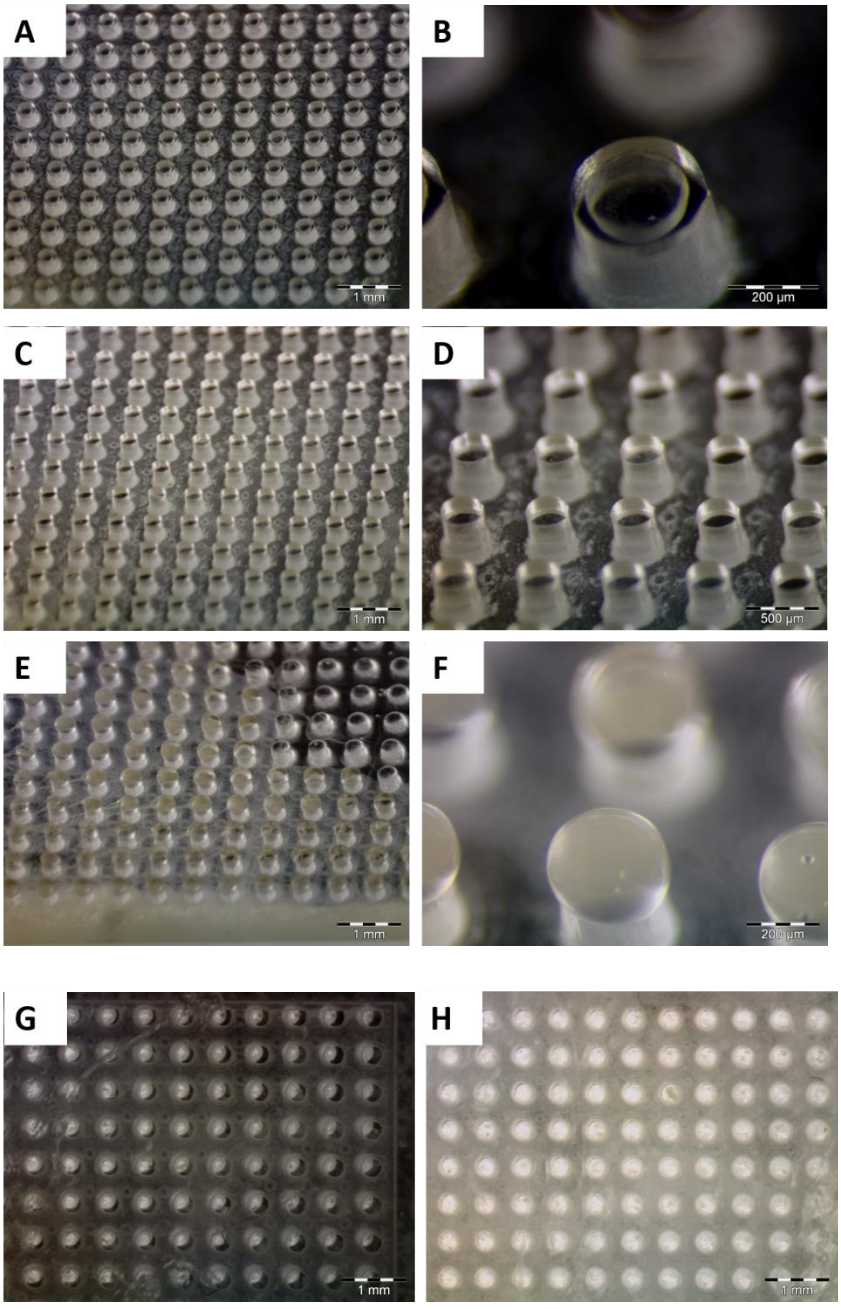

Figure 6.2 Hollow in a half pillars for the breaking step A,B; Bulk pillars for the harvesting C,D; Glue-like solution on the edges of pillars E,F; Misalignment due to PDMS shrinkage G; Alignment after including 1,8 % error H

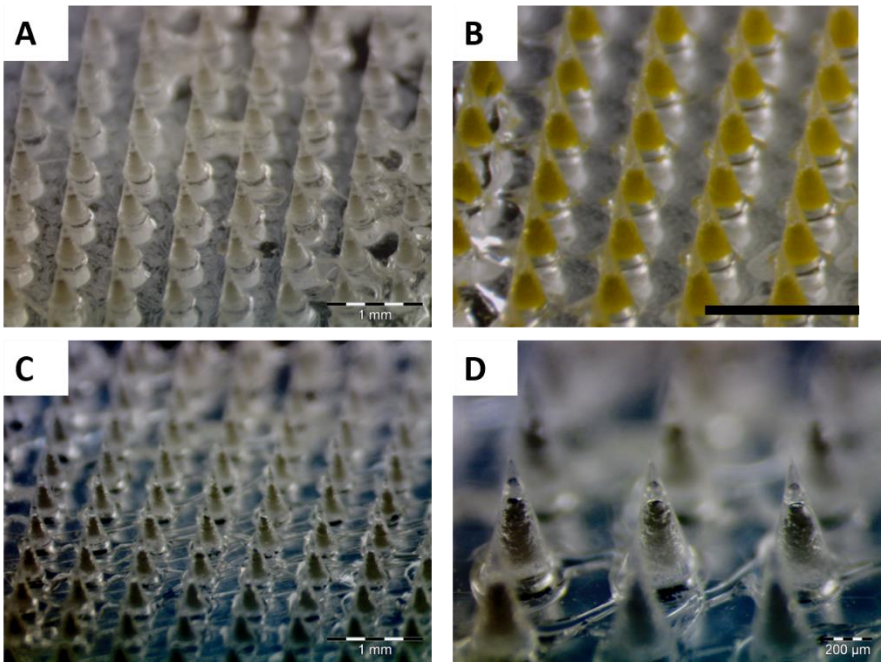

Figure 6.3 Examples of µPs MNs integrated with bulk pillars

5.4 Mechanical characterization

Mechanical characterization is essential to evaluate the behavior of microneedles, especially for the dissolvable category. Typically, the fracture force is examined to determine the load which miconeedles can withstand. The analysis of fracture force ensures that µPs MNs do not bend or fracture during skin insertion. According to the ASTM D695-10 standard, dissolvable µPs MN underwent a compressive test to evaluate the fracture force. Compressive tests are widely employed because they mimic the insertion of MNs within the skin. A 1 kN cell was used to evaluate the mechanical behavior of a complete array of 256 microneedles. The force-displacement curve drops when the failure force is achieved, which is considered the maximum load the MNs can withstand. The fracture force corresponds to 85 N, which converts into 0.33 N/needle (Fig. 6.4A). Addiotnally, the failure force of the IP-S positive master (Fig. 6.4 D) was analyzed and was equal to 245 N, which converts into 0,96 N/needle. The curves of dissolvable patches were comparable to positive master ones. A more sensitive cell was also implemented to investigate the fracture force of microneedles. Compressive tests using a 10 N cell were carried out with 4 microneedles samples. The fracture force resulted in 1,5 N, which converts into 0,375 N/needle (Fig. 6.4B). These values are definitively higher than the limits required to pierce the stratum corneum. 0,375>0,06-0,1 N/needle (J. H. Park et al., 2005; Shu et al., 2021).In general, the resistive

force of the skin is 3.18 x 10^6 N/m^2 (Davis et al., 2004). These tests were performed on microneedles without pillars.

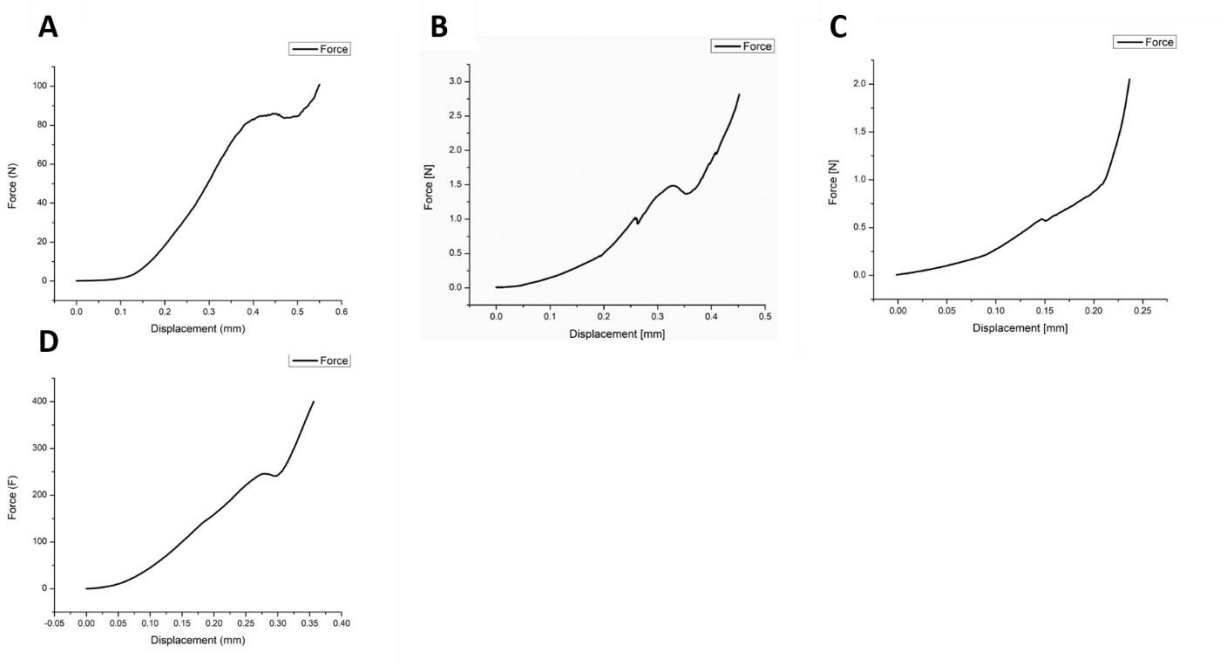

Figure 6.4 Failure force of a dissolvable complete array of 256 needles A (1 kN cell); Failure force of dissolvable sintered sample B (10 N cell); Failure force of dissolvable not sintered sample C (10 N cell); Failure force of IP-S positive master D (1 kN cell)

Moreover, a remarkable observation was made by comparing the failure forces of samples with and without exposure to solvent vapors to achieve the sintering effect. The failure force of the sample without exposure to solvent vapors was determined and found to be equal to 1 N (0,25N/needle) (Fig. 6.4 C). Considering that, the sintering effect should ensure a higher value of the load the microneedles can withstand to. Despite that, this effect did not consistently emerge in each comparison (10 samples) of sintered-not sintered samples. Factors such as the sensitivity of the cell and variations in environmental conditions may affect the outcomes. A wider exploration of the phenomenon is planned forthcoming.

Additionally, a stress-strain curve was derived by failure-force data. The criterion of similar triangles was used to consider the variable section of cones. The volume may be considered constant during compression, assuming the load is perpendicular to the cones (Du et al., 2021). The tip radius was considered 0,9 μm for the first value of stress. The stress response is high at the beginning of the compression plate stroke and rapidly decreases, assuming a plastic material behavior, which suggests that this contributes to incomplete implantation within the skin. Pillars

are supposed to concentrate the pressure on the base area, thus harnessing the initial response of the microneedles to pierce the skin and complete penetration, assuming the lowering of the resistive force of the skin once the stratum corneum is pierced.

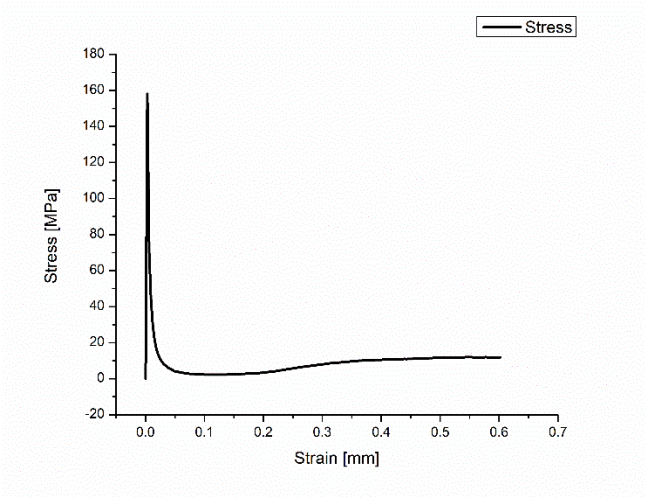

Figure 6.5 Stress-Strain of µPs MNs

5.5 Full thickness skin model characterization

An endogenous–human skin equivalent (Casale et al., 2016, 2018) was employed to assess the dissolution properties of the tip compartment, ensuring cargo release within a few minutes, and the capability to be fully implanted. This model mimics human skin behavior. PMMA chambers were prepared to host the skin model during the insertion process. The compressive test station was customized to mimic the insertion using an applicator to eliminate variability due to the operator. The insertion was set to provide implantation at a rate of 0.5 mm/s, pressing the samples on the model for 180 seconds, considering the superior limit of applied force as 20 N, the average value of human pressure using thumb (Bauleth-Ramos et al., 2023; Larrañeta et al., 2014). Customized patches were fabricated to match the model dimensions (Fig. 6.6 A), and sulphorhodamine B was loaded as a dye in the tip. The skin model was placed in the chamber onto the lower plate and the microneedle patch mounted onto the upper plate (Fig. 6.6 C,H). The tips were fully dissolved after 180 seconds (Fig. 6.6 B), achieving proper implantation and µPs were released within the skin model (Fig. 6.6 E,F). The force-displacement curve of the test is reported (Fig. 6.6 I), and mimics the non-linear behavior of human skin. Post-indentation immunofluorescence is also shown (Fig. 6.6 G), revealing the subsequent micro-channel matching

the dimensions of µPs MNs. Collagen surrounds the channel, and the blue and green dots identify fibroblasts and keratinocytes nuclei, respectively.

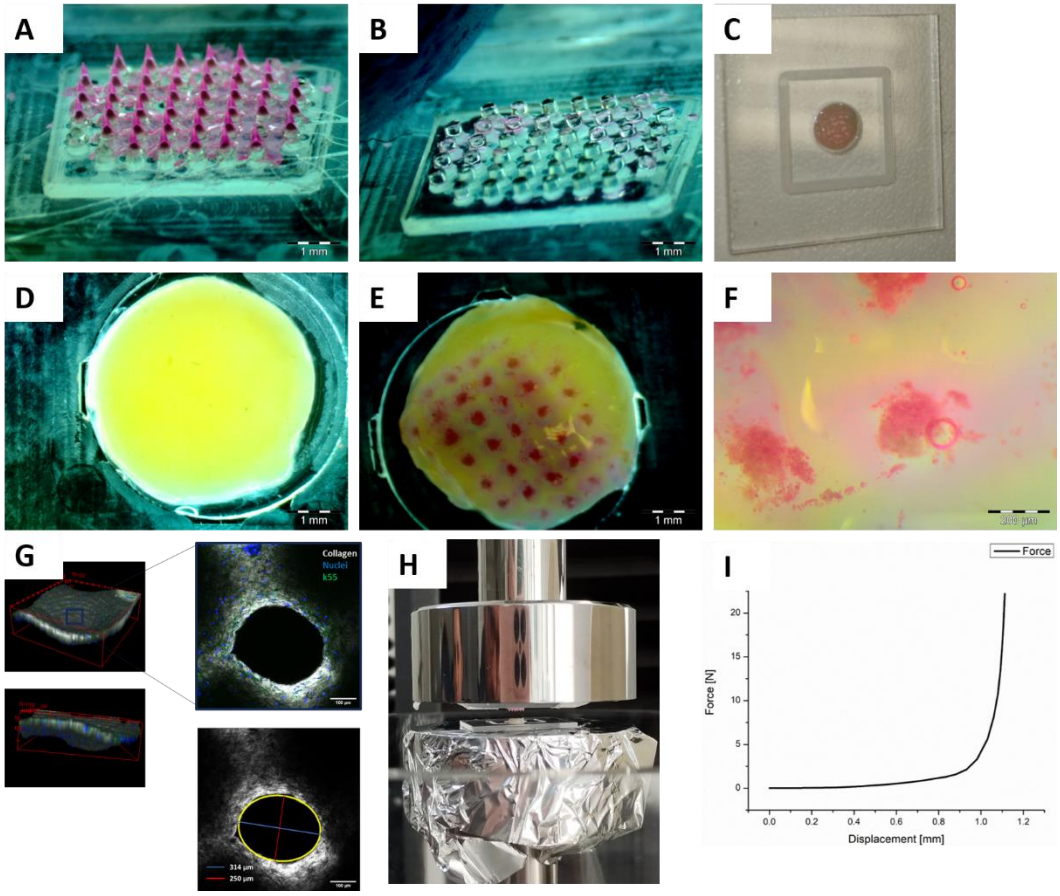

Figure 6.6 Pillar-based µPs MNs customized for skin equivalent model A; dissolution of µPs MNs after 180s B; PMMA chamber to host the skin model C; Endogenous–Human skin equivalent before application of µPs MNs D; Array of µPs MNs totally inserted in Endogenous–Human skin equivalent model E; Magnification of PLGA particles released within the model F; Immunofluorescence after implantation test, it confirms total implantation considering the axes dimensions were 314 µm and 250 µm G; Customized set up to conduct the experiment H; Displacement-Force curve pulled out after the implantation I

5.6 *Ex-vivo* pig skin

Ex-vivo pig skin was employed to assess µPs MNs features in conditions similar to the previous test with the skin equivalent model. It emerged that higher forces were required to properly implant the µPs MNs compared to the previous test. Consequently, 40 N was set as the upper limit for achieving a proper implantation. Typical forces used to push microneedles against skin range to 25-50 N (Larrañeta et al., 2014).This difference may be attributed to the removal of skin tissue from its natural environment. In ordinary conditions, the skin is subject to pre-conditioning stress due to elastin and collagen. In *ex vivo* conditions, the fibers tend to crimp, leading to the relaxation of the skin sample and easier accommodation of mechanical behavior under applied loads,

obtaining more intense deformations before complete implantation of the µPs MNs. Further experiments using skin in a pre-conditioning state, mimicking *in vivo* conditions, are planned to demonstrate how the pillars reduce the force required. Moreover, implantation test using microneedles without pillars were carried out, and implantation was not achieved. The pattern and delivery of PLGA µPs are evident in the picture. In histology pictures, the piercing of stratum corneum is clear, and the dermis was reached (Fig. 6.7).

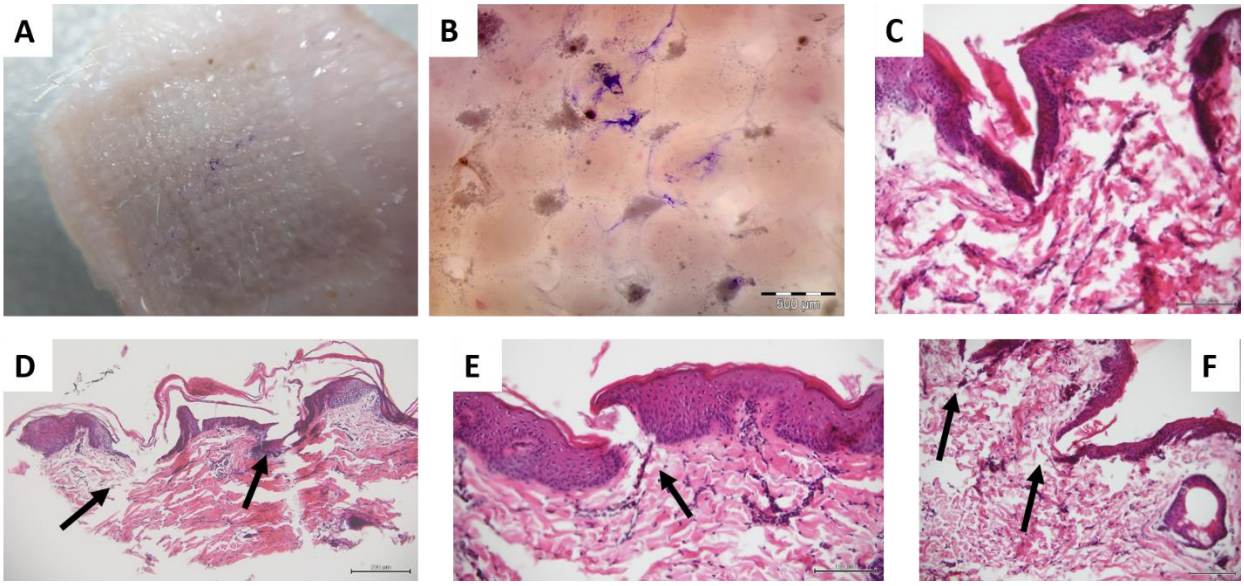

Figure 6.7 implantation of pillar-based µPs MNs in ex vivo pig skin A,B; Histology sections of implantation of pillar-based µPs MNs in ex vivo pig skin C-F

6 Applications

6.1 Introduction for MNs targeting different barriers

Microneedles, originally developed for transdermal drug delivery, have found diverse applications in various other administration pathways, including oral, buccal, intramyocardial, and ocular routes. In oral administration, microneedles can directly inject pharmaceuticals into the intestinal epithelia, overcoming gastrointestinal mucus barriers and enhancing drug bioavailability (Abramson et al., 2019). In the context of buccal delivery, microneedles enable the direct transfer of drugs into the systemic circulation, bypassing hepatic first-pass metabolism. Furthermore, microneedles provide a means for localized drug application at high concentrations directly to the

affected sites, particularly in intramyocardial or ocular delivery scenarios. Despite the versatility of microneedle technology, the application of microneedle technology faces certain challenges due to the less accessible nature of many delivery sites. These challenges are partly attributed to the limited operational areas, such as the small and sensitive regions of the eye and oral cavity, or the deep tissue locations within the human body, including the heart and intestines. Consequently, these physiological constraints necessitate the development of more sophisticated microneedle designs to enable efficient and effective drug delivery (Le et al., 2023).

6.2 Customized µPs MNs for industrial partner

MNs-based technology may target barriers different from skin. µPs MNs platform was investigated to be customized according to the demand of the private partner for an industrial application. µPs MNs were required to modify several features with the purpose to endure in physiological conditions. The customized features included:

1. Harvesting layer
2. Mechanical behavior of polymers
3. Dissolution rate of the tip compartment
4. Specific Drug-loaded PLGA µPs

1) Pillars were replaced with a layer provided by the partner. The harvesting solution was modified to ensure adhesion the layer. The platform needed to be adapted to a very flexible layer, with the purpose of reproducing even rolling movements. The harvesting solution was renewed: a blend of PVP, hydroxyethyl cellulose (HEC), Glycerol and Tween 80 was produced. PVP/HEC mass ratio was equal to 14. Additionally, oxygen plasma treatment was integrated to enhance the adhesion between the harvesting solution and the layer. This harvesting solution made possible to have a flexible harvesting layer.

2) In order to have a complete flexible patch, HA was replaced by HEC as well. The blend solution for the tip compartment was given by a blend of PVP, HEC and Tween 80 (2% w/V). This time PVP/HEC mass amount was equal to 15, considering 80 mg/mL was the superior limit for concave-shaped microneedles. HEC both in tip and harvesting solution allowed to have a flexible patch, capable of moving together with the layer. On the other hand, HEC increased the swelling effect of polymeric blend, leading to have cavities smaller within the body of the microneedles.

3) As shown in previous sections, µPs MNs dissolve in a few minutes, the challenge was to tune the dissolution time of tip compartment to target the barrier of interest, and release the PLGA µPs. Hard efforts were necessary to find out the right conditions to slow the dissolution of the tip compartment. Spray coating technique was implemented to coat µPs MNs with a PLGA solution. A customized system was set to fulfil the goal, combining instruments of spray coating, spin coating and syringe pump. A SCHLICK Two-Substance Nozzle 970 S8 was used to spray PLGA solution. Different parameters contribute in implementing the technique: typology of coating, time of deposition, flow rate of the solution, air pressure, nozzle opening, nozzle-sample distance, rotation of the sample for uniform deposition and relative rpm. PLGA 1% w/V was dissolved in a solution of Ethyl acetate and DMC (1:4), the sample was placed on the holder of a spin coating machine to induce the rotation of the sample setting 150 rpm while air pressure was set at 0,5 bar. A thin and uniform layer of PLGA was deposited on the samples in order to decrease the dissolution rate and remodeling it from 2-3 min to longer time.

4) Double emulsion method was adapted to encapsulate the drug of interest in PLGA µPs. The double emulsion method is described in experimental section.

In the end, the patches exhibited a flexible behavior, slower dissolution rate and proper drug release.

6.2.1 Fabrication Process

The fabrication process of µPs MNs was carried out as the usual process, taking into account the exposed modifications. Shortly, 150 µL of PVP, HEC, Tween 80 solution was casted on PDMS stamp. Degassing and dehydration were used to dry the polymeric sample. Furtherly, µPs were loaded in cavities of samples and then they were subjected to Etoh/DMC (8:1) vapor for sintering step. The substrate underwent oxygen plasma treatment (1 min at 50 W) and 150 µL of PVP, HEC, Glycerol, Tween 80 solution was casted on the layer. By using an hot plate, it was dried. Furtherly, µPs MNs were placed on a spin coater sample holder to harness the rotation of the instrument and exposed to PLGA (PLA:PGA 50:50) (1% w/V) spray solution (SCHLICK Two-Substance Nozzle 970 S8). The solution was infused through a syringe pump connected to the nozzle (Standard Infuse/Withdraw Pump 11 Pico Plus Elite, Harvard).

6.2.2 Results

µPs MNs were lifted off from the substrate. The flexibility of the array without cracking phenomena on both substrate and microneedles can be appreciated in Fig. 6.8 A-E. The flexibility was crucial to achieve in order to ensure rolling movements. This result allowed for further investigating into dissolution properties. This typology of microneedles revealed an adequate fracture force, although the mechanical properties were lower the PVP/HA formulation. The mechanical fracture force of PVP/HEC was 45 N, which means 0,18 N/needle. Higher flexibility implied a lower fracture force, but still enough according to the state of art (Fig. 6.8 F).

Empty concave-shaped microneedles were exposed to a PLGA spray coating solution employing FITC as a dye (Fig. 6.9 C,D). Confocal microscopy was then used to investigate the shape of microneedles, the uniformity of the deposition and the reduction in tip diameter resolution. The green signal represents FITC. Morphologically, microneedles maintained their conical shape and the deposition of the PLGA solution appeared uniform on the substrate and on the needle's surface. However, a loss of tip diameter resolution was evident, resulting in 19 µm. PLGA-coated µPs MNs are presented in Fig. 6.9 A,B. The roughness is different in the picture, and a comparison between the tips is presented.

For drug release studies under physiological conditions, µPs were dissolved in 1.5 mL of PBS (pH 7.4). At various time points, 1 mL of the solution was removed and analyzed by fluorescence. Figure 7 A illustrates that µPs containing the drug released 63.9% (mean value, SD $\pm$ 1.48) after 4 hours. This procedure was replicated to dissolve µPs MNs (without PLGA coating) and Figure 7 B shows correspondence between both types of release.

With regards to the characterization tests of dissolution, the samples were delivered to the private partner. A specific media was used to assay slower dissolution properties of the platform. After 3 min it still showed an impermeable behavior. After 1h, the cargo was not released yet, but initial swelling effects and some dissolved spots were evident (Fig. 7.1). After 2.25 h, samples were dissolved and the cargo was released. Cryo sections show complete penetration into the tissue of the PLGA-coated µPs MNs in ex vivo model (Fig. 7 C-D).

In conclusion, customization was achieved. It was the proof of a first attempt to modify several properties of the platform by starting from a robust protocol.

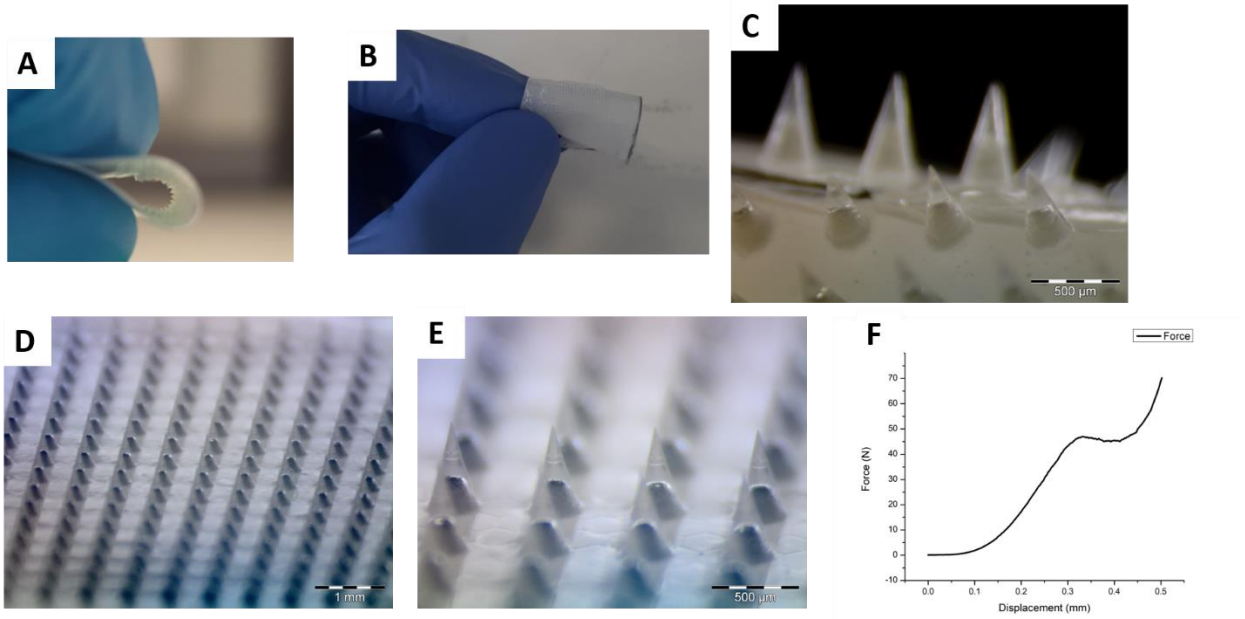

Figure 6.8 Flexible behavior of PVP/HEC µPs MNs A-C; PVP/HEC µPs MNs on substrate D,E; Fracture force of PVP/HEC MNs F

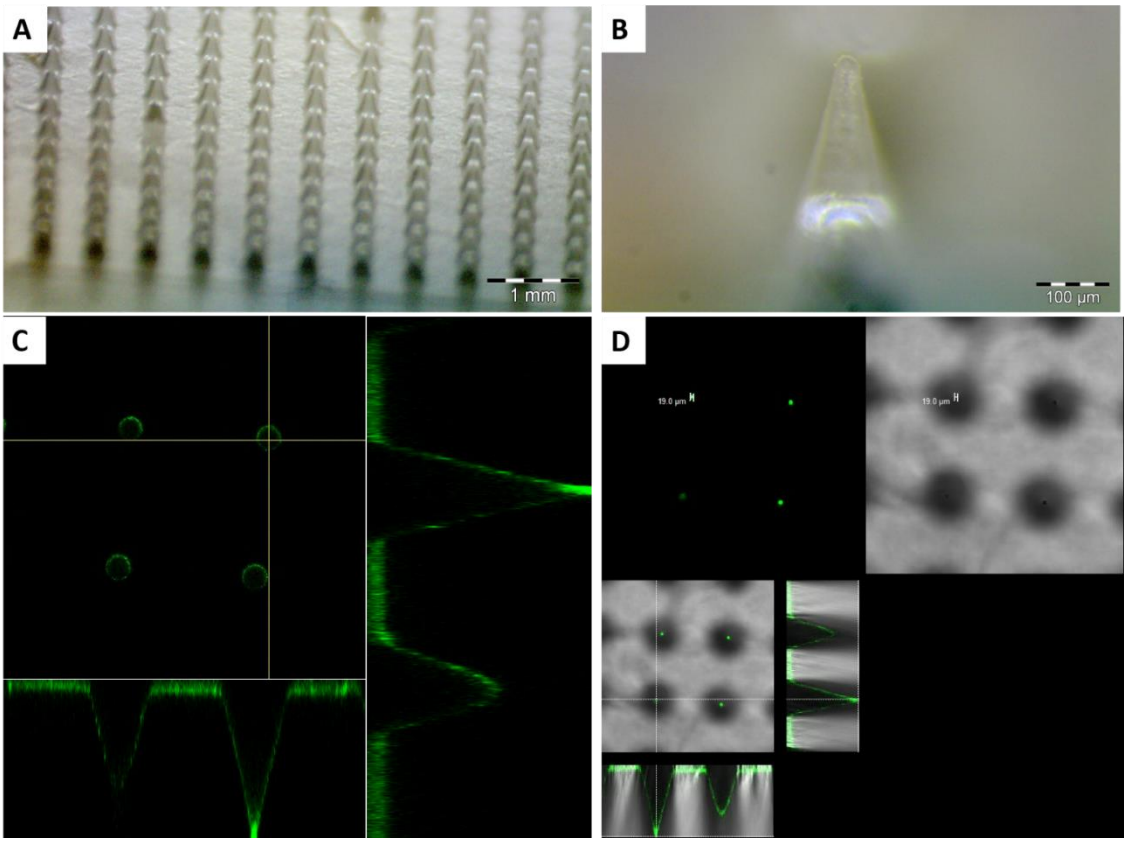

Figure 6.9 PLGA-coated PVP/HEC µPs MNs A,B; PLGA-FITC coated PVP/HEC µPs MNs to investigate deposition properties C,D

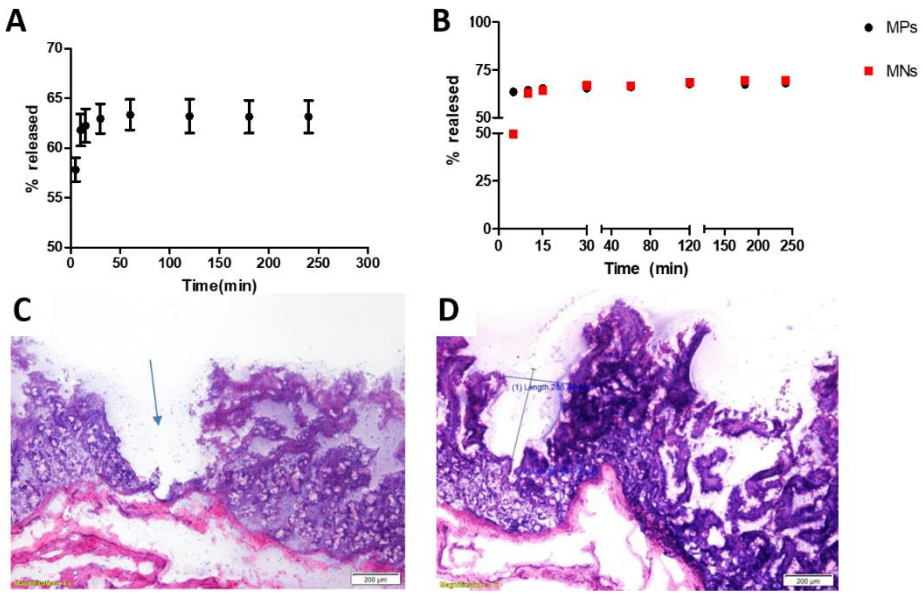

Figure 7 Drug release from PLGA µPs A; Drug release from PVP/HEC µPs MNs B; PLGA-coated µPs MNs in ex vivo model C,D

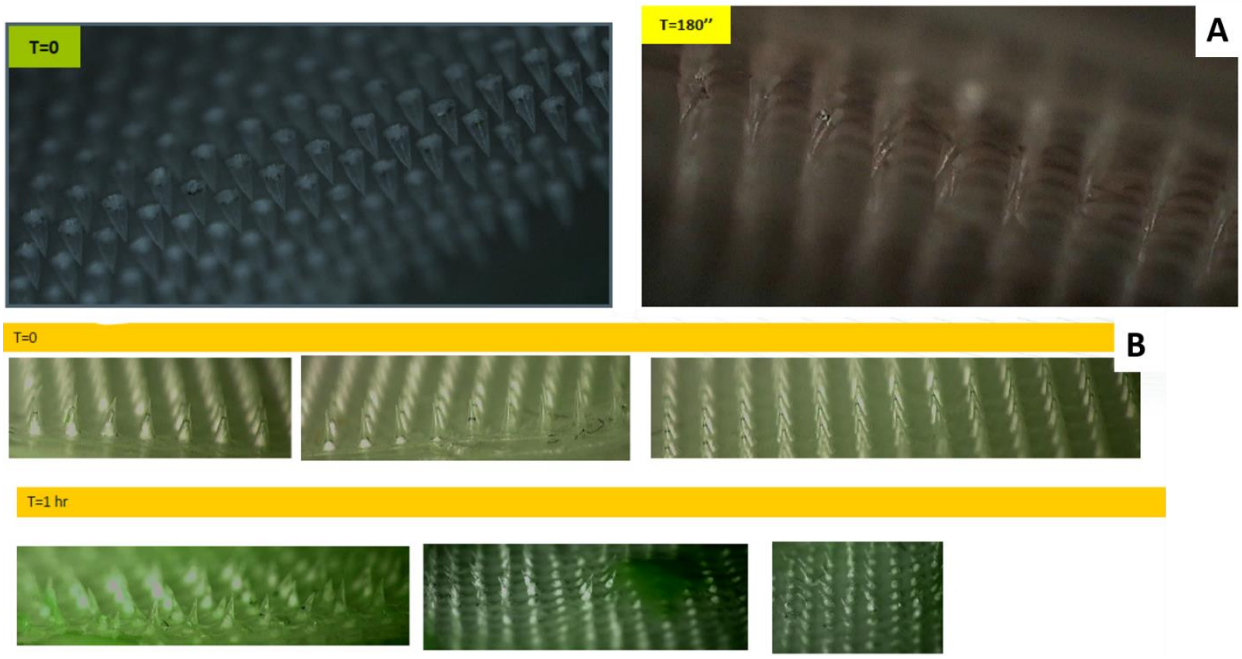

Figure 7.1 Dissolution properties of PLGA-coated PVP/HEC µPs MNs in physiological fluid

6.3 Introduction in triple negative breast cancer application

The triple negative breast cancer (TNBC) represents 10-20% of all breast cancers and it is characterized by the lack of three common breast cancer biomarkers, such as estrogen, progesterone and epidermal growth factor receptor 2. The absence of specific drug-receptor bindings is responsible of its aggressiveness and difficulty on the treatment. Current therapy relies

on classic chemotherapy, resulting in a poor response and high side effects. Immunotherapy explores the role of the immune system, giving it a pivotal role in cancer treatment. The immune system, with its complex mechanisms, protects against external pathogenic stimuli, with T cells playing a crucial function. These cells express on their surface some proteins that can activate or deactivate an immune response, called checkpoint proteins. Briefly, checkpoint proteins make T cells become active, for example when an infection is present. Different checkpoints make T cells deactivated, because they may attack healthy cells and tissues. In this context, cancer cells express high levels of these latter proteins deactivating T cells and suppressing their ability to recognize cancer cells. TNBC calls for novel therapies: immunotherapy is based on the usage of monoclonal antibody to block checkpoint proteins and for this reason they are called checkpoint inhibitors. The goal is to suppress cancer cells mechanism of deactivating T cells, allowing these cells to recognize and attack cancer cells (Akyala et al., 2018; Hu & McArthur, 2018; Shokooh et al., 2022). FDA has recently approved the use of monoclonal antibodies in combination with paclitaxel for the treatment of TNBC. Typically, such molecules face challenges in passing through the skin barrier and are not stable at room temperature . In light of this introduction, µPs MNs were explored to improve drug tumor targeting within a Fondazione Veronesi project.

6.4 µPs MNs for the treatment of the Triple negative breast cancer

µPs MNs were investigated for drug tumor targeting with the aim of enhancing antibody and paclitaxel stability and, as a consequence, increasing their therapeutic properties and reducing their side effects. The platform is customized for the delivery of three different drugs: a proteolytic enzyme, such as collagenase, was loaded into the polymeric solution used for the tip compartment, while paclitaxel and monoclonal antibody were separately loaded in µPs. Collagenase was intended to degrade the extracellular collagen matrix to promote the delivery of the drugs encapsulated in the µPs. This approach allows to protect the drugs from proteinases when they are released in the plasma, theoretically. The polymeric blend for the tip compartment was adapted for including collagenase while preserving mechanical properties concurrently.

6.4.1 Experimental section of µPs MNs for the treatment of the Triple negative breast cancer

A Tris buffer (Tris 25 mM, CaCl3 10 mM, pH 7.2) was prepared and used to dissolve Collagenase A (0.226 U/mg, Roche) at a concentration of 2.3 mg/mL. µPs MNs were prepared replacing 70

µL of Milliq water with 70 µL of Collagenase A dissolved in Tris buffer. The fabrication process of the tip compartment proceeded without any modifications.

The µPs were obtained using the water/oil/water double emulsion/solvent evaporation technique, as previously documented. This method facilitated the encapsulation of two different drugs; specifically, monoclonal antibody was encapsulated in the first water phase, while paclitaxel was loaded in the oil phase. Additionally, to achieve highly porous µPs, ammonium bicarbonate (ABC) was employed as a gas foaming porous agent. Specifically, 100 µL of a 7.5 mg/mL ABC solution was incorporated into the initial emulsion to produce highly porous particles. The water phase included 200 µL of monoclonal Antibody-Atto647 at a concentration of 0.69 mg/mL, while the oil phase consisted of 100 µL of paclitaxel (PXT) at 5mg/mL in acetonitrile loaded in dimetilcarbonate (DMC). µPs with only monoclonal antibody or PXT separately were prepared as control samples.

Confocal microscopy (Leica SP5 microscope, Wetzlar, Germany) was used to exmine the different formulations of µPs, as well as the multicompartmental structure of the microcones, to assess the molecular signal within them. Specifically, fluorescence images were captured with an HCX IRAPO L 25×/0.95 water objective and a 488 nm laser for excitation, as previously outlined.

The average size and Polydispersity Index (PDI) of both µPs were determined through static light scattering (Mastersizer 3000, Malvern Instruments, Malvern, UK) at a concentration of 3 mg/mL in water.

The morphology of µPs was examined using SEM microscopy. Briefly, 20 µL were placed on a standard SEM pin stub and analyzed with FESEM ULTRA-PLUS (Zeiss) (Milan, Italy) at 5 kV using the SE_2 detector. Additionally, the internal porous structure of the µPs was investigated using a 2 mm thick PDMS cured at 80 °C for 30 min. After cooling, µPs were positioned on it, and another PDMS layer (2 mm thick) covered them. Subsequently, the solid PDMS block was frozen in liquid nitrogen (–196 °C) and cut using the Leica CryoUltra Microtome EM-FC7-UC7 (Milan, Italy).

For in vitro indentation preliminary tests, a 3D in vitro dermis equivalent model was prepared. The model was prepared by incorporating the Triple-negative Breast Cancer Cell Line MDA-MB 231 into a collagen matrix. The cells were cultured in a complete medium, comprising Dulbecco's

Modified Eagle's Medium (DMEM) supplemented with 20% FBS, 1% glutamine, 1% non-essential amino acids, and 100 U mL−1 penicillin, 100 mg mL−1 streptomycin. Cultivation took place in 100 mm diameter cell culture dishes within a controlled, humidified atmosphere at 37 °C and 5% CO_2. The medium was refreshed every 2–3 days.

Collagen gels were formed using rat-tail collagen solution (ibidi®), reconstituted following the manufacturer's guidelines, and employed to assess the in vitro co-activity of collagenase-µPs MNs. A suspension of 6 × 10^4 MDA-MB-231 cells in 300 µL of 4 mg mL−1 collagen solution was poured into a flourish. The system was then incubated at 37 °C for 30 min to facilitate collagen fibrillogenesis, followed by the addition of fresh cell culture medium to the gel.

The Instron station was used to assess mechanical properties of collagenase-loaded µPs MNs at a rate of 1.1 mm/min through a compressive test.

6.4.2 Results

This typology of microneedles revealed adequate fracture force, 0,34 N/needle, and adaptability to the process (Fig. 7.2). The amount of collagenase was optimized to not affect mechanical properties. Confocal microscopy was used to assess the multi-compartmental nature of the platform. In Fig. 7.2 B, collagenase in the tip and the PXT particles in the body of the microneedles are clearly visible.

A detailed study of µPs morphology was conducted using confocal microscopy, employing two different fluorophores: Atto 488 for paclitaxel (PXT) and Atto 647 for the antibody. The perfect shape of our µPs is evident in Figures 7.3 A and D, where the green signal represents PXT, blue indicates the antibody, and in Figure G shows µPs with both drugs, represented by a merge of the two colors. The correct shape was also assessed using SEM microscopy (Fig. 7.3 B,E,H), confirming uniformity and diameter through Mastersizer analysis (Fig. 7.4).

For drug release studies under physiological conditions, µPs with only PXT, only the antibody, and a combination of both were dissolved in 1.5 mL of PBS (pH 7.4). At various time points, 1 mL of the solution was removed and analyzed by fluorescence. 100% EE for PXT and 50% for the antibody were obtained separately. Similar results were confirmed in multifunctional µPs when combining PXT and antibody (Fig. 7.3 C, F, I). Figure C illustrates that µPs containing only PXT released 100% after 4 hours, as expected for a small molecule like PXT. Antibody-loaded µPs

released 50% of the drug after 24 hours. Crucially, multifunctional µPs loaded with both drugs exhibited consistent release patterns, indicating that even in this type of µPs, the pharmacokinetic properties of the drugs remained unchanged.

A skin collagen model was produced to scrutinize ability of microneedles and the release of active substances. In detail, cells derived from human TNBC were cultured in a layer of collagen forming a 3D model of skin. After the formation of the layer, the three conFiguretions (PXT- µPs, antibody-µPs, PXT-antibody- µPs) of µPs MNs were indented and the release of drug loaded- µPs was studied by confocal microscopy. The insertion of microneedles is reported in the figure 7.5 A. Cells within the collagen fibers are visible in figure 7.5 B, while in figure C, the release of µPs after 1 h from insertion of MNs is observable. The green signal indicates PXT, while the blue signal highlighted in the blue spot represents the antibody signal. The blue signal is weak, confirming a slower release in comparison with PXT µPs. Moreover, in figure C collagenase was included in MNs, while in Figure D, µPs MNs were collagenase-free. In Figure D, a lower percentage of drugs is detectable, giving a reason of collagenase acting as an enhancer of drug release. Before applying for in-vivo trials, *ex-vivo* mouse skin implantation was performed. This experiment was carried out loading FITC as dye in PLGA µPs, to avoid wasting PXT and antibody. Confocal microscopy was used to assess pillar-based µPs-MNs implantation. The inner part of the skin was placed on the sample holder of the confocal microscope. Observing the green signal of the FITC, they were properly inserted into the skin and it is clear how the body of µPs crossed from side to side, because the typical array is visible (Fig. 7.5 E).

Collagen models were also used to perform a cellular µPs toxicity assay. Interesting results were obtained: higher toxicity was expressed by PXT-µPs, even in healthy breast cells, after 72 h. Lower toxicity was expressed by antibody-µPs. Due to that, toxicity of empty µPs was evaluated in control cell line (Fig. 7.6). The best result was obtained for multifunction µPs. A combined effect between antibody and PXT was observed, where toxicity in breast cells was evident and no toxicity in healthy cell also at 72 hours. At any time, no toxicity in both cell lines was observed for empty µPs.

In conclusion, promising results were obtained. The platform showed adaptability in this context and *in vivo* experiments are underway.

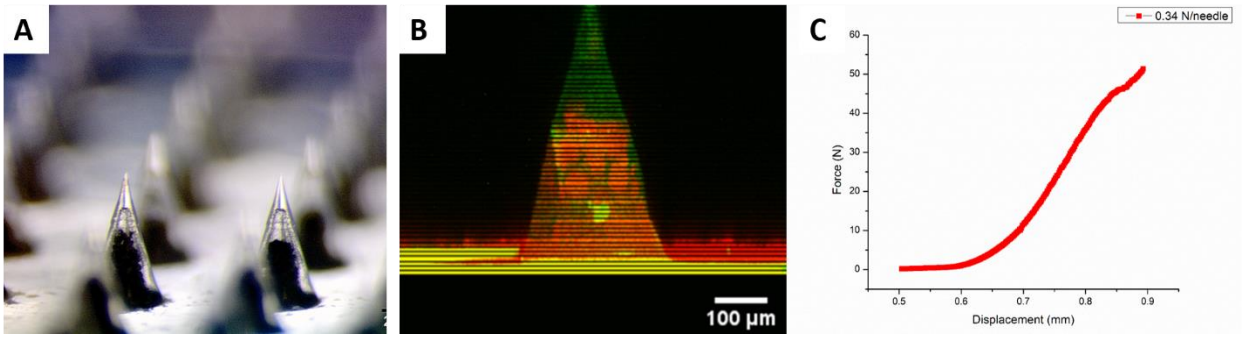

Figure 7.2 Collagenase-loaded PVP/HA µPs MNs

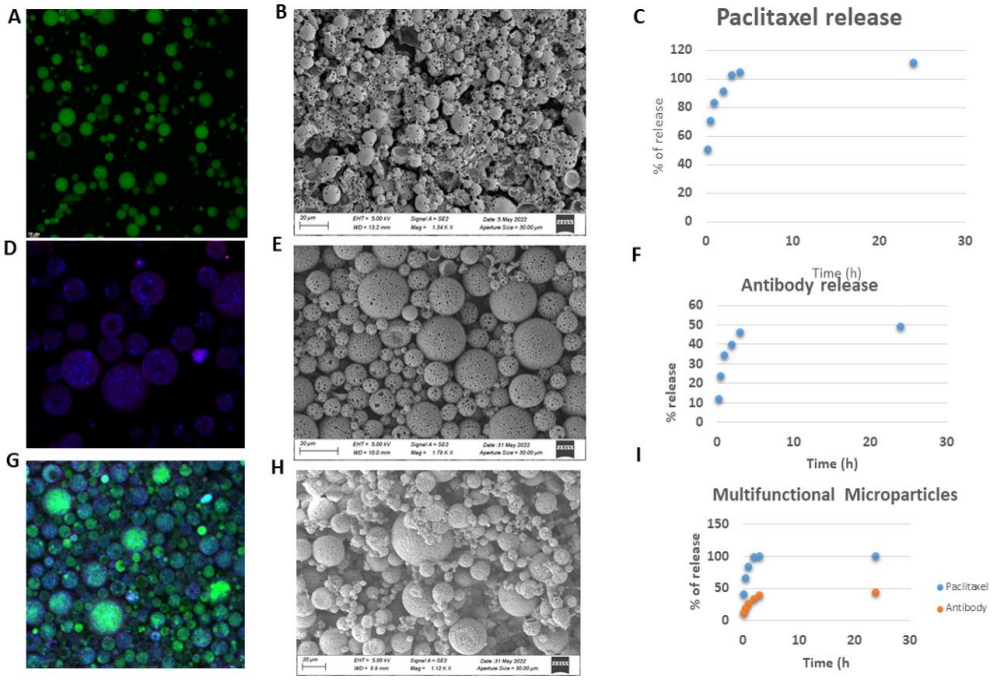

Figure 7.3 Confocal investigation of µPs loaed with PXT (A), antibody (D), merge of the signals (G); SEM morphological investigations of µPs B, E, H; Release properties of PXT-loaded µPs (C), antibody-loaded µPs (F), multifunctional PXT-loaded and antibody-loaded µPs (I)

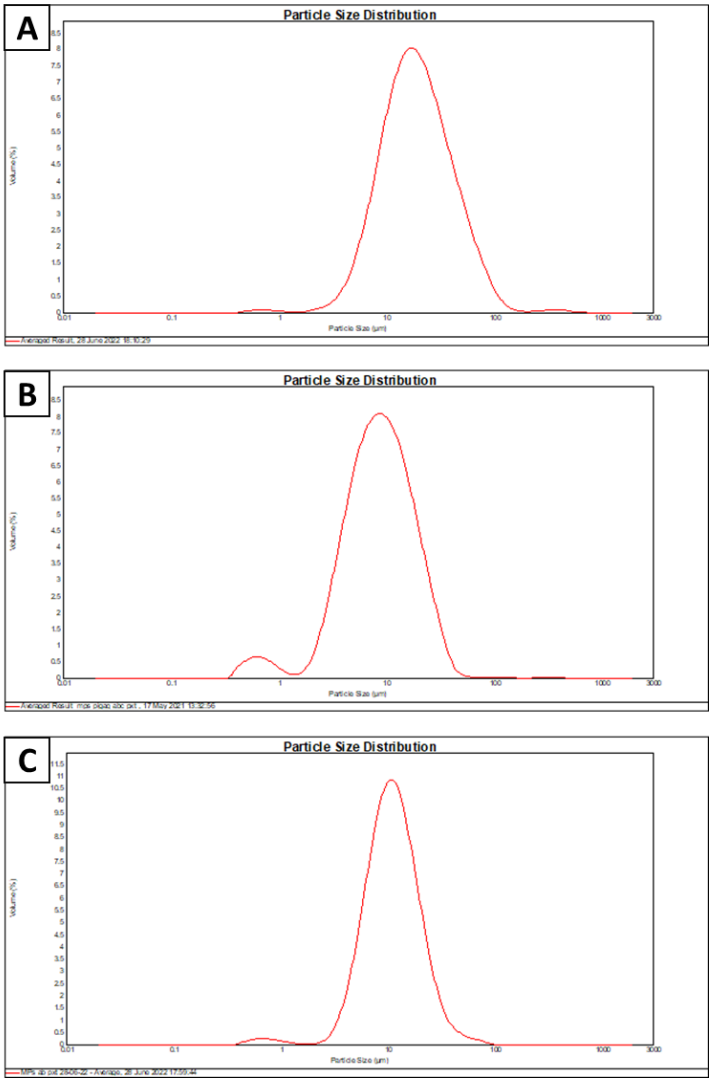

Figure 3 Mastersizer analysis: A PXT-µPs $D_{average}$= 8.70±2.1 µm, B Ab-µPs $D_{average}$= 14.7±2. µm, C Multifunct-µPs $D_{average}$= 10.9±1.6 µm

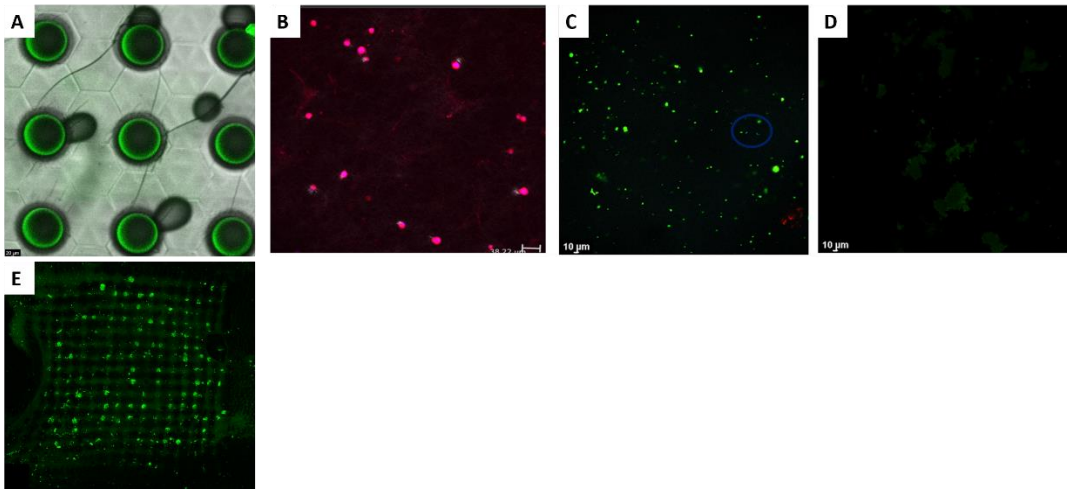

Figure 7.5 Collagen implantation A-D; Ex vivo mouse skin implantation E

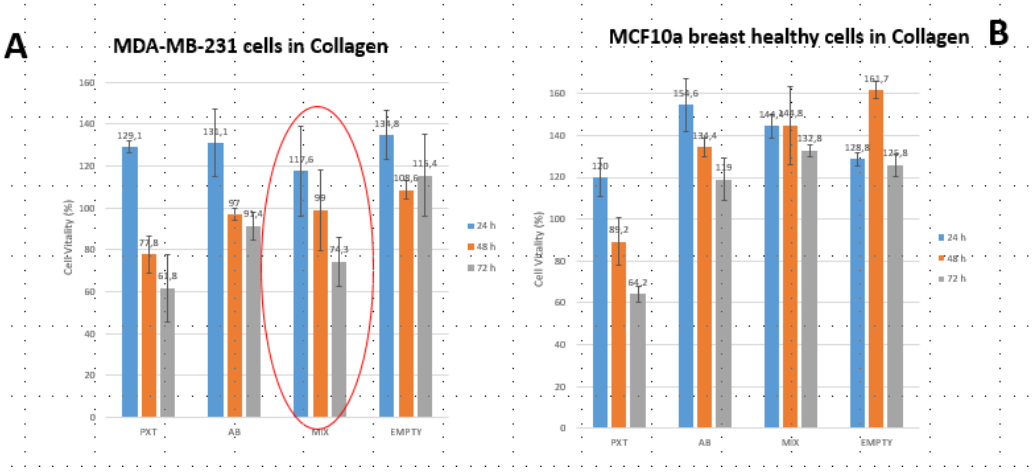

Figure 7.6 Collagen models were also used to perform a cellular µPs toxicity assay

6.5 Introduction in MNs for mRNA delivery

Microneedles (MNs) enhance the efficacy of vaccines by facilitating intradermal delivery of antigens directly to the epidermis and dermis, which are rich in antigen-presenting cells (APCs), a crucial component of the immune response. This targeted delivery to APC-abundant areas has the potential to amplify the immunogenicity of the vaccine, resulting in a more robust and effective immune response. By capitalizing on the dense presence of immune cells in these skin layers, the interaction between the vaccine and the body's immune system is optimized. In particular, dissolvable MNs are especially promising for vaccines application as they rapidly release the payload after dissolution to APCs. One of their key advantages is the preservation of the activity of vaccine components within a polymeric matrix at room temperature, avoiding the need for a

cold chain, which is necessary for current vaccines. The COVID-19 pandemic elucidated the significance of mRNA vaccines and the challenges to overcome such as suboptimal vaccine storage, distribution infrastructures and scarcity of healthcare professionals. In addressing the critical need for efficient mass vaccination strategies, particularly in low- and middle-income countries, MNs offer several advantages. These include ease of self-administration, minimal discomfort, enhanced shelf life, and the ability to circumvent the need for cold chain logistics. The adoption of this technology could revolutionize vaccine distribution in resource-limited settings, representing a significant stride towards global health equity in vaccination efforts. However, it is crucial to incorporate large-scale logics into the strategy for fabricating microneedles, as discussed in more detail in Chapter 1.

6.6 µPs-MNs for mRNA delivery

Based on the robustness of both the fabrication process for microneedles and µPs carriers, the versatility and adaptability of µPs-MNs platform shown in previous applications, it is under investigation for mRNA delivery. It is inserted within the PNRR (National Recovery and Resilience Plan) project "National Center for Gene Therapy and Drugs based on RNA Technology" for a potential further application in the vaccine field. Considering the easiness of mRNA in being degraded, µPs-MNs are explored to efficiently deliver active mRNA at room temperature. In order to ensure that, the structure of mRNA needs to be preserved by PLGA shell of µPs. Considering the APC's uptake of particles plays a crucial role in the transport to the lymph nodes and in the subsequent immune response, distinct strategies are underway. How the size affects the cellular uptake is not clear at all (Benne et al., 2016; Di et al., n.d.; Ji et al., 2022; D. Lee et al., 2023b). Larger size (micro) particles persist longer in the injection site and draining to lymph nodes, while smaller size partciles (nano) have greater chance of being taken up by the cells at the hosting site. Discovering the better strategy, from the engineering of polymeric carriers point of view, for mRNA administration is challenging. A combination of micro and nano particles to provide a novel version of sustained release is even possible. µPs MNs are explored in this field currently, preliminary results are promising to proceed in this direction.

6.6.1 Fabrication of µPs for mRNA delivery

The µPs were obtained using the water/oil/water double emulsion/solvent evaporation technique, according to the following steps:

1. 83 mg PLGA and 17 mg of PLURONIC F68 dissolved in 1 mL of DCM

2. 200 µL of mRNA solution was added to the oil phase and homogenized for 30s at 15.000 rpm

3. First Emulsion was poured into 10 mL 2%v/w PVA and homogenized for 1 min at 20.000 rpm

4. The second emulsion was pured into 30 mL and homogenized for 3h at 450 rpm with a paddle stirrer (Heidolph RZR 2102 control). This allowed the DCM evaporation.

5. µPs were washed three times with RNase free water by centrifuging at 10,000 rpm for 15 min at 4°C (SL16R Centrifuge, Thermoscientific, USA)

6. Lyophilized for 3 days (HetoPowerDry PL6000 Freeze Dryer, Thermo Electron Corp., USA; −50°C, 0.73 hPa) and stored at −80°C.

[1] The mRNA solution was the internal water phase
[1] The oil phase is represented by PLGA + Pluronic F68 in DCM.
[1] 2% PVA is the external water phase

6.6.2 Results

Pillar-based µPs-MNs (PVP/HA) were prepared including sulphorhodamine Bin the tip compartment , as dye, and FITC was loaded in µPs as dye as well. *In vivo* tests on a murine model were performed to assess the implantation capabilities of µPs-MNs exploring further mRNA delivery. They were pushed on mouse back by thumb. The animal was sacrificed and the area of interest was included in PAF 4% to preserve structural morphology. Confocal microscopy was used to investigate the implantation abilities. Considering confocal investigation did not followed immediately implantation test, µPs were likely dissolved in PAF solution (considering 96 % is given by aqueous phase) but the channels due to microneedles penetration were visible, confirming achieving insertion (Fig. 7.7).

Scanning electron microscopy (SEM) and confocal microscopy analysis highlighted a porous structure of mRNA-loaded µPs.

To confirm the presence of mRNA within the µPs and assess their stability, agarose gel electrophoresis was conducted (Fig. 7.8). It was anticipated that the most robust systems would exhibit minimal migration under the influence of the electric field. The samples, including mRNA µPs released at 30 min, 1h, 2h, and 24h, empty µPs, and pure mRNA (500 ng) at a concentration

of 0.250 mg/mL, were prepared with loading dye (40 µL). The samples underwent horizontal electrophoresis using 1.2% agarose gels. Electrophoresis was performed in Tris-acetate-EDTA (TAE) buffer, consisting of 40 mM tris(hydroxymethyl)aminomethane base, 20 mM acetic acid, and 1 mM EDTA at pH 8.0, and ran at 70 V for 35 min. Gel visualization occurred under a transilluminator following staining with Sybergreen. mRNA was still stable after encapsulation and a progressive release was ensured until 24 h.

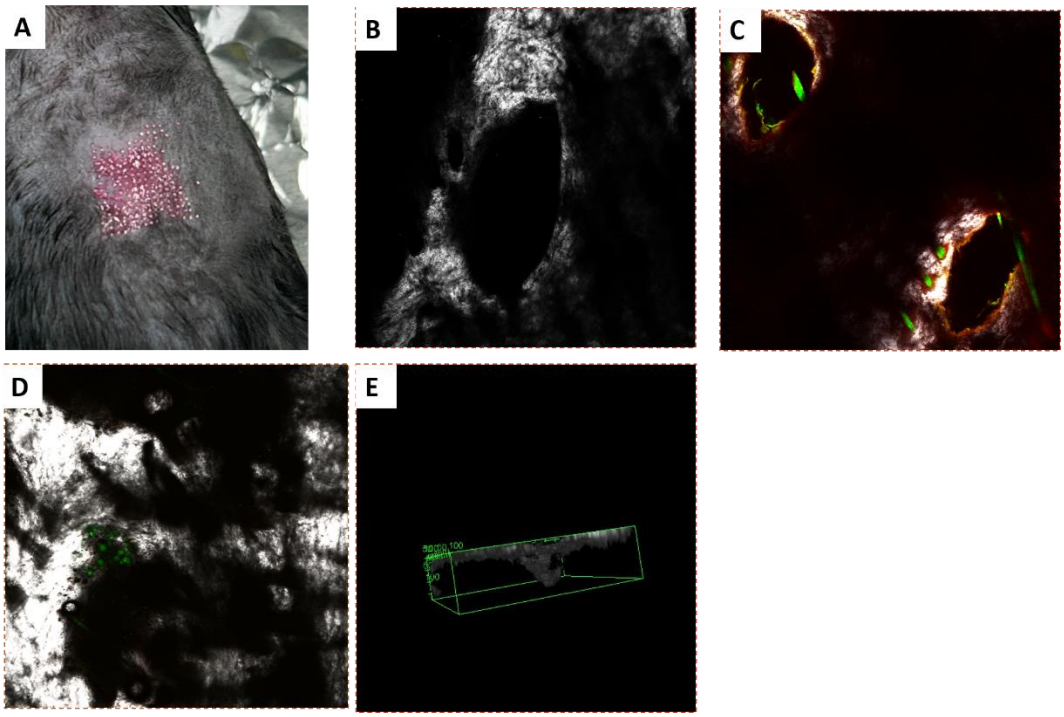

Figure 7.7 Implantation of µPs-MNs in in vivo mouse model

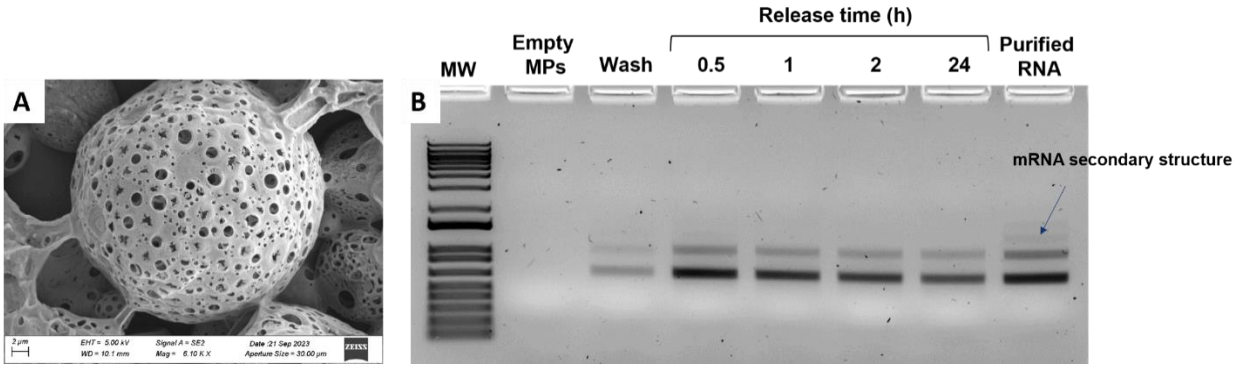

Figure 7.8 Agarose gel electrophoresis to confirm the presence of mRNA

7 Conclusions and Future Developments

Polymeric materials have really improved the controlled release of a drug over time. However, efforts are still required towards more user-friendly pharmaceutical systems and to make patient self-sufficient. Safety, efficacy and usability appear to be the key factors in this context. MNs offer a solution that enables patients to self-administer drugs, avoiding the risk of diseases transmission as well. MNs can accommodate a wide range of molecules, from cosmetic applications to vaccine delivery.

The process of incorporating drugs into MNs is a significant hurdle in their development for drug delivery purposes, influenced by various factors. It is essential to take into account the physical and chemical properties of the drugs, the materials used to fabricate the MNs, as well as the manufacturing technique, and the strength and stability of the compounds. These factors collectively impact the kind and amount of drug that can be loaded into MNs.

Herein, μPs MNs have been adapted in different scenarios and showed their versatility, due to the robustness of the fabrication process. While, they do not satisfy the magic formula of "One size fits all", the combination of MNs with PLGA μPs makes possible their assessment in a broad spectrum of drug delivery applications. Consequently, they are under investigation for their potentiality in mRNA delivery within a PNRR project, addressing the growing need for large-scale production and rapid vaccine development. Indeed, the newly developed mRNA technology can be further potentiated in combination with μPs MNs acquiring all the advantages of this tool in terms of efficacy, storage, painless, no toxic wastes, no cross infection among others. Moreover, the fabrication process is time saving in comparison with similar technologies and an automation of the process is in an early stage in order to move forward a large-scale approach.

8 References

Abramson, A., Caffarel-Salvador, E., Soares, V., Minahan, D., Tian, R. Y., Lu, X., Dellal, D., Gao, Y., Kim, S., Wainer, J., Collins, J., Tamang, S., Hayward, A., Yoshitake, T., Lee, H. C., Fujimoto, J., Fels, J., Frederiksen, M. R., Rahbek, U., … Traverso, G. (2019). A luminal unfolding microneedle injector for oral delivery of macromolecules. *Nature Medicine*, *25*(10), 1512–1518. https://doi.org/10.1038/s41591-019-0598-9

Ahmed Saeed AL-Japairai, K., Mahmood, S., Hamed Almurisi, S., Reddy Venugopal, J., Rebhi Hilles, A., Azmana, M., & Raman, S. (2020). Current trends in polymer microneedle for transdermal drug delivery. In *International Journal of Pharmaceutics* (Vol. 587). Elsevier B.V. https://doi.org/10.1016/j.ijpharm.2020.119673

Akhtar, N., Singh, V., Yusuf, M., & Khan, R. A. (2020). Non-invasive drug delivery technology: Development and current status of transdermal drug delivery devices, techniques and biomedical applications. In *Biomedizinische Technik* (Vol. 65, Issue 3, pp. 243–272). De Gruyter Open Ltd. https://doi.org/10.1515/bmt-2019-0019

Akyala, A. I., Verhaar, A. P., & Peppelenbosch, M. P. (2018). Immune checkpoint inhibition in gastric cancer: A systematic review. *Journal of Cellular Immunotherapy*, *4*(2), 49–55. https://doi.org/10.1016/j.jocit.2018.05.001

Alkilani, A. Z., McCrudden, M. T. C., & Donnelly, R. F. (2015a). Transdermal drug delivery: Innovative pharmaceutical developments based on disruption of the barrier properties of the stratum corneum. In *Pharmaceutics* (Vol. 7, Issue 4, pp. 438–470). MDPI AG. https://doi.org/10.3390/pharmaceutics7040438

Alkilani, A. Z., McCrudden, M. T. C., & Donnelly, R. F. (2015b). Transdermal drug delivery: Innovative pharmaceutical developments based on disruption of the barrier properties of the stratum corneum. In *Pharmaceutics* (Vol. 7, Issue 4, pp. 438–470). MDPI AG. https://doi.org/10.3390/pharmaceutics7040438

Amani, H., Shahbazi, M. A., D'Amico, C., Fontana, F., Abbaszadeh, S., & Santos, H. A. (2021). Microneedles for painless transdermal immunotherapeutic applications. *Journal of Controlled Release*, *330*, 185–217. https://doi.org/10.1016/j.jconrel.2020.12.019

Anders, G. (1956). *L'uomo è antiquato I: Vol. I*. Bollati Boringhieri.

Ando, D., Ozawa, A., Sakaue, M., Yamamoto, E., Miyazaki, T., Sato, Y., Koide, T., & Izutsu, K. ichi. (2023). Fabrication and Characterization of Dissolving Microneedles for Transdermal Drug Delivery of Apomorphine Hydrochloride in Parkinson's Disease. *Pharmaceutical Research*. https://doi.org/10.1007/s11095-023-03621-x

Andranilla, R. K., Anjani, Q. K., Hartrianti, P., Donnelly, R. F., & Ramadon, D. (2023). Fabrication of dissolving microneedles for transdermal delivery of protein and peptide drugs: polymer materials and solvent casting micromoulding method. In *Pharmaceutical Development and Technology* (Vol. 28, Issue 10, pp. 1016–1031). Taylor and Francis Ltd. https://doi.org/10.1080/10837450.2023.2285498

Avcil, M., & Çelik, A. (2021). Microneedles in drug delivery: Progress and challenges. In *Micromachines* (Vol. 12, Issue 11). MDPI. https://doi.org/10.3390/mi12111321

Awasthi, R., Manchanda, S., Das, P., Velu, V., Malipeddi, H., Pabreja, K., Pinto, T. D. J. A., Gupta, G., & Dua, K. (2018). Poly(vinylpyrrolidone). In *Engineering of Biomaterials for Drug Delivery Systems: Beyond Polyethylene Glycol* (pp. 255–272). Elsevier Inc. https://doi.org/10.1016/B978-0-08-101750-0.00009-X

Ayorinde, F. O., Gelain, S. V., Johnson, J. H., & Wan, L. W. (2000). Analysis of some commercial polysorbate formulations using matrix-assisted laser desorption/ionization time-of-flight mass spectrometry. *Rapid Communications in Mass Spectrometry*, *14*(22), 2116–2124. https://doi.org/10.1002/1097-0231(20001130)14:22<2116::AID-RCM142>3.0.CO;2-1

Battisti, M., Vecchione, R., Casale, C., Pennacchio, F. A., Lettera, V., Jamaledin, R., Profeta, M., Di Natale, C., Imparato, G., Urciuolo, F., & Netti, P. A. (2019). Non-invasive Production of Multi-Compartmental Biodegradable Polymer Microneedles for Controlled Intradermal Drug Release of Labile Molecules. *Frontiers in Bioengineering and Biotechnology*, *7*. https://doi.org/10.3389/fbioe.2019.00296

Bauleth-Ramos, T., El-Sayed, N., Fontana, F., Lobita, M., Shahbazi, M.-A., & Santos, H. A. (2023). Recent approaches for enhancing the performance of dissolving microneedles in drug delivery applications. *Materials Today*, *63*, 239–287. https://doi.org/10.1016/j.mattod.2022.12.007This

Benne, N., van Duijn, J., Kuiper, J., Jiskoot, W., & Slütter, B. (2016). Orchestrating immune responses: How size, shape and rigidity affect the immunogenicity of particulate vaccines. In *Journal of Controlled Release* (Vol. 234, pp. 124–134). Elsevier B.V. https://doi.org/10.1016/j.jconrel.2016.05.033

Casale, C., Imparato, G., Urciuolo, F., & Netti, P. A. (2016). Endogenous human skin equivalent promotes in vitro morphogenesis of follicle-like structures. *Biomaterials*, *101*, 86–95. https://doi.org/10.1016/j.biomaterials.2016.05.047

Casale, C., Imparato, G., Urciuolo, F., Rescigno, F., Scamardella, S., Escolino, M., & Netti, P. A. (2018). Engineering a human skin equivalent to study dermis remodelling and epidermis senescence in vitro after UVA exposure. *Journal of Tissue Engineering and Regenerative Medicine*, *12*(7), 1658–1669. https://doi.org/10.1002/term.2693

Chen, M. C., Chan, H. A., Ling, M. H., & Su, L. C. (2017). Implantable polymeric microneedles with phototriggerable properties as a patient-controlled transdermal analgesia system. *Journal of Materials Chemistry B*, *5*(3), 496–503. https://doi.org/10.1039/c6tb02718k

Cheng, A., Sun, W., Xing, M., Zhang, S., & Gao, Y. (2022a). The hygroscopicity of polymer microneedles on the performance of dissolving behavior for transdermal delivery. *International Journal of Polymeric Materials and Polymeric Biomaterials*, *71*(1), 72–78. https://doi.org/10.1080/00914037.2020.1798442

Cheng, A., Sun, W., Xing, M., Zhang, S., & Gao, Y. (2022b). The hygroscopicity of polymer microneedles on the performance of dissolving behavior for transdermal delivery. *International Journal of Polymeric Materials and Polymeric Biomaterials*, *71*(1), 72–78. https://doi.org/10.1080/00914037.2020.1798442

Chu, L. Y., Choi, S. O., & Prausnitz, M. R. (2010). Fabrication of dissolving polymer microneedles for controlled drug encapsulation and delivery: Bubble and pedestal microneedle designs. *Journal of Pharmaceutical Sciences*, *99*(10), 4228–4238. https://doi.org/10.1002/jps.22140

Chu, L. Y., Ye, L., Dong, K., Compans, R. W., Yang, C., & Prausnitz, M. R. (2016). Enhanced Stability of Inactivated Influenza Vaccine Encapsulated in Dissolving Microneedle Patches. *Pharmaceutical Research*, *33*(4), 868–878. https://doi.org/10.1007/s11095-015-1833-9

Dahan, A., Miller, J. M., & Amidon, G. L. (2009). Prediction of solubility and permeability class membership: Provisional BCS classification of the world's top oral drugs. In *AAPS Journal* (Vol. 11, Issue 4, pp. 740–746). https://doi.org/10.1208/s12248-009-9144-x

Dalvi, M., Kharat, P., Thakor, P., Bhavana, V., Singh, S. B., & Mehra, N. K. (2021). Panorama of dissolving microneedles for transdermal drug delivery. In *Life Sciences* (Vol. 284). Elsevier Inc. https://doi.org/10.1016/j.lfs.2021.119877

Davis, S. P., Landis, B. J., Adams, Z. H., Allen, M. G., & Prausnitz, M. R. (2004). Insertion of microneedles into skin: Measurement and prediction of insertion force and needle fracture force. *Journal of Biomechanics*, *37*(8), 1155–1163. https://doi.org/10.1016/j.jbiomech.2003.12.010

De Alteriis, R., Vecchione, R., Attanasio, C., De Gregorio, M., Porzio, M., Battista, E., & Netti, P. A. (2015). A method to tune the shape of protein-encapsulated polymeric microspheres. *Scientific Reports*, *5*. https://doi.org/10.1038/srep12634

Demuth, P. C., Garcia-Beltran, W. F., Ai-Ling, M. L., Hammond, P. T., & Irvine, D. J. (2013). Composite dissolving microneedles for coordinated control of antigen and adjuvant delivery kinetics in transcutaneous vaccination. *Advanced Functional Materials*, *23*(2), 161–172. https://doi.org/10.1002/adfm.201201512

Di, J., Du, Z., Wu, K., Jin, S., Wang, X., Li, T., & Xu, Y. (n.d.). *Biodistribution and Non-linear Gene Expression of mRNA LNPs Affected by Delivery Route and Particle Size*. https://doi.org/10.1007/s11095-022-03166-5/Published

Donnelly, R. F. (2012). *Microneedle-mediated transdermal and intradermal drug delivery*. Wiley-Blackwell.

Donnelly, R. F. (2017). How can microneedles overcome challenges facing transdermal drug delivery? In *Therapeutic Delivery* (Vol. 8, Issue 9, pp. 725–728). Newlands Press Ltd. https://doi.org/10.4155/tde-2017-0028

Donnelly, R. F., Morrow, D. I. J., Singh, T. R. R., Migalska, K., McCarron, P. A., O'Mahony, C., & Woolfson, A. D. (2009). Processing difficulties and instability of carbohydrate microneedle arrays. *Drug Development and Industrial Pharmacy*, *35*(10), 1242–1254. https://doi.org/10.1080/03639040902882280

Donnelly, R. F., Singh, T. R. R., Tunney, M. M., Morrow, D. I. J., McCarron, P. A., O'Mahony, C., & Woolfson, A. D. (2009). Microneedle arrays allow lower microbial penetration than hypodermic needles in vitro. *Pharmaceutical Research*, *26*(11), 2513–2522. https://doi.org/10.1007/s11095-009-9967-2

Doraiswamy, A., Jin, C., Narayan, R. J., Mageswaran, P., Mente, P., Modi, R., Auyeung, R., Chrisey, D. B., Ovsianikov, A., & Chichkov, B. (2006). Two photon induced polymerization of organic-inorganic hybrid biomaterials for microstructured medical devices. *Acta Biomaterialia*, *2*(3), 267–275. https://doi.org/10.1016/j.actbio.2006.01.004

Du, G., & Sun, X. (2020). Current Advances in Sustained Release Microneedles. *Pharmaceutical Fronts*, *02*(01), e11–e22. https://doi.org/10.1055/s-0040-1701435

Du, G., Zhang, Z., He, P., Zhang, Z., & Sun, X. (2021). Determination of the mechanical properties of polymeric microneedles by micromanipulation. *Journal of the Mechanical Behavior of Biomedical Materials*, *117*. https://doi.org/10.1016/j.jmbbm.2021.104384

Ebadi, N., & Asadi, G. (n.d.). *The Motive behind Technology Integration*. Retrieved January 16, 2024, from https://opentextbooks.uregina.ca/universityteaching/chapter/technology-makes-it-easier/

Economidou, S. N., & Douroumis, D. (2021). 3D printing as a transformative tool for microneedle systems: Recent advances, manufacturing considerations and market potential. In *Advanced Drug Delivery Reviews* (Vol. 173, pp. 60–69). Elsevier B.V. https://doi.org/10.1016/j.addr.2021.03.007

Elseviers, M. M., Arias-Guillén, M., Gorke, A., & Arens, H. J. (2014). Sharps injuries amongst healthcare workers: Review of incidence, transmissions and costs. In *Journal of Renal Care* (Vol. 40, Issue 3, pp. 150–156). Wiley-Blackwell. https://doi.org/10.1111/jorc.12050

Faraji Rad, Z., Prewett, P. D., & Davies, G. J. (2021). High-resolution two-photon polymerization: the most versatile technique for the fabrication of microneedle arrays. In *Microsystems and Nanoengineering* (Vol. 7, Issue 1). Springer Nature. https://doi.org/10.1038/s41378-021-00298-3

Galimberti, U. (2013). *I miti del nostro tempo*. Universale Feltrinelli.

Gill, H. S., & Prausnitz, M. R. (2007). Does Needle Size Matter? Hypodermic Needles. In *Journal of Diabetes Science and Technology* (Vol. 1, Issue 5). www.journalofdst.org

Glycerol. (n.d.).

Gualeni, B., Coulman, S. A., Shah, D., Eng, P. F., Ashraf, H., Vescovo, P., Blayney, G. J., Piveteau, L. D., Guy, O. J., & Birchall, J. C. (2018). Minimally invasive and targeted

therapeutic cell delivery to the skin using microneedle devices. *British Journal of Dermatology*, *178*(3), 731–739. https://doi.org/10.1111/bjd.15923

Han, B.-C. (2021). *La società senza dolore*. Einaudi.

Hashmi, S., Ling, P., Hashmi, G., Reed, M., Gaugler, R., & Trimmer, W. (1995). Genetic transformation of nematodes using arrays of micromechanical piercing structures. *BioTechniques*, *19*(5), 766–770.

Henry, S., Mcallister, D. V, Allen, M. G., And, |, & Prausnitz, M. R. (1998). *Microfabricated Microneedles: A Novel Approach to Transdermal Drug Delivery*. https://doi.org/10.1021/js980042

Hosseinipalangi, Z., Golmohammadi, Z., Ghashghaee, A., Ahmadi, N., Hosseinifard, H., Mejareh, Z. N., Dehnad, A., Aghalou, S., Jafarjalal, E., Aryankhesal, A., Rafiei, S., Khajehvand, A., Nasab, M. A., & Kan, F. P. (2022). Global, regional and national incidence and causes of needlestick injuries: a systematic review and meta-analysis. In *Eastern Mediterranean Health Journal* (Vol. 28, Issue 3, pp. 233–241). World Health Organization. https://doi.org/10.26719/emhj.22.031

Hu, Z. I., & McArthur, H. L. (2018). Immunotherapy in Breast Cancer: the New Frontier. In *Current Breast Cancer Reports* (Vol. 10, Issue 2, pp. 35–40). Current Medicine Group LLC 1. https://doi.org/10.1007/s12609-018-0274-y

Huang, S., Liu, H., Huang, S., Fu, T., Xue, W., & Guo, R. (2020). Dextran methacrylate hydrogel microneedles loaded with doxorubicin and trametinib for continuous transdermal administration of melanoma. *Carbohydrate Polymers*, *246*. https://doi.org/10.1016/j.carbpol.2020.116650

Ita, K. (2015). Transdermal delivery of drugs with microneedles—potential and challenges. *Pharmaceutics*, *7*(3), 90–105. https://doi.org/10.3390/pharmaceutics7030090

Jamaledin, R., Makvandi, P., Yiu, C. K. Y., Agarwal, T., Vecchione, R., Sun, W., Maiti, T. K., Tay, F. R., & Netti, P. A. (2020). Engineered Microneedle Patches for Controlled Release of Active Compounds: Recent Advances in Release Profile Tuning. In *Advanced Therapeutics* (Vol. 3, Issue 12). Blackwell Publishing Ltd. https://doi.org/10.1002/adtp.202000171

Jeong, W. Y., Kwon, M., Choi, H. E., & Kim, K. S. (2021). Recent advances in transdermal drug delivery systems: a review. In *Biomaterials Research* (Vol. 25, Issue 1). BioMed Central Ltd. https://doi.org/10.1186/s40824-021-00226-6

Ji, A., Xu, M., Pan, Y., Diao, L., Ma, L., Qian, L., Cheng, J., & Liu, M. (2022). Lipid Microparticles Show Similar Efficacy With Lipid Nanoparticles in Delivering mRNA and Preventing Cancer. *Pharmaceutical Research*. https://doi.org/10.1007/s11095-022-03445-1

Joodaki, H., & Panzer, M. B. (2018). Skin mechanical properties and modeling: A review. In *Proceedings of the Institution of Mechanical Engineers, Part H: Journal of Engineering in*

Medicine (Vol. 232, Issue 4, pp. 323–343). SAGE Publications Ltd. https://doi.org/10.1177/0954411918759801

Joshi, N., Azizi Machekposhti, S., & Narayan, R. J. (2023). Evolution of Transdermal Drug Delivery Devices and Novel Microneedle Technologies: A Historical Perspective and Review. *JID Innovations*, *3*(6), 100225. https://doi.org/10.1016/j.xjidi.2023.100225

Jünger, E. (1997). *Foglie e Pietre*. Adelphi.

Kanitakis, J. (2002). Anatomy, histology and immunohistochemistry of normal human skin. *European Journal of Dermatology*, *12*(4), 390–401.

Kim, J., Park, S., Nam, G., Choi, Y., Woo, S., & Yoon, S. H. (2018). Bioinspired microneedle insertion for deep and precise skin penetration with low force: Why the application of mechanophysical stimuli should be considered. *Journal of the Mechanical Behavior of Biomedical Materials*, *78*, 480–490. https://doi.org/10.1016/j.jmbbm.2017.12.006

Kim, S., Yang, H., Eum, J., Ma, Y., Fakhraei Lahiji, S., & Jung, H. (2020). Implantable powder-carrying microneedles for transdermal delivery of high-dose insulin with enhanced activity. *Biomaterials*, *232*. https://doi.org/10.1016/j.biomaterials.2019.119733

Kobayashi, Y., Okamoto, A., & NISHINARIt, K. (1994). *0006-355X(94)EOOl6-N VISCOELASTICITY OF HYALURONIC ACID WITH DIFFERENT MOLECULAR WEIGHTS*.

Koh, K. J., Liu, Y., Lim, S. H., Loh, X. J., Kang, L., Lim, C. Y., & Phua, K. K. L. (2018). Formulation, characterization and evaluation of mRNA-loaded dissolvable polymeric microneedles (RNApatch). *Scientific Reports*, *8*(1). https://doi.org/10.1038/s41598-018-30290-3

Kolarsick, P. A., Ann Kolarsick, M., & Goodwin, C. (2006). *Anatomy and Physiology of the Skin*.

Kurakula, M., & Rao, G. S. N. K. (2020). Pharmaceutical assessment of polyvinylpyrrolidone (PVP): As excipient from conventional to controlled delivery systems with a spotlight on COVID-19 inhibition. In *Journal of Drug Delivery Science and Technology* (Vol. 60). Editions de Sante. https://doi.org/10.1016/j.jddst.2020.102046

Lagreca, E., Onesto, V., Di Natale, C., La Manna, S., Netti, P. A., & Vecchione, R. (2020). Recent advances in the formulation of PLGA microparticles for controlled drug delivery. In *Progress in Biomaterials* (Vol. 9, Issue 4, pp. 153–174). Springer Science and Business Media Deutschland GmbH. https://doi.org/10.1007/s40204-020-00139-y

Larrañeta, E., Lutton, R. E. M., Woolfson, A. D., & Donnelly, R. F. (2016). Microneedle arrays as transdermal and intradermal drug delivery systems: Materials science, manufacture and commercial development. In *Materials Science and Engineering R: Reports* (Vol. 104, pp. 1–32). Elsevier Ltd. https://doi.org/10.1016/j.mser.2016.03.001

Larrañeta, E., Moore, J., Vicente-Pérez, E. M., González-Vázquez, P., Lutton, R., Woolfson, A. D., & Donnelly, R. F. (2014). A proposed model membrane and test method for microneedle insertion studies. *International Journal of Pharmaceutics*, *472*(1–2), 65–73. https://doi.org/10.1016/j.ijpharm.2014.05.042

Le, Z., Yu, J., Quek, Y. J., Bai, B., Li, X., Shou, Y., Myint, B., Xu, C., & Tay, A. (2023). Design principles of microneedles for drug delivery and sampling applications. In *Materials Today* (Vol. 63, pp. 137–169). Elsevier B.V. https://doi.org/10.1016/j.mattod.2022.10.025

Lee, D., Huntoon, K., Lux, J., Kim, B. Y. S., & Jiang, W. (2023a). Engineering nanomaterial physical characteristics for cancer immunotherapy. *Nature Reviews Bioengineering*, *1*(7), 499–517. https://doi.org/10.1038/s44222-023-00047-3

Lee, D., Huntoon, K., Lux, J., Kim, B. Y. S., & Jiang, W. (2023b). Engineering nanomaterial physical characteristics for cancer immunotherapy. *Nature Reviews Bioengineering*, *1*(7), 499–517. https://doi.org/10.1038/s44222-023-00047-3

Lee, K. J., Jeong, S. S., Roh, D. H., Kim, D. Y., Choi, H. K., & Lee, E. H. (2020). A practical guide to the development of microneedle systems – In clinical trials or on the market. In *International Journal of Pharmaceutics* (Vol. 573). Elsevier B.V. https://doi.org/10.1016/j.ijpharm.2019.118778

Leone, M., Romeijn, S., Slütter, B., O'Mahony, C., Kersten, G., & Bouwstra, J. A. (2020). Hyaluronan molecular weight: Effects on dissolution time of dissolving microneedles in the skin and on immunogenicity of antigen. *European Journal of Pharmaceutical Sciences*, *146*. https://doi.org/10.1016/j.ejps.2020.105269

Love, A. S., & Love, R. J. (2021). Considering Needle Phobia among Adult Patients During Mass COVID-19 Vaccinations. In *Journal of Primary Care and Community Health* (Vol. 12). SAGE Publications Inc. https://doi.org/10.1177/21501327211007393

Makvandi, P., Kirkby, M., Hutton, A. R. J., Shabani, M., Yiu, C. K. Y., Baghbantaraghdari, Z., Jamaledin, R., Carlotti, M., Mazzolai, B., Mattoli, V., & Donnelly, R. F. (2021). Engineering Microneedle Patches for Improved Penetration: Analysis, Skin Models and Factors Affecting Needle Insertion. In *Nano-Micro Letters* (Vol. 13, Issue 1). Springer Science and Business Media B.V. https://doi.org/10.1007/s40820-021-00611-9

Marschuk Tz, M. K., Bernkop-Schnu, A., & Rch, K. (2000). Oral peptide drug delivery: polymer}inhibitor conjugates protecting insulin from enzymatic degradation in vitro. In *Biomaterials* (Vol. 21).

Marshall, S., Sahm, L. J., & Moore, A. C. (2016). Microneedle technology for immunisation: Perception, acceptability and suitability for paediatric use. In *Vaccine* (Vol. 34, Issue 6, pp. 723–734). Elsevier Ltd. https://doi.org/10.1016/j.vaccine.2015.12.002

Mikszta, J. A., Alarcon, J. B., Brittingham, J. M., Sutter, D. E., Pettis, R. J., & Harvey, N. G. (2002). NEW TECHNOLOGY Improved genetic immunization via micromechanical

disruption of skin-barrier function and targeted epidermal delivery. In *NATURE MEDICINE • VOLUME* (Vol. 8, Issue 4). http://medicine.nature.com

Miranda, I., Souza, A., Sousa, P., Ribeiro, J., Castanheira, E. M. S., Lima, R., & Minas, G. (2022). Properties and applications of PDMS for biomedical engineering: A review. In *Journal of Functional Biomaterials* (Vol. 13, Issue 1). MDPI. https://doi.org/10.3390/jfb13010002

Mistilis, M. J., Bommarius, A. S., & Prausnitz, M. R. (2015). Development of a thermostable microneedle patch for influenza vaccination. *Journal of Pharmaceutical Sciences*, *104*(2), 740–749. https://doi.org/10.1002/jps.24283

Morris, L. S., & Schulz, R. M. (1992). Patient compliance—an overview. In *Journal of Clinical Pharmacy and Therapeutics* (Vol. 17, Issue 5, pp. 283–295). https://doi.org/10.1111/j.1365-2710.1992.tb01306.x

Nagarkar, R., Singh, M., Nguyen, H. X., & Jonnalagadda, S. (2020). A review of recent advances in microneedle technology for transdermal drug delivery. In *Journal of Drug Delivery Science and Technology* (Vol. 59). Editions de Sante. https://doi.org/10.1016/j.jddst.2020.101923

Nestle, F. O., Di Meglio, P., Qin, J. Z., & Nickoloff, B. J. (2009). Skin immune sentinels in health and disease. In *Nature Reviews Immunology* (Vol. 9, Issue 10, pp. 679–691). https://doi.org/10.1038/nri2622

Nguyen, H. X. (2023). *Microneedles: the future of drug delivery* (CRC Press Taylor&Francis Group, Ed.; First).

Noh, I., Lee, K., & Rhee, Y. S. (2022). Microneedle systems for delivering nucleic acid drugs. In *Journal of Pharmaceutical Investigation* (Vol. 52, Issue 3, pp. 273–292). Springer. https://doi.org/10.1007/s40005-021-00558-4

Noreen, A., Zia, K. M., Tabasum, S., Khalid, S., & Shareef, R. (2020). A review on grafting of hydroxyethylcellulose for versatile applications. In *International Journal of Biological Macromolecules* (Vol. 150, pp. 289–303). Elsevier B.V. https://doi.org/10.1016/j.ijbiomac.2020.01.265

Oh, E. J., Park, K., Kim, K. S., Kim, J., Yang, J. A., Kong, J. H., Lee, M. Y., Hoffman, A. S., & Hahn, S. K. (2010). Target specific and long-acting delivery of protein, peptide, and nucleotide therapeutics using hyaluronic acid derivatives. In *Journal of Controlled Release* (Vol. 141, Issue 1, pp. 2–12). https://doi.org/10.1016/j.jconrel.2009.09.010

Olatunji, O., Das, D. B., Garland, M. J., Belaid, L., & Donnelly, R. F. (2013). Influence of array interspacing on the force required for successful microneedle skin penetration: Theoretical and practical approaches. *Journal of Pharmaceutical Sciences*, *102*(4), 1209–1221. https://doi.org/10.1002/jps.23439

Orenius, T., LicPsych, Säilä, H., Mikola, K., & Ristolainen, L. (2018). Fear of Injections and Needle Phobia Among Children and Adolescents: An Overview of Psychological, Behavioral, and Contextual Factors. *SAGE Open Nursing*, *4*. https://doi.org/10.1177/2377960818759442

Parikh, J. K., Vallabhbhai, S., Raval, A., Engineer, C., & Parikh, J. (2011). Review on Hydrolytic Degradation Behavior of Biodegradable Polymers from Controlled Drug Delivery System Article in Trends in Biomaterials and Artificial Organs · Review on Hydrolytic Degradation Behavior of Biodegradable Polymers from Controlled Drug Delivery System. In *Trends Biomater. Artif. Organs* (Vol. 25, Issue 2). http://www.sbaoi.org

Park, J. H., Allen, M. G., & Prausnitz, M. R. (2005). Biodegradable polymer microneedles: Fabrication, mechanics and transdermal drug delivery. *Journal of Controlled Release*, *104*(1), 51–66. https://doi.org/10.1016/j.jconrel.2005.02.002

Park, S. C., Kim, M. J., Baek, S. K., Park, J. H., & Choi, S. O. (2019). Spray-formed layered polymer microneedles for controlled biphasic drug delivery. *Polymers*, *11*(2). https://doi.org/10.3390/POLYM11020369

Phatale, V., Vaiphei, K. K., Jha, S., Patil, D., Agrawal, M., & Alexander, A. (2022). Overcoming skin barriers through advanced transdermal drug delivery approaches. In *Journal of Controlled Release* (Vol. 351, pp. 361–380). Elsevier B.V. https://doi.org/10.1016/j.jconrel.2022.09.025

Prausnitz, M. R. (2004). Microneedles for transdermal drug delivery. *Advanced Drug Delivery Reviews*, *56*(5), 581–587. https://doi.org/10.1016/j.addr.2003.10.023

Prausnitz, M. R. (2017). Engineering Microneedle Patches for Vaccination and Drug Delivery to Skin MNP: microneedle patch. *Annu. Rev. Chem. Biomol. Eng*, *8*, 177–200. https://doi.org/10.1146/annurev-chembioeng

Prokop, A., & Davidson, J. M. (2008). Nanovehicular intracellular delivery systems. *Journal of Pharmaceutical Sciences*, *97*(9), 3518–3590. https://doi.org/10.1002/jps.21270

Qin, M., Du, G., & Sun, X. (2021). Recent Advances in the Noninvasive Delivery of mRNA. *Accounts of Chemical Research*, *54*(23), 4262–4271. https://doi.org/10.1021/acs.accounts.1c00493

Raj M, K., & Chakraborty, S. (2020). PDMS microfluidics: A mini review. In *Journal of Applied Polymer Science* (Vol. 137, Issue 27). John Wiley and Sons Inc. https://doi.org/10.1002/app.48958

Ramadon, D., McCrudden, M. T. C., Courtenay, A. J., & Donnelly, R. F. (2022). Enhancement strategies for transdermal drug delivery systems: current trends and applications. *Drug Delivery and Translational Research*, *12*(4), 758–791. https://doi.org/10.1007/s13346-021-00909-6

Rapiti, E., Prüss, A., Yvan, Ü., Series, H., Prüss-Üstün, A., Campbell-Lendrum, D., Corvalán, C., & Woodward, A. (2005). *Sharps injuries Assessing the burden of disease from sharps injuries to health-care workers at national and local levels World Health Organization Protection of the Human Environment Geneva 2005*.

Römgens, A. M., Bader, D. L., Bouwstra, J. A., Baaijens, F. P. T., & Oomens, C. W. J. (2014). Monitoring the penetration process of single microneedles with varying tip diameters. *Journal of the Mechanical Behavior of Biomedical Materials*, *40*, 397–405. https://doi.org/10.1016/j.jmbbm.2014.09.015

Ronnander, P., Simon, L., & Koch, A. (2020). Experimental and mathematical study of the transdermal delivery of sumatriptan succinate from polyvinylpyrrolidone-based microneedles. *European Journal of Pharmaceutics and Biopharmaceutics*, *146*, 32–40. https://doi.org/10.1016/j.ejpb.2019.11.007

Roter, D. L., Hall, J. A., Merisca, R., Nordstrom, B., Cretin, D., & Svarstad, B. (1998). Effectiveness of Interventions to Improve Patient Compliance: A Meta-Analysis Author(s). In *Care* (Vol. 36, Issue 8). http://www.jstor.orgURL:http://www.jstor.org/stable/3766882

Sabri, A. H., Kim, Y., Marlow, M., Scurr, D. J., Segal, J., Banga, A. K., Kagan, L., & Lee, J. B. (2020). Intradermal and transdermal drug delivery using microneedles – Fabrication, performance evaluation and application to lymphatic delivery. In *Advanced Drug Delivery Reviews* (Vol. 153, pp. 195–215). Elsevier B.V. https://doi.org/10.1016/j.addr.2019.10.004

Sabri, A. H., Ogilvie, J., Abdulhamid, K., Shpadaruk, V., McKenna, J., Segal, J., Scurr, D. J., & Marlow, M. (2019). Expanding the applications of microneedles in dermatology. In *European Journal of Pharmaceutics and Biopharmaceutics* (Vol. 140, pp. 121–140). Elsevier B.V. https://doi.org/10.1016/j.ejpb.2019.05.001

Sadeghi, I., Byrne, J., Shakur, R., & Langer, R. (2021). Engineered drug delivery devices to address Global Health challenges. In *Journal of Controlled Release* (Vol. 331, pp. 503–514). Elsevier B.V. https://doi.org/10.1016/j.jconrel.2021.01.035

Sartawi, Z., Blackshields, C., & Faisal, W. (2022). Dissolving microneedles: Applications and growing therapeutic potential. In *Journal of Controlled Release* (Vol. 348, pp. 186–205). Elsevier B.V. https://doi.org/10.1016/j.jconrel.2022.05.045

Schramm, L. L., Stasiuk, E. N., & Marangoni, D. G. (2003). Surfactants and their applications. In *Annual Reports on the Progress of Chemistry - Section C* (Vol. 99, pp. 3–48). Royal Society of Chemistry. https://doi.org/10.1039/B208499F

Shokooh, M. K., Emami, F., Duwa, R., Jeong, J. H., & Yook, S. (2022). Triple-negative breast cancer treatment meets nanoparticles: Current status and future direction. In *Journal of Drug Delivery Science and Technology* (Vol. 71). Editions de Sante. https://doi.org/10.1016/j.jddst.2022.103274

Shu, W., Heimark, H., Bertollo, N., Tobin, D. J., O'Cearbhaill, E. D., & Annaidh, A. N. (2021). Insights into the mechanics of solid conical microneedle array insertion into skin using the

finite element method. *Acta Biomaterialia*, *135*, 403–413. https://doi.org/10.1016/j.actbio.2021.08.045

Sullivan, S. P., Murthy, N., & Prausnitz, M. R. (2008). Minimally invasive protein delivery with rapidly dissolving polymer microneedles. *Advanced Materials*, *20*(5), 933–938. https://doi.org/10.1002/adma.200701205

Supe, S., & Takudage, P. (2021). Methods for evaluating penetration of drug into the skin: A review. In *Skin Research and Technology* (Vol. 27, Issue 3, pp. 299–308). John Wiley and Sons Inc. https://doi.org/10.1111/srt.12968

Trommer, H., & Neubert, R. H. H. (2006). Overcoming the stratum corneum: The modulation of skin penetration. A review. *Skin Pharmacology and Physiology*, *19*(2), 106–121. https://doi.org/10.1159/000091978

Vecchione, R., Pitingolo, G., Guarnieri, D., Falanga, A. P., & Netti, P. A. (2016). From square to circular polymeric microchannels by spin coating technology: A low cost platform for endothelial cell culture. *Biofabrication*, *8*(2). https://doi.org/10.1088/1758-5090/8/2/025005

Vert, M., Mauduit, J., & Li, S. (n.d.). *Biodegradation of PLA/GA polymers: increasing complexity*.

Victor, A., Ribeiro, J., & F. Araújo, F. (2019). Study of PDMS characterization and its applications in biomedicine: A review. *Journal of Mechanical Engineering and Biomechanics*, *4*(1), 1–9. https://doi.org/10.24243/JMEB/4.1.163

Wang, C., Ye, Y., Hochu, G. M., Sadeghifar, H., & Gu, Z. (2016). Enhanced Cancer Immunotherapy by Microneedle Patch-Assisted Delivery of Anti-PD1 Antibody. *Nano Letters*, *16*(4), 2334–2340. https://doi.org/10.1021/acs.nanolett.5b05030

Wang, Q. L., Ren, J. W., Chen, B. Z., Jin, X., Zhang, C. Y., & Guo, X. D. (2018a). Effect of humidity on mechanical properties of dissolving microneedles for transdermal drug delivery. *Journal of Industrial and Engineering Chemistry*, *59*, 251–258. https://doi.org/10.1016/j.jiec.2017.10.030

Wang, Q. L., Ren, J. W., Chen, B. Z., Jin, X., Zhang, C. Y., & Guo, X. D. (2018b). Effect of humidity on mechanical properties of dissolving microneedles for transdermal drug delivery. *Journal of Industrial and Engineering Chemistry*, *59*, 251–258. https://doi.org/10.1016/j.jiec.2017.10.030

Wang, Q. L., Zhu, D. D., Liu, X. B., Chen, B. Z., & Guo, X. D. (2016). Microneedles with controlled bubble sizes and drug distributions for efficient transdermal drug delivery. *Scientific Reports*, *6*. https://doi.org/10.1038/srep38755

Wang, Q., Yao, G., Dong, P., Gong, Z., Li, G., Zhang, K., & Wu, C. (2015). Investigation on fabrication process of dissolving microneedle arrays to improve effective needle drug distribution. *European Journal of Pharmaceutical Sciences*, *66*, 148–156. https://doi.org/10.1016/j.ejps.2014.09.011

Wang, Y., Zhang, Z., Luo, J., Han, X., Wei, Y., & Wei, X. (2021). mRNA vaccine: a potential therapeutic strategy. In *Molecular Cancer* (Vol. 20, Issue 1). BioMed Central Ltd. https://doi.org/10.1186/s12943-021-01311-z

Yadav, P. R., Munni, M. N., Campbell, L., Mostofa, G., Dobson, L., Shittu, M., Pattanayek, S. K., Uddin, M. J., & Bhusan Das, D. (2021). Translation of polymeric microneedles for treatment of human diseases: Recent trends, Progress, and Challenges. In *Pharmaceutics* (Vol. 13, Issue 8). MDPI. https://doi.org/10.3390/pharmaceutics13081132

Yang, H. W., Ye, L., Guo, X. D., Yang, C., Compans, R. W., & Prausnitz, M. R. (2017). Ebola Vaccination Using a DNA Vaccine Coated on PLGA-PLL/γPGA Nanoparticles Administered Using a Microneedle Patch. *Advanced Healthcare Materials*, *6*(1). https://doi.org/10.1002/adhm.201600750

Yang, P., Lu, C., Qin, W., Chen, M., Quan, G., Liu, H., Wang, L., Bai, X., Pan, X., & Wu, C. (2020). Construction of a core-shell microneedle system to achieve targeted co-delivery of checkpoint inhibitors for melanoma immunotherapy. *Acta Biomaterialia*, *104*, 147–157. https://doi.org/10.1016/j.actbio.2019.12.037

Yao, G., Quan, G., Lin, S., Peng, T., Wang, Q., Ran, H., Chen, H., Zhang, Q., Wang, L., Pan, X., & Wu, C. (2017). Novel dissolving microneedles for enhanced transdermal delivery of levonorgestrel: In vitro and in vivo characterization. *International Journal of Pharmaceutics*, *534*(1–2), 378–386. https://doi.org/10.1016/j.ijpharm.2017.10.035

You, Y., Tian, Y., Yang, Z., Shi, J., Kwak, K. J., Tong, Y., Estania, A. P., Cao, J., Hsu, W. H., Liu, Y., Chiang, C. L., Schrank, B. R., Huntoon, K., Lee, D. Y., Li, Z., Zhao, Y., Zhang, H., Gallup, T. D., Ha, J. H., … Lee, A. S. (2023). Intradermally delivered mRNA-encapsulating extracellular vesicles for collagen-replacement therapy. *Nature Biomedical Engineering*, *7*(7), 887–900. https://doi.org/10.1038/s41551-022-00989-w

Yu, J., Wang, J., Zhang, Y., Chen, G., Mao, W., Ye, Y., Kahkoska, A. R., Buse, J. B., Langer, R., & Gu, Z. (2020). Glucose-responsive insulin patch for the regulation of blood glucose in mice and minipigs. *Nature Biomedical Engineering*, *4*(5), 499–506. https://doi.org/10.1038/s41551-019-0508-y

Zhang, L., Guo, R., Wang, S., Yang, X., Ling, G., & Zhang, P. (2021). Fabrication, evaluation and applications of dissolving microneedles. In *International Journal of Pharmaceutics* (Vol. 604). Elsevier B.V. https://doi.org/10.1016/j.ijpharm.2021.120749

Zhang, X. P., Wang, B. B., Li, W. X., Fei, W. M., Cui, Y., & Guo, X. D. (2021). In vivo safety assessment, biodistribution and toxicology of polyvinyl alcohol microneedles with 160-day uninterruptedly applications in mice. *European Journal of Pharmaceutics and Biopharmaceutics*, *160*, 1–8. https://doi.org/10.1016/j.ejpb.2021.01.005